TRANS **NOW**

TRANSPORTATION NORTHWEST

Final Report TNW2012-07

Research Project Agreement No. 701719

Finite Element Evaluation of Pervious Concrete Pavement for Roadway Shoulders

Ashraful Alam, Graduate Research Assistant,
Civil and Environmental Engineering
Washington State University

Liv Haselbach, Associate Professor
Civil and Environmental Engineering
Washington State University

William Cofer, Professor
Civil and Environmental Engineering
Washington State University

A report prepared for

Transportation Northwest (TransNow)
University of Washington
112 More Hall, Box 352700
Seattle, Washington 98195-2700

and

Washington State Department of Transportation

October 2011

TECHNICAL REPORT STANDARD TITLE PAGE

1. REPORT NO. TNW2012-07	2. GOVERNMENT ACCESSION NO.	3. RECIPIENT'S CATALOG NO.	
4. TITLE AND SUBTITLE Finite Element Evaluation of Pervious Concrete Pavement for Roadway Shoulders		5.REPORT DATE 10/2011 6. PERFORMING ORGANIZATION CODE 701719	
7. AUTHOR(S) William Cofer, Liv Haselbach, Ashraful Alam		8. PERFORMING ORGANIZATION REPORT NO. TNW2012-07	
9. PERFORMING ORGANIZATION NAME AND ADDRESS Transportation Northwest Regional Center X (TransNow) Box 352700, 112 More Hall University of Washington Seattle, WA 98195-2700		10. WORK UNIT NO. 11. CONTRACT OR GRANT NO. DTRT07-G-0010	
12. SPONSORING AGENCY NAME AND ADDRESS United States Department of Transportation Office of the Secretary of Transportation 1200 New Jersey Ave, SE Washington, D.C. 20590		13. TYPE OF REPORT AND PERIOD COVERED Final Technical Report 14. SPONSORING AGENCY CODE	
15. SUPPLEMENTARY NOTES			
Stormwater quantity control is an important issue that needs to be addressed in roadway and ancillary transportation facility design. Pervious concrete has provided an effective solution for storm runoff for parking lots, sidewalks, bike trails, and other applications. It should be readily adaptable for use on roadway shoulders. Being a relatively new material for use in pavement for roadways, there is a lack of knowledge of the strength and behavior of pervious concrete slabs. While standard procedures for rigid pavement design with Portland cement concrete have been recommended, there are fundamental differences with pervious concrete pavement. These include a variation in concrete strength and stiffness through the depth of a slab and differences in the subgrade. Also, the main concern for a shoulder is the need to withstand wheel loadings from encroaching truck traffic. Both the strength of the pervious concrete pavement and the interface with the mainline pavement must be evaluated. Typically, tiebars are used at the interface to connect the shoulder and mainline slabs. The capacity and durability of pervious concrete at the tiebars is unknown, and steel reinforcing may not be an option with pervious systems. While full scale testing of pervious concrete pavement is desirable, a preliminary evaluation can be performed quickly and economically through computer simulation. The Finite Element Method is a proven technique for the evaluation of solids and structures. With this approach, a number of loading scenarios can be applied to various pavement configurations to determine pavement capacity and evaluate the importance of connections with tiebars. The results of these analyses can be used to guide a full-scale testing program and help develop design procedures.			
17. KEY WORDS Pervious Concrete		18. DISTRIBUTION STATEMENT No restrictions.	
19. SECURITY CLASSIF. (of this report) None	20. SECURITY CLASSIF. (of this page) None	21. NO. OF PAGES 79	22. PRICE

DISCLAIMER

The contents of this report reflect the views of the authors, who are responsible for the facts and the accuracy of the information presented herein. This document is disseminated under the sponsorship of the Department of Transportation University Transportation Centers Program, in the interest of information exchange. The U.S. Government assumes no liability for the contents or use thereof.

Executive Summary

Finite Element Evaluation of Pervious Concrete Pavement for Roadway Shoulders

Pervious concrete is a sustainable paving material that has complex matrix and material characteristics due to the inherent porosity within the material. It has been in use for many years for low volume traffic applications, sidewalks, and parking lots. Lack of understanding of the stress and deflection characteristics of this novel material under traffic loading is one of the reasons for its limited use. There are several different ways to evaluate the stress characteristics of any type of structure; one of them is experimental investigation on built structures, another approach is application of finite element modeling methods. In this research, the finite element method has been used to evaluate the stress and deflection characteristics of pervious concrete pavement systems.

Traditional pavement systems are complex multi-layer configurations of different materials. Pervious concrete systems have even more complexity with their inherent and variable porosity in addition to the multi-layer configuration. This study began with the development of a finite element modeling technique specific to pervious concrete systems. The modeling procedure used a simplified vertical porosity distribution in the previous concrete layer with the assumption of perfect bond between the interfaces of the different material layers. The pervious concrete layer was divided into three vertical sections (top quarter, middle half, and bottom quarter), each with a specified porosity based on the average placement porosity and previous research on typical porosity distributions in pervious concrete layers. Additional material property relationships in the pervious concrete layer have been obtained from previous research of a field site in Oregon, and previous laboratory investigations. Different thicknesses in the pervious concrete and subbase layer were considered. All the modeling analyses were for static loading conditions and linear material properties.

The stresses obtained from the analyses were compared with material strength data and also compared to pavement condition index rating data. It was found that if the pavement condition index data is defined to represent cyclic loading, the required thickness needs a factor of safety of approximately two (2) compared to the static loading analysis. In addition, expanded finite element models for typical material properties and tire pressures indicate that pervious concrete might be appropriate for high volume traffic applications such as highway shoulders. Finally, considerations for dowel bars between pervious concrete and traditional pavement sections were discussed and not considered to be necessary based on the performance of the applications reviewed.

Acknowledgement

The authors gratefully acknowledge the contribution of Will Goede and Evolution Paving, since the material characteristics and comparative study have been performed based on these previous studies. The authors also appreciate University Recreation Center at WSU for the permission of research on the pervious concrete sidewalk and Michelle Boyer, Andrew Easley, and Cory Tobin for their assistance in evaluating the performance of sidewalk at WSU. Finally, the authors are grateful to TransNOW for the financial support for this research.

Table of Contents

List of Tables

List of Figures

Chapter 1
Introduction

1.1 Problem Statement

Stormwater runoff from the built environment is an important issue that needs to be addressed in roadway and ancillary transportation facility design. Low Impact Development (LID) is a suite of stormwater best management practices (BMPs) that are under development for prevention or control of this runoff. With LID, the hydrology of a developed site is designed to mimic the natural hydrological cycle as much as possible, while still maintaining the functional needs of the facility. One important practice of LID is to infiltrate rainwater as close as possible to the location where the stormwater would have been infiltrated naturally at the site. This will cause fewer changes to the site characteristics, including those below grade.

Pervious concrete is a relatively new paving material, unique from traditional concrete pavements because water can pass through its highly porous structure. Pervious concrete is considered to be a LID BMP, and its use can have many benefits, such as water pollution removal, maintenance of groundwater levels, increased driver safety, improved land utilization, and decreased road noise (Tennis et al., 2004; ACI Committee 522, 2006).

Currently, pervious concrete is commonly used for low frequency, relatively light loading applications such as sidewalks and parking lots. If adapted for use on roadway shoulders, it would also serve to infiltrate highway runoff close to the rainwater source and reduce the need for much of the currently designed stormwater control infrastructure provided in roadway right-of-ways (ROWs). However, additional knowledge of the strength and behavior of pervious concrete slabs is needed to more effectively implement their use for roadway shoulders. While standard procedures for rigid pavement design with portland cement concrete have been recommended for light applications with minor modifications (Delatte, 2008), there are still fundamental differences with pervious concrete pavement. These include a variation in concrete strength and stiffness through the depth of the pervious concrete slab due to its vertical porosity distribution resulting from the placement techniques, which is important for environmental and durability reasons, and also differences in the subbase and subgrade (Haselbach and Freemon, 2006). The subbase is typically used for stormwater storage and the subgrade is usually not compacted to levels common for typical pavement placements.

The main concern for a highway shoulder is the need to withstand wheel loadings from encroaching truck traffic. Before pervious concrete can be extensively used for such demanding applications, its unique material characteristics and structural performance must be incorporated into design methods.

The most commonly used thickness design methods for traditional concrete pavement are the AASHTO (1993) design guide and the Portland Cement Association's (PCA) (1984) design procedure (ACI Committee 325, 2002). The former is an empirical approach, based on tests from the late 1950's (Delatte, 2008). The latter is a mechanistic approach that is more readily updated to reflect the characteristics of pervious concrete. Here, detailed finite element (FE) analysis is used to determine the stresses and deflections at critical locations in the slab. Factors such as finite slab dimensions, location of wheel loads, and load transfer at joints and cracks are included (Garber and Hoel, 2002). This type of FE analysis can be a first step for evaluating the use of pervious concrete for roadway shoulders and, ultimately, for mainline slabs.

1.2 Objectives

The main objective of the work of this report is to provide guidance for the development of thickness design procedures for pervious concrete pavement. These criteria might then serve as a basis for the design of roadway shoulders for highways in Washington State.

Objective 1: Perform a literature search for finite element modeling of pervious concrete with respect to its structural performance.

Objective 2: Propose an FE modeling technique that includes the special characteristics of pervious concrete placements, primarily its vertical porosity distribution, its unique subbase for stormwater storage, and its uncompacted subgrade.

Objective 3: Validate this model against a known application of pervious concrete that received high loading.

Objective 4: Use the validated FE model to develop a range of design simulations.

Objective 5: Correlate the design with highway stormwater storage and preliminarily consider the possible use of dowels for connection to the mainline slabs.

1.3 Approach

The Finite Element Method of computer analysis is a well accepted approach for the structural analysis of pavement slabs (Huang, 2004; Garber and Hoel, 2002; Delatte, 2008). One version of it has been used in this research.

Typical model methodologies used in these analyses consisted of the following:

- The pervious concrete slab was built of solid elements to capture the full three dimensional stress states at the point of load application. It has three layers of elements through its thickness to include the variation of stiffness properties that have been observed in pervious concrete due to its vertical porosity distribution. Relevant material properties include modulus of elasticity, Poisson's ratio, flexural strength, and compressive strength. The values used were based on a survey of the literature and those obtained recently through testing at Washington State University (Goede, 2009).
- The subbase and subgrade were also modeled with solid elements to capture three dimensional effects.
- Loading was applied from tire footprints at critical locations. For stress, the critical location is with the wheels at the edge of the slab at approximately mid-span, as shown in Figure 1.1a. For maximum deflection, the critical location of the wheel is at the edge of the pavement as shown in Figure 1.1b. In addition to these, the wheel location was considered at the center of the pavement (Figure 1.1c) to compare the FE analysis results with the classical analytical theory for traditional concrete pavement.

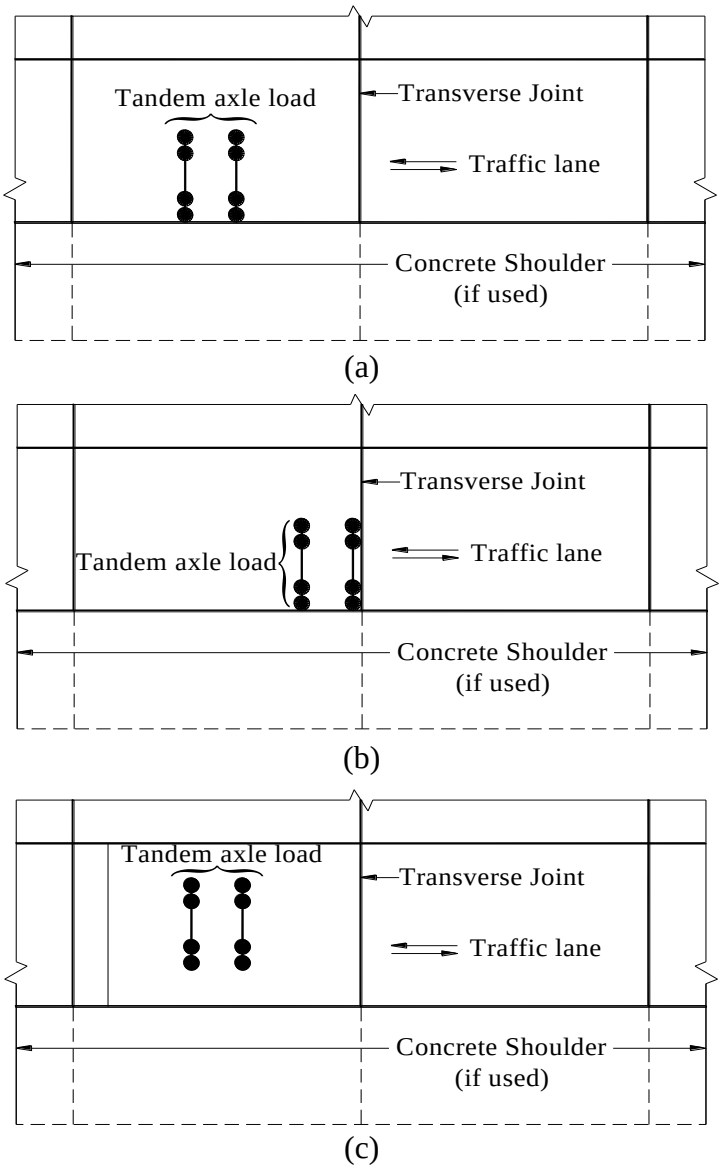

Figure 1.1: Wheel location at (a) edge for critical stress, (b) corner for critical deflection and (c) center of the pavement (After Huang, 2004 and Alam et al., 2011a)

There were several possible choices for finite element software that could be used for this project. EverFE (Davids, 2010) is freely available software specially designed to analyze jointed plain concrete pavement systems, with the ability to construct models having most of the desired features listed previously. However, this option was discarded because the complex material characteristics of pervious concrete cannot be as readily modeled using this software. Another option was to use general purpose software, such as ADINA (ADINA, 2010) or ABAQUS (ABAQUS, 2010). Preliminary two dimensional (2-D) analyses of pervious concrete pavements were performed to evaluate the software performance in terms of modeling with the ADINA and ABAQUS software packages. Example models for deflection in the pavement from both types of software are shown in Figure 1.2.

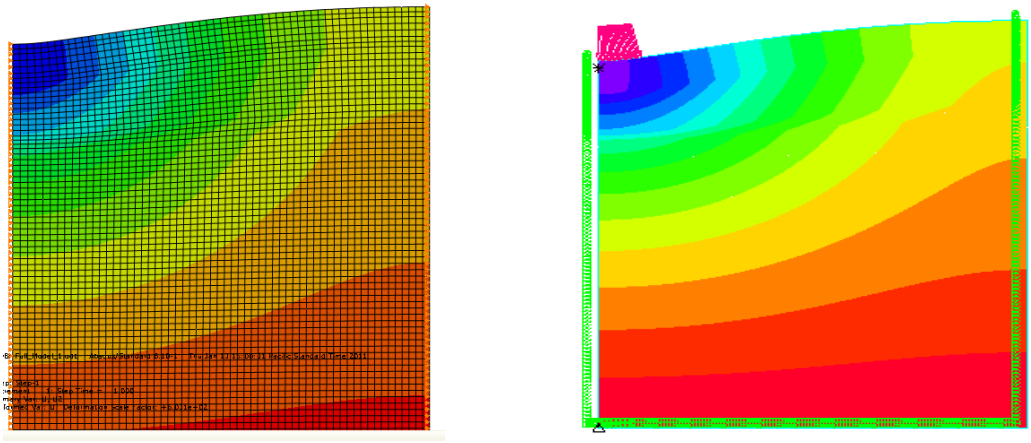

(a) (b)

Figure 1.2: Deflection contour for 2-D pervious concrete pavement analysis obtained from (a) ABAQUS, (b) ADINA

Both of the models from these two software packages appear to have appropriate deflection, tensile stress and compressive stress patterns and were found to be capable of performing the desired analyses with reasonable efficiency. However, the researchers in this proposal have greater familiarity with ADINA. Therefore, ADINA was selected for the FE analyses of the pervious concrete pavement.

1.4 Expected Benefits

The results of this project will provide much of the background needed to preliminarily design pervious concrete pavement for highway shoulder usage. It is anticipated that these will provide the basis for the design of test sections and those sections further used to validate and improve the models in the future. If permeable pavements can be used for transportation projects, they will have a large impact on reducing the additional infrastructure needed for stormwater management. More importantly, their use will aid in the transition to the incorporation of Low Impact Development technologies within the state of Washington and beyond.

CHAPTER 2
BACKGROUND

2.1 Pervious Concrete

Many studies have been performed to investigate the material characteristics of pervious concrete. These studies agree that increasing the porosity of pervious concrete typically decreases the strength of the material. The compressive strength of pervious concrete could vary from 500 psi (3.45 MPa) to 4000 psi (27.58MPa) (Onstenk et al., 1993; Tennis, et al., 2004; Vassilikou et al., 2011), while the typical traditional concrete compressive strength ranges from 3000 psi (20.68 MPa) to 7000 psi (48.26 MPa) (McCormac and Nelson, 2005). Typical pervious concrete and traditional concrete flexural strengths range between 150 to 550 psi and 350 to 600 psi, respectively (Tennis, et al., 2004; Wang, et al., 2007). However, pervious concrete strengths higher than typical traditional concrete strengths are obtainable through the use of admixtures and could reach up to 8000 psi (55.16 MPa) (Yang and Jiang, 2003). Tennis et al., (2004) recommend pervious concrete porosities between 15 and 25 percent for adequate infiltration capabilities and strengths. Even though compressive and flexural strength is primarily dependent on porosity, aggregate size, shape, and gradation can also affect the strength of pervious concrete (Crouch, et al., 2007; Yang, et al., 2008).

The structural performance of pervious concrete has also been studied. Delatte et al. (2007) performed distress surveys on 18 different pervious concrete field installations. Of the 18 installations observed, 15 showed only minimal raveling, and 12 showed no cracking. Wanielista and Chopra (2007) reported on the performance of a pervious concrete shoulder installed in an interstate rest area parking lot. After being monitored for a year, no visual wear was observed. However, it was noted that strength tests should be performed on the pervious concrete pavement. Rohne and Izevbekhai (2009) described the construction and early performance of a pervious concrete test cell in Minnesota at the MnROAD facility. There, the cell was subjected to periodic loading from 80-kip and 102-kip 5-axle semi-trailers. The overall surface condition was surveyed and, while some raveling was observed at the surface, further degradation was not present and cores exhibited no macro cracking. It was concluded that pervious concrete can withstand stresses in the same range as those on standard pavements. Deflections were larger, however.

In another investigation into structural performance, Goede and Haselbach (2011) performed distress surveys on two different field sites. The distress survey results were used to calculate a pavement condition index (PCI) using the procedure described in ASTM Standard D6433 (2007). One of the sites had been subjected to equivalent loading as a “Collector” street (as defined by ACI Committee 325, 2002) in use for between 8 and 80 years. They concluded that the high PCI ratings of the thicker pervious concrete sections indicated that pervious concrete, when properly designed, is capable of being used for most “Residential” streets and many “Collector” streets for typical design life durations while exhibiting satisfactory structural performance (Goede and Haselbach, 2010).

2.2 Pavement Types

The pavement types, which are being adopted for LID, are referred to as permeable pavements. These include pervious concrete, porous asphalt, permeable pavers and open-grid pavement systems (Ferguson, 2005). These are being used instead of more traditional pavements.

The three major types of traditional pavements are flexible pavements, rigid pavements and composite pavements (Huang, 2004). The first two pavement types are differentiated by the type of binder material used, with asphalt being used as the binder material for flexible pavement

and cement being used for rigid pavement. Composite pavement is a combination of Portland cement concrete (PCC) and hot mix asphalt (HMA). Typically, the most desirable combination in a composite pavement is the use of PCC in the bottom layer and HMA as a top layer.

Rigid pavements, also known as conventional concrete pavements, are further subdivided based on the joints and reinforcement used. The common types are JPCP (Jointed Plain Concrete Pavement), JRCP (Jointed Reinforced Concrete Pavement), CRCP (Continuously Reinforced Concrete Pavement) and PCP (Prestressed Concrete Pavement) (Huang, 1993). The four types of traditional concrete pavement are shown in Figure 2.1.

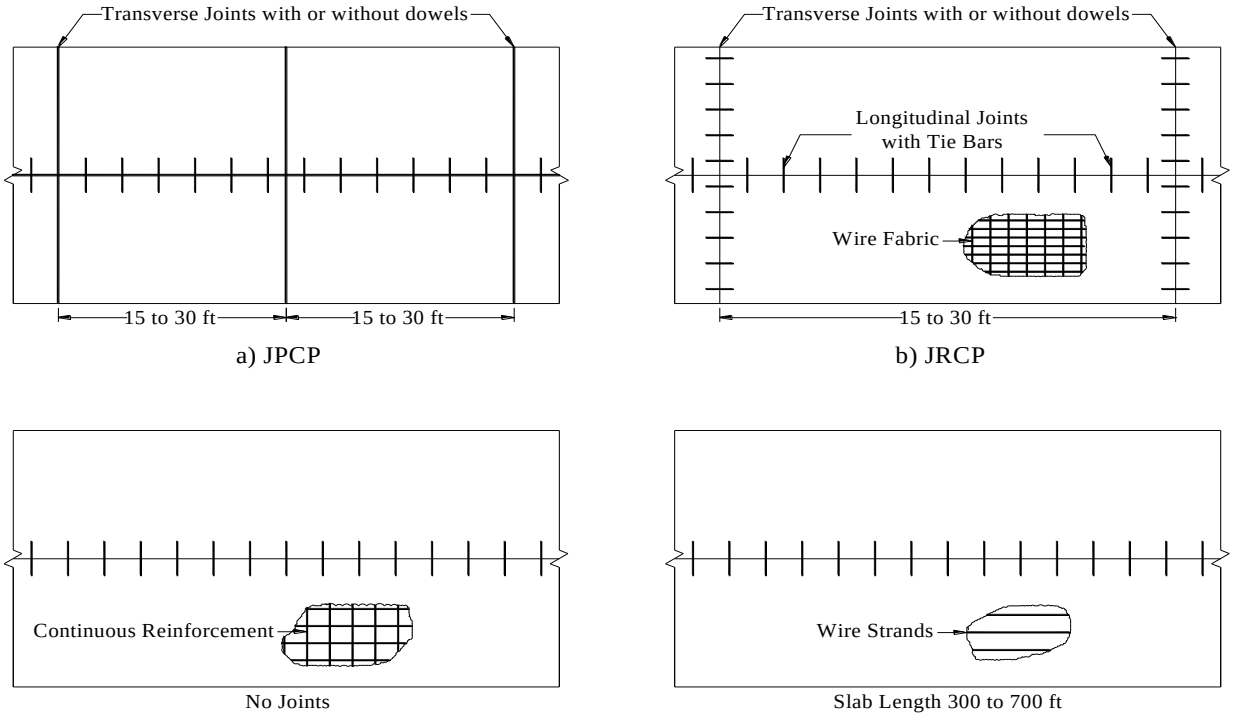

Figure 2.1: Different types of concrete pavements (Huang, 2004)

In the literature, JPCP has two different definitions. According to PCA (1984), JPCP is a plain concrete pavement with no reinforcement and no doweled joints, while Huang (2004) defined JPCP as plain concrete pavements with dowel bars in the longitudinal joints and transverse joints constructed with or without dowels. Aggregate interlocks are assumed to transfer loads at the joints if there is no dowel bar. However, the practice of using dowel bars varies from state to state in the United States. While the western and southwestern states use aggregate interlocking for load transfer in joints, southeastern states use dowel bars most frequently and the other regions use both as a general practice (Huang, 2004).

The other traditional pavement types use reinforcement in the mainline slab as well as in the longitudinal joints and transverse or contraction joints. The maximum recommended joint spacing for JPCP is 15 ft when no dowels are used in the joint and 20 ft for doweled joints. For JRCP, the joint spacing is 40 ft and, usually, there is no contraction/ transverse joint in CRCP and PCP. For PCP, the slab length varies from 300 ft to 760 ft (Huang, 2004).

There are three layers through the depth of traditional rigid pavements (Figure 2.2). These are the concrete layer, the subbase layer, and the subgrade or soil below. The depth of the

concrete layer and subbase layer vary depending on the anticipated volume of traffic and loading over the pavement. In earlier designs, the concrete layer was frequently placed directly over the soil or subgrade, but inclusion of a subbase has become almost mandatory as the weight and volume of traffic has increased, and pumping of the pavement has been recognized as an issue (Huang, 2004).

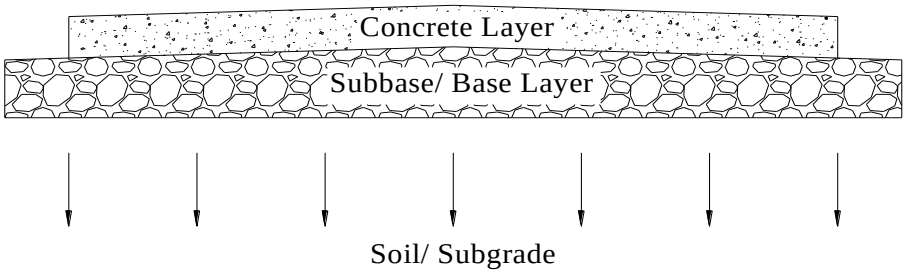

Figure 2.2: Cross section along the depth of a rigid concrete pavement

For pervious concrete pavement systems, the depth of the subbase layer is typically much greater as compared to traditional concrete pavement because of the need for increased storage volume for its intended use as a detention pond, and also when frost depth considerations require that the water be contained deeper in the system. The subgrade of pervious concrete systems is also commonly not compacted because it is required to maintain the infiltration capability of the natural soil in order for the system to function for stormwater management. There are a few exceptions to this when the collected stormwater is not infiltrated due to other environmental concerns such as high water tables, but usually the subgrade is either not compacted, or if inadvertently compacted during construction, scarified or otherwise amended to restore appropriate infiltration rates.

2.3 FE Modeling of Pavement

FE analysis, as compared to other modeling techniques, can uniquely represent structures of arbitrary complex geometry, and may more adequately resemble the actual body or region or the modeled systems (Cook et. al, 2004). Another advantage of FE modeling is that it takes less time compared to experimental study. However, validation of FE analysis is important in order to establish the compatibility of practical applications and analytical theory. Once validated, then parametric studies can be performed for prototype models using FE analysis without the construction of physical models.

For roads and pavement, two- and three-dimensional FE modeling and analysis can be applicable for many structural investigations, such as:

- static and dynamic analysis,
- identification of material properties,
- linear and nonlinear analysis,
- pavement response and behavior simulations,
- load transfer,
- temperature effects and thermal stress analysis,
- road surface temperature prediction and curling stresses,
- permanent deformations,
- pavement discontinuities and contact problems,
- dynamic response irregularities,
- moving loads,

- frost protection,
- interface shear stress,
- pavement soil interaction,
- stability of roads and intersections, and
- fatigue cracking (Mackerle, 1998).

FE modeling and analysis demonstrating most of the aforementioned variables have been performed for traditional rigid and flexible pavements, and some FE modeling and analysis have also been performed for porous asphalt pavement (Mackerle, 1998). However, the application of the FE method for pervious concrete pavement is quite new. It has been applied for percolation and transport characteristics of pervious concrete as compared with field installations (Bentz, 2008). In that study, FE numerical algorithms were developed to model the microstructure of pervious concrete and the associated percolation characteristics were determined for pervious concrete. It has also been used for preliminary modeling of heat transfer in pervious concrete systems (Boyer et al., 2012)

2.4 Material Properties

FE structural analyses require a number of properties of the material based on the type of analysis. For a static analysis, the required material properties are modulus of elasticity and Poisson's ratio of the corresponding material. Since a pervious concrete pavement system typically has three layers (pervious concrete layer, subbase layer and subgrade layer), the properties of these materials all need to be determined. Various values for these properties have been compiled based on literature reviews and laboratory analyses at Washington State University (WSU) and are summarized in the following sections.

2.4.1 *Soil/Subgrade*

The modulus of elasticity and Poisson's ratio are important parameters in determining the settlement of the subgrade or soil. Bowles (1996) has reported a list of values for the modulus of elasticity and Poisson's ratio of various soil types that are listed in Table 2.1 and Table 2.2, respectively.

Table 2.1: Moduli of elasticity of soils (Bowles, 1996)

Soil Type		Modulus of Elasticity
		ksi (GPa)
Clay	Very soft	0.29-2.18 (0.002-0.015)
	Soft	0.73-3.63 (0.005-0.025)

	Medium	2.18-7.25 (0.015-0.05)
	Hard	7.25-14.5 (0.05-0.1)
	Sandy	3.63-36.26 (0.025-0.25)
Glacial Till	Loose	1.45-21.76 (0.01-0.15)
	Dense	21.76-39.16 (0.15-0.27)
	Very dense	72.52-208.85 (0.5-1.44)
Loess		2.130-8.7 (0.015-0.06)
Sand	Silty	0.73-2.9 (0.005-0.02)
	Loose	1.45-3.63 (0.01-0.025)
	Dense	7.25-11.75 (0.05-0.081)
Sand and Gravel	Loose	7.25-21.76 (0.05-0.15)
	Dense	14.5-29.0(0.1-0.2)
Shale		21.76-725.0 (0.15-5.0)
Silt		0.29-2.9 (0.002-0.02)

Table 2.2: Poisson's ratio of soil (Bowles, 1996)

Soil Type	Poisson's ratio
Most clay soil	0.4-0.5
Saturated clay soil	0.45-0.50
Cohesionless – medium and dense	0.3-0.4
Cohesionless – loose to medium	0.2-0.35

Coduto (1994) has listed the modulus of elasticity and Poisson's ratio of soils based on the drainage condition of the soil, either drained or undrained. It is a function of the coefficient of permeability or hydraulic conductivity, and the applied loading rate. The drained condition is described when the drainage rate is higher than the loading rate and the undrained condition occurs under the opposite conditions. Usually, the drained condition is more frequent in sandy soils because of higher coefficients of permeability, and undrained conditions occur more frequently in clay soils since the hydraulic conductivity is low. However, both sandy and clayey soils can experience either of the drained conditions. Table 2.3 and Table 2.4 are the summaries of the moduli of elasticity and Poisson's ratio based on the drainage condition of various soils.

Table 2.3: Modulus of elasticity of soil (Coduto, 1994)

Soil Type		Modulus of Elasticity
		ksi (GPa)
Undrained Condition	Soft Clay	0.21 – 1.39 (0.0015 – 0.01)
	Medium Clay	0.69 – 6.94 (0.005 – 0.05)

	Stiff Clay	2.08 – 10.41 (0.015 – 0.075)
Drained Condition	Soft Clay	0.035 – 0.21 (0.0003 – 0.0015)
	Medium Clay	0.069 – 0.49 (0.0005 – 0.0035)
	Stiff Clay	0.17 – 2.78 (0.0012 – 0.02)
	Loose Sand	1.39 – 3.47 (0.01 – 0.025)
	Medium dense sand	2.78 – 8.33 (0.02 – 0.06)
	Dense sand	6.94 – 13.89 (0.05 – 0.1)
Sandstone		972.0 – 2780 (7.0 – 20.0)
Granite		3470 – 6940 (25.0 – 50.0)

Table 2.4: Poisson's ratio of soil (Coduto, 1994)

Soil Type	Poisson's ratio
Saturated soil, undrained condition	0.50
Partially saturated clay	0.30 – 0.40
Dense sand, drained condition	0.30 – 0.40
Losse sand, drained condition	0.10 – 0.30
Sandstone	0.25 – 0.30
Granite	0.23 – 0.27

Higher drainage rates in the subgrade level are generally preferred for rigid pavements so that water pumping does not occur under the pavement, which might compromise its stability (Huang, 2004). However, pumping is not necessarily an issue for permeable pavements, but the higher drainage rates might be important for the stormwater management calculations.

2.4.2 *Aggregate/Subbase*

The modulus of elasticity of granite and limestone ranges between 2,000 ksi to 7,000 ksi (13.8 GPa to 48.3 GPa), and sandstone has a comparatively lower modulus of elasticity which varies from 1,000 ksi to 5,000 ksi (6.9 GPa to 34.5 GPa) (Somayaji, 2001). Note that there are various rock types which do not obey the Hooke's law of elasticity. Granite and limestone exhibit a linearly elastic stress-strain relationship while sandstone with a porous structure shows nonlinear stress-strain relationship at very small stresses.

Adu-Osei et al. (2001) have conducted numerous tests on unbound limestone aggregate to characterize the behavior of base materials under traffic loads. The modulus of elasticity they found ranges from 10.1 ksi (0.067 GPa) to 510.0 ksi (0.35 GPa) with an average value of 29.3 ksi (0.20 GPa) and the average Poisson's ratio was 0.399 (0.336 – 0.441).

2.4.3 *Pervious Concrete*

Material characteristics of pervious concrete used in FEA have been adapted from Goede (2009) and also Ghafoori and Dutta (1995) for this research. The full development of the equations used for the material characterization may be found in a previous work (Alam et al., 2011b), repeated below for completeness.

Goede (2009) investigated the mechanical properties of pervious concrete to evaluate the structural performance of pervious concrete pavements. Material characterization tests were performed on pervious concrete samples extracted from existing pavement and also on specimens prepared in the laboratory. Flexural strength, compressive strength, and porosity have been determined for the cores extracted from the pavement site. Based on experimental data,

relationships between flexural strength and compressive strength and between flexural strength and porosity were established. For laboratory prepared samples, porosity, compressive strength, modulus of elasticity, and Poisson's ratio were determined, and a relationship between the modulus of elasticity and compressive strength was developed.

The cores extracted from the pavement site were found to have an average unit weight of 118 pcf (1890 kg/m3), an average flexural strength of 294 psi (2.03 MPa), an average compressive strength of 3089 psi (21.30 MPa), and a mean porosity of 21%. The relationship between flexural strength and compressive strength and between flexural strength and porosity were expressed in Equation 2.1 and Equation 2.2, respectively, by Goede.

$$MOR = 5.3\sqrt{f_c^{'}} \tag{2.1}$$

$$MOR = -1105\sqrt{P} + 800 \tag{2.2}$$

where MOR is the flexural strength (psi), $f_c^{'}$ is compressive strength (psi), and P (%) is the porosity.

For the laboratory prepared samples of Goede (2009), the average unit weight was 116 pcf (1858 kg/m^3), the average compressive strength was 1540 psi (10.62 MPa), the average modulus of elasticity was 1923.67 ksi (13.3 GPa), the average Poisson's ratio was 0.22, and the mean porosity was 27%. Additional relationships were developed for the modulus of elasticity in terms of the unit weight and the compressive strength of pervious concrete, and for the compressive strength in terms of the porosity of the pervious concrete samples. Both are given in Equation 2.3 and Equation 2.4.

$$E = 39.1 w_{pc}^{1.5} \sqrt{f_c^{'}} \tag{2.3}$$

$$f_c^{'} = -16600P + 6350 \tag{2.4}$$

where E is the modulus of elasticity (psi), w_{pc} is unit weight of pervious concrete (pcf), $f_c^{'}$ is compressive strength (psi) and P is the porosity of pervious concrete (%).

Although there were no experimental data for the modulus of elasticity for cores extracted from the site in the work by Goede (2009), the modulus of elasticity can be estimated from Equation 2.3 for the known compressive strengths of the pervious concrete cores extracted from the site. However, the compressive strengths of the field cores were almost twice as large as the compressive strengths of laboratory prepared samples due to porosity variations and the addition of admixture in the field placement. Thus, the modulus of elasticity of the pervious concrete samples from the site could only be estimated using an extrapolation of the compressive strength relationship to the modulus of elasticity as determined in the laboratory. Based on a linear approximation of the site data, the relationship between compressive strengths and porosity for pervious concrete were represented by Goede (2009) as:

$$P = -18.37 \ln\left(f_c^{'}, s \right) + 168.04 \tag{2.5}$$

$$P = -8.31 \ln\left(f_c^{'} \right) + 88.1 \tag{2.6}$$

where $f_c^{'}, s$ and $f_c^{'}$ are the compressive strength of pervious concrete at the site and at laboratory respectively, in units of psi.

The relationship of compressive strength of pervious concrete at the site and for laboratory prepared sample based on porosity from Equations 2.5 and 2.6 can then be written as:

$$f_c^{'} = e^{\left[2.2\ln\left(f_c^{'}, s\right) - 9.6\right]} \tag{2.7}$$

Thus from Equation 2.3 the modulus of elasticity in pervious concrete at the site can be expressed as:

$$E, s = 39.1 w_{pc}^{1.5} \left[e^{\left\{2.2\ln\left(f_c^{'}, s\right) - 9.6\right\}} \right]^{1/2} \tag{2.8}$$

where E, s is the modulus of elasticity of pervious concrete at the site.

When the modulus of elasticity is calculated from Equation 2.8, it appears to be larger than the modulus of elasticity in traditional concrete, as the recommended modulus of elasticity equation of tradition concrete by ACI 318 (2008) is given by:

$$E_{TC} = 33 w_{TC} \sqrt{f_{TC}^{'}} \tag{2.9}$$

where E_{TC}, w_{TC}, $f_{TC}^{'}$ is the modulus of elasticity, unit weight and compressive strength of traditional concrete.

Thus, the extrapolation from the more porous laboratory data measured by Goede (2009) might represent an overestimate. This seems reasonable as porosity is a three dimensional characteristic and compressive stresses are usually applied in only one direction. However, Ghafoori and Dutta (1995) have developed a modulus of elasticity equation in terms of unit weight and compressive strength of pervious concrete for more applicable ranges of porosity, given by:

$$E = 32.88 w_{pc} \sqrt{f_{pc}^{'}} \tag{2.10}$$

where E is the modulus of elasticity of pervious concrete.

Using Equation 2.10, the modulus of elasticity of pervious concrete at the site can be re-written as:

$$E, s = 32.88 w_{pc}^{1.5} \left[e^{\left\{2.2\ln\left(f_c^{'}, s\right) - 9.6\right\}} \right]^{1/2} \tag{2.11}$$

Equation 2.11 provides an acceptable and conservative value of modulus of elasticity of pervious concrete at the site, assuming that the pervious concrete will have a lower modulus of elasticity as compared to traditional concrete.

These derived equations provide the associated material characteristic relationships for a specific porosity of pervious concrete, but porosity in the pervious concrete layer in a typical placement varies from top to bottom and this porosity variation can have a significant effect on the strength of the pervious concrete (Haselbach and Freeman, 2006). Haselbach and Freeman (2006) have developed a series of expressions for vertical porosity distribution in a typical pervious concrete placement that has received an approximate ten percent compression during placement from the top surface. In addition to relating porosity in terms of depth, they have also

developed a simplified set of porosity distribution equations for the top quarter, the middle half, and the bottom quarter of a pervious concrete column based on the average porosity of that full column. The top typically has a lower porosity, the middle has an average porosity and the bottom has a higher porosity. These vertical section porosities can then be used to estimate various properties in these vertical sections of the pervious concrete layer. For instance, the top of the column with the lowest porosity would usually control the stormwater flow into a pervious concrete slab, as the lower porosity here would be the infiltration bottleneck for flow. The higher porosity in the lower section would be important in determining the strength properties, particularly the flexural strength limitations of a slab with an applied surface point load.

The simplified set of equations of porosity distribution along the depth of the pavement are expressed as follows (Haselbach and Freeman, 2006):

$$P_{top} = 1.07P_{mean} - 7 \tag{2.12}$$

$$P_{mid} = P_{mean} \tag{2.13}$$

$$P_{bottom} = 0.93P_{mean} + 7 \tag{2.14}$$

where P_{mean} is the known mean porosity as a ratio of the volume of the voids to the total volume, and P_{top}, P_{mid}, and P_{bottom} are the average top, middle, and bottom porosities, respectively.

Based on the mean porosity of the sample from a placement, porosities for the three vertical sections of the pervious concrete layer can be estimated from Equations 2.12, 2.13, and 2.14. Once these porosities are determined, the compressive strengths of the sample at the site can be determined from Equations 2.1 and 2.2 for the corresponding vertical sections in the pervious concrete layer. Finally, the modulus of elasticity of the sample at the site can be obtained from Equation 2.11 for the top, middle, and bottom vertical sections of the pervious concrete layer.

Chapter 3
Field Site Evaluations by Finite Element Modeling and Analysis

3.1 Introduction

One way to validate FE model and analysis results is to compare with known field application results. In this chapter, one of the field sites evaluated by Goede (2009) is modeled using finite element methods and the analysis results were then compared with the data obtained from the field. The results of this analysis and comparisons are summarized herein (Alam et al., 2011b).

The available field data includes pavement geometry, unit weight, porosity, modulus of elasticity, compressive and flexural strength of pervious concrete, and pavement condition index (PCI) values. While pavement geometry, unit weight, porosity, and modulus of elasticity were used in the pre-processing phase to model the field application, compressive and flexural strength of pervious concrete and the pavement condition index (PCI) value were used in the post processing phase to compare the results and validity of the FE model.

3.2 Pervious Pavement Placement at Site (Goede, 2009)

Two pervious concrete placements were evaluated by Goede (2009). One placement was at Salem, Oregon and another one at Kent, Washington. Since detailed material characteristic data were only available for the Salem, Oregon site, only this site was modeled and evaluated by FE methods. The Salem Oregon placement served as the main drive for a concrete producer.

3.2.1 *Pavement Geometry*

At the Salem, Oregon site, 4000 square feet of the pervious concrete drive, which was further divided into sixteen (16) panels, was investigated (Figure 3.1). The eight panels in the ingress side were subjected to empty concrete truck loading, while the eight egress panels were subjected to full concrete truck loads. All the loads and the number and type of trucks were recorded in the company manifests.

Figure 3.1: Photo of pervious concrete placement at Salem, OR (Goede, 2009)

The different panels in the driveway had varying material characteristics, specifically intended to represent a range of design variables for which some were expected to fail under the subjected loads and others were expected to be more than adequate. The design properties for each of these panels are listed in Table 3.1. The 3/8 inch maximum aggregate size as listed does not contain any other sizes, but the 5/8 inch crushed rock contained a mixture of 75% 5/8 inch to ¼ inch and 25% 3/8 inch aggregate, and the ½ inch crushed rock composed of 75% ½ inch to ¼ inch crushed aggregate and 25% quarter-ten (< ¼ inch) crushed rock.

Table 3.1: Pervious concrete pavement panel property summary at Salem, OR (Goede, 2009)

Panel No	Thickness	Maximum aggregate size	Aggregate type	Age	Compaction	Truck loading type
	in (mm)	in (mm)		yr		
1	7.5 (190.5)	3/8 (9.53)	Round Rock	6	½ in heavy roller	Empty
2	10 (254)	5/8 (15.88)	Crushed Rock	5	Heavy weighted Fresno	Full
3	10 (254)	5/8 (15.88)	Crushed Rock	6	½ in heavy roller	Empty
4	7 (177.8)	5/8 (15.88)	Crushed Rock	5	Heavy weighted Fresno	Full
5	8 (203.2)	5/8 (15.88)	Crushed Rock	6	½ in heavy roller	Empty
6	5 (127)	½ (12.7)	Crushed Rock	5	Heavy weighted Fresno	Full
7	6 (152.4)	5/8 (15.88)	Crushed Rock	6	½ in heavy roller	Empty
8	5 (127)	3/8 (9.53)	Round Rock	5	Heavy weighted Fresno	Full
9	4 (101.6)	5/8 (15.88)	Crushed Rock	6	½ in heavy roller	Empty
10	4 (101.6)	3/8 (9.53)	Round Rock	5	Heavy weighted Fresno	Full
11	4 (101.6)	3/8 (9.53)	Round Rock	6	None	Empty
12	4 (101.6)	3/8 (9.53)	Round Rock	5	Heavy rolled from 4.5 in to 4 in	Full
13	6 (152.4)	3/8 (9.53)	Round Rock	6	None	Empty
14	6 (152.4)	3/8 (9.53)	Round Rock	6	None	Full
15	8 (203.2)	3/8 (9.53)	Round Rock	6	None	Empty
16	8 (203.2)	3/8 (9.53)	Round Rock	6	None	Full

The ½-inch heavy roller in the compaction column refers to the fact that a heavy roller was used to compact the pervious concrete ½-inch. Heavy weighted Fresno refers to being compacted by a Fresno float, a hand tool for surface compaction and leveling. Admixtures were also used to increase the workability, hardness and other properties of the concrete panels, but the names and types of the admixtures used were not disclosed by the installation company. Pavement ages listed in Table 3.1 reflect the age in 2009, the year when the survey was performed. The two different ages refer to the fact that initially in 2003 all the sixteen panels were placed, but subsequently the panels numbered 2, 4, 6, 8, 10 and 12 were removed and replaced in 2004. The ten panels remaining from 2003 were usually described as *Phase I construction*, and the six panels replaced in 2004 were usually described as *Phase II construction*. The joints in the pavement were full depth saw cut.

No specific information was given about the thickness of the subbase and characteristics of the subgrade. However, it was reported that the thickness of the subbase in these panels varied from 4 inches to 10 inches, depending on the thickness of the pervious concrete layer. The aggregate size in the subbase layers varied from ¾ inch to 1½ inches and these layers acted as stormwater recharge beds. Above the natural subgrade layer there was also a special subgrade layer of one inch minus rock that more closely resembles layers under traditional concrete pavement. When placed there was also a 12-inch thickened edge extending approximately one foot from the outside perimeter of the pavement. Additional information on the subbase could

not be obtained as the driveway was demolished in 2009. It was from this demolition work that the samples were made available for laboratory analysis by Goede (2009).

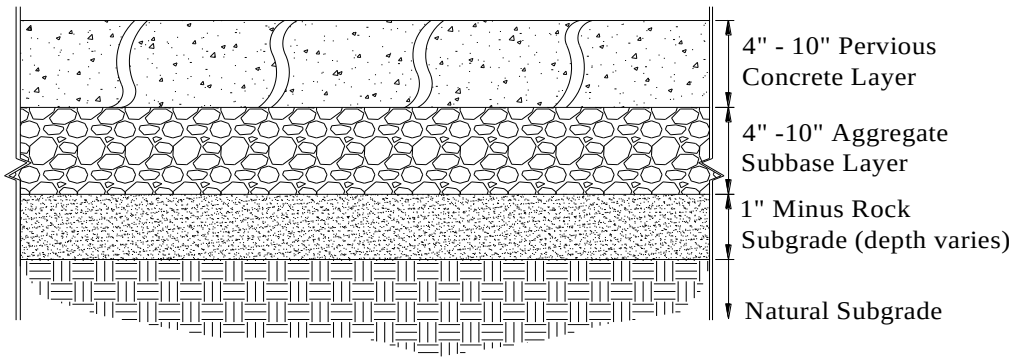

Figure 3.2: Pavement section

3.2.2 *Truck Type and Loading in the Pavement*

The test site in Salem Oregon was a service road into and out of the concrete mixing plant. The entering trucks were typically empty, and the trucks were loaded when exiting the plant. It was estimated based on truck manifests that approximately 40 trucks (Figure 3.3) on average passed through each direction every day. Thus, the Phase I panels experienced 85000 truck loads during the six years and the Phase II panels experienced 70000 truck loads at the time of distress survey. The weights of the trucks were on average 65000 lbs when full, and 30000 lbs when empty. With two booster axles, the trucks used in transporting the concrete had five axles. The booster axles were used when the truck was full and typically raised when the truck was empty.

Figure 3.3: Typical concrete truck type used at both sites (Goede, 2009)

3.2.3 *Material Properties Obtained for Site Extracted Cores*

As previously noted, Goede (2009) performed material characterization tests on the pervious concrete samples extracted from the Oregon site and also on samples prepared in the laboratory. The material characterizations of the laboratory prepared samples aided in developing correlations between the material properties that could not be tested on field extracted samples as discussed in the Section 2.4.3.

The material properties that were investigated are porosity, exfiltration rate, flexural strength, compressive strength, modulus of elasticity, and Poisson's ratio. Material characterization tests were executed following various methods. Flexural strength tests were performed by third point loading test (ASTM C78, 2002). ASTM C39 (2005) was followed for the compression strength tests and ASTM C469 (2002) was used to determine the modulus of elasticity and Poisson's ratio of the sample. As there were no appropriate ASTM standards for the pervious concrete porosity test, the test method developed by Montes et al. (2005) was used to calculate the total porosity for the pervious concrete sample. The material properties obtained from these tests for the field extracted samples are listed in Table 3.2 for the various corresponding panels.

Table 3.2: Material properties for samples extracted from the Evolution Paving Site (Goede, 2009)

Panel No	Depth of Pervious Concrete Layer	Truck Loading Condition	Unit Weight	Flexural Strength	Compressive Strength	Core Porosity
	in (mm)		pcf (kg/m^3)	psi (MPa)	psi (MPa)	%
1	7.5 (191)	No	122 (1952)	297 (2.05)	3520 (24.27)	15
2	10 (254)	Yes	111	--	1780	27
3	10 (254)	No	127	--	5030	13
4	7 (178)	Yes	117 (1872)	284 (1.96)	2940 (20.27)	22
5	8 (203)	No	118 (1888)	329 (2.27)	2900 (19.99)	21
6	5 (127)	Yes	112 (1792)	206 (1.42)	2260 (15.58)	26
7	6 (152)	No	--	--	--	--
8	5 (127)	Yes	113 (1808)	275 (1.90)	2840 (19.58)	24
9	4 (102)	No	--	--	--	--
10	4 (102)	Yes	--	--	--	--
11	4 (102)	No	109	--	2520	32
12	4 (102)	Yes	116	--	2730	23
13	6 (152)	No	120 (1920)	260 (1.79)	2880 (19.86)	22
14	6 (152)	Yes	122 (1952)	--	4200	15
15	8 (203)	No	--	--	--	--
16	8 (203)	Yes	124 (1984)	407 (2.81)	3470 (23.92)	13
Average			118	294	3089	21

3.2.4 Pavement Distress Survey

Goede (2009) also performed distress surveys for the two different pervious concrete placements. Based on manifests of concrete trucks traversing these two placements over periods of from 1.5 to 6 years, it was determined that the placements had been subjected to stresses equivalent to approximately 20 years repetitive loading as *Collector Streets*. The Pavement

Condition Index (PCI) of both of these placements was then determined based on using distress survey results. The distress survey began with evaluating the structural performance of the pavement and relied on a variation of the PCI methodology for standard pavements (ASTM, 2009). PCI is a numerical value that ranges between 0-100. Zero represents the worst condition of the pavement and 100 is the best possible score, indicating that the pavement condition is good. There are numerous versions of the ASTM standard for determining the PCI. The standard used in the original study was ASTM D 6433-07 and the most recent standard for the PCI rating is ASTM D 6433-09. These two standards have no difference (Figure 3.4) in rating the pavement in terms of both numerical value and pavement condition. The colors in Figure 3.4 are suggested by ASTM to represent corresponding pavement condition.

Rating	ASTM D6433 2007	ASTM D6433 2009
100	Good	Good
85	Satisfactory	Satisfactory
70	Fair	Fair
55	Poor	Poor
40	Very Poor	Very Poor
25	Serious	Serious
10	Failed	Failed
0		

Figure 3.4 PCI rating comparison for ASTM D6433-07 and ASTM D6433-09

The PCI rating calculation starts with identifying the type and severity of distress in a pavement slab. The different types of distresses in concrete pavements include blowup, corner break, longitudinal cracks, faulting of transverse joints and cracks, lane/shoulder drop off or heave, pumping, longitudinal joint faulting, edge punch-out, corner spalling, swell, transverse or diagonal cracks, and durability 'D' cracking (Huang, 2004; Miller and Bellinger, 2003). Considering these factors and their severity, PCI values were evaluated for each individual panel (Table 3.3) at the Evolution Paving site.

Table 3.3: PCI values for panels from the Evolution Paving Site (Goede, 2009)

Panel No	Depth of Pervious Concrete Layer in (mm)	Truck Loading Condition	PCI	2007/2009ASTM Rating
1	7.5 (191)	No	48	Poor
2	10 (254)	Yes	87	Good
3	10 (254)	No	89	Good
4	7 (178)	Yes	86	Good
5	8 (203)	No	87	Good
6	5 (127)	Yes	77	Satisfactory
7	6 (152)	No	26	Very Poor
8	5 (127)	Yes	8	Failed
9	4 (102)	No	27	Very Poor
10	4 (102)	Yes	8	Failed
11	4 (102)	No	8	Failed
12	4 (102)	Yes	8	Failed
13	6 (152)	No	8	Failed
14	6 (152)	Yes	8	Failed
15	8 (203)	No	60	Fair
16	8 (203)	Yes	50	Poor

3.3 FE Modeling of the Field Site

The modeling of any structure by the finite element method is a sequence of activities which start with creating the geometry of the structures to be analyzed, followed by determining the analysis type to be used (i.e. static, dynamic), assigning the material property, load, and boundary conditions, and then assigning the meshing patterns of the elements used in the analyses. The application of FE methods for stress and deflection in pervious concrete is new and the modeling analysis for the evaluation of the pervious pavement site followed a uniquely developed vertical porosity distribution technique (Alam et al., 2011a).

3.3.1 *Pavement Configuration*

The pervious concrete pavement drive from the Oregon site consisted of sixteen unique (i.e. thickness, aggregate size, admixture) individual panels as shown in Figure 3.1. In the FE model, only one panel was modeled at a time, taking advantage of their isolation. Each panel had a dimension of 20 ft (6096 mm) in the longitudinal direction and 15 ft (4572 mm) in the transverse direction with 12 inch (300 mm) extension into the subbase layer at the perimeter of the pavement panel. Since the material properties of pervious concrete vary along the depth of the pervious concrete layer, as discussed in Section 2.4.3, this pervious concrete layer was further subdivided into three vertical sections (top quarter, middle half and bottom quarter). In addition, under the concrete was a subbase layer above the soil/subgrade layer (Figure 3.5).

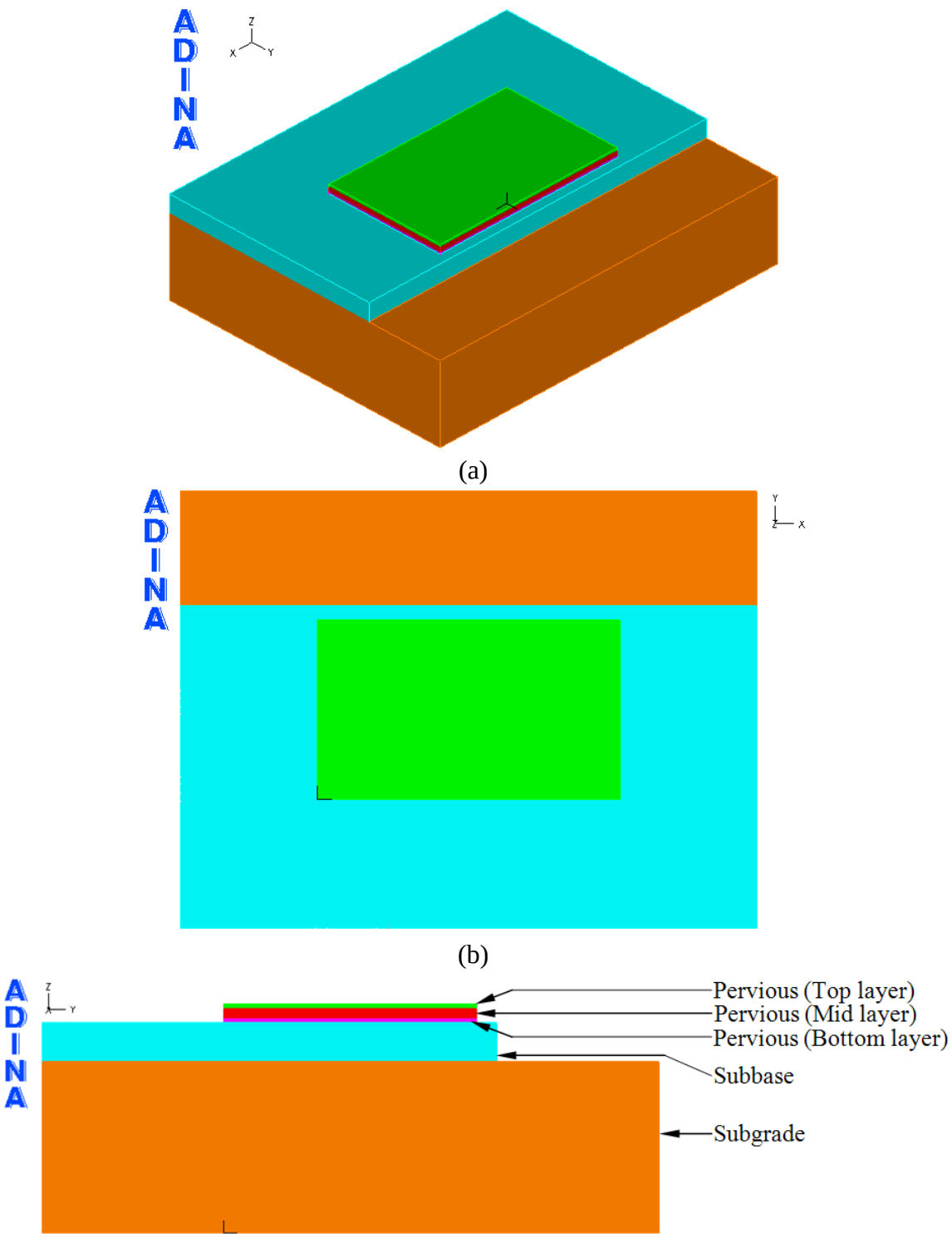

Figure 3.5: Pavement model subdivision by depth used in the ADINA model (a) 3-D view, (b) Plan view of the pavement (x-y plane) and (c) Elevation of the pavement (y-z plane)

To compare with the field panels, four different thicknesses in the pervious concrete layer were used. These are 5-inch (127 mm), 6-inch (152 mm), 7-inch (178 mm) and 8-inch (203 mm). The thickness of the subbase layer was 4 inches (102 mm) and 10 inches (254 mm), representing the minimum and maximum thicknesses of the subbase at the site. The subbase was further extended 12 inches (305 mm) around the outside edge of the pavement to mimic the layout of the field application. The additional 1-inch minus rock layer was not considered in the modeling. The subgrade layer thickness was 108 inches (2743 mm) which represents the infinite boundary of this layer in the lateral direction and vertical direction under the subbase layer. (It was found after many iterative analyses that there were no significant changes in the deflection and stresses of the pavement if the subgrade layer was extended beyond 108 inches (2743 mm)). Note that for a similar two-dimensional FE analysis of pavement the total depth of the pavement system was recommended to be 90 inches (2286 mm) (Cho et al., 1996).

3.3.2 *Mechanical Properties of the Materials used in FE analysis*

The details of how the material properties of the pervious concrete, subbase and subgrade from the Oregon site were determined were discussed in Section 2.4. For the subbase and subgrade moduli of elasticity, the lower values were chosen to be on the conservative side (Table 3.4) in the analysis process. For the pervious concrete layer, the porosity values of the corresponding vertical sections were calculated based on the mean porosity of 21% (field sample) using Equations 2.12, 2.13 and 2.14. For these porosities, the compressive strengths of the pervious concrete depth sections were determined from Equations 2.1 and 2.2. Finally, the moduli of elasticity of pervious concrete for the depth sections were calculated using Equation 2.11, as presented in Table 3.4. The Poisson's ratio for the entire pervious layer was kept constant. The modulus of elasticity of the subgrade that was used was based on medium clay soil. All the materials were considered to be isotropic in each depth section, and thus the moduli of elasticity and Poisson's ratio remained the same in all directions.

Table 3.4: Material properties for FE analysis

Material		Modulus of Elasticity	Poisson's Ratio
		ksi (GPa)	
Pervious Concrete	Top quarter	3858.0	0.22
	Middle half	2385.0	0.22
	Bottom quarter	1405.0	0.22
Subbase		20.0	0.40
Subgrade		5.0	0.40

3.3.3 *Tire Configuration and Pressure*

The concrete trucks used at the Oregon site were tridem axle with the rear one as single axle wheel and the other two are dual axle wheels. The rear single axle wheel was a booster axle and was used outside of the site. Thus, the tire configuration used in the modeling is tandem axle dual wheel. The wheel configurations, along with the tire footprint on the pavement, are shown in Figure 3.6. The dual wheel tandem axle in the middle of the truck held 45,000 lbs (200 KN), exerting a 100 psi (690 KPa) pressure on each wheel when loaded with concrete.

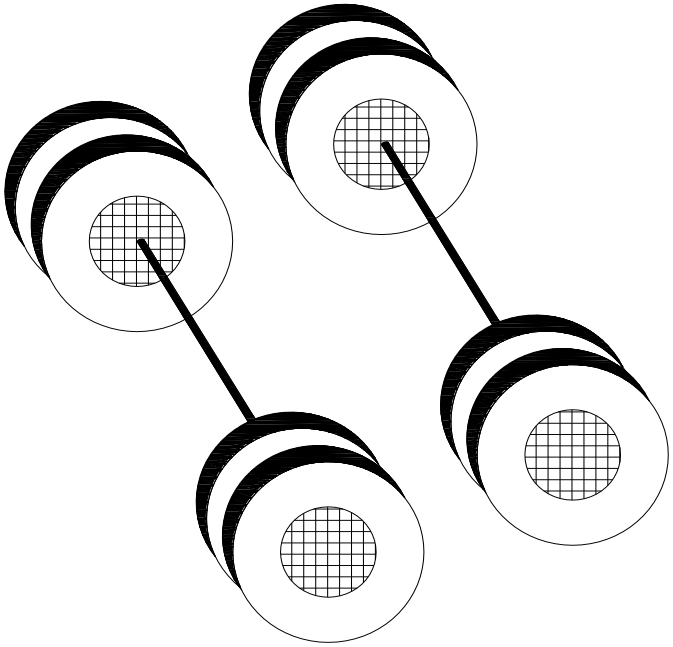

(a)

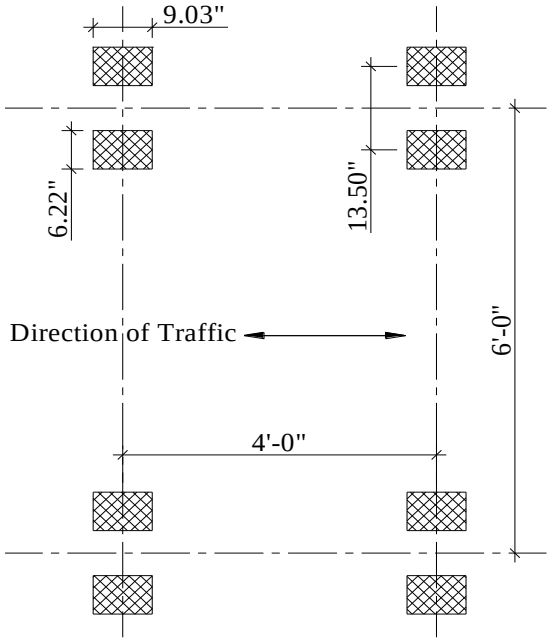

(b)

Figure 3.6: Tandem axle dual wheel: (a) Isometric representation; (b) Tire contact area configuration above the pavement

3.3.4 *Boundary Condition, Symmetry, Meshing, and Element Type*

Proper boundary conditions, identification of symmetry in the structure, appropriate meshing sizes in various portions of the model, and the choice of element type are some of the important parameters that need to be balanced for adequate detailing of the model, while also optimizing computer resource, modeling, and computing time. The bottom of the modeled pavement panel remained fixed, while the sides of the pavement panel represented a symmetric boundary condition. Taking advantages of the line of symmetry, only half of the pavement was modeled

for edge loading (Figure 3.7) and center loading (Figure 3.8) while the full panel was modeled for corner loading (Figure 3.9) since there is no line of symmetry for the wheel location at the corner of the pavement.

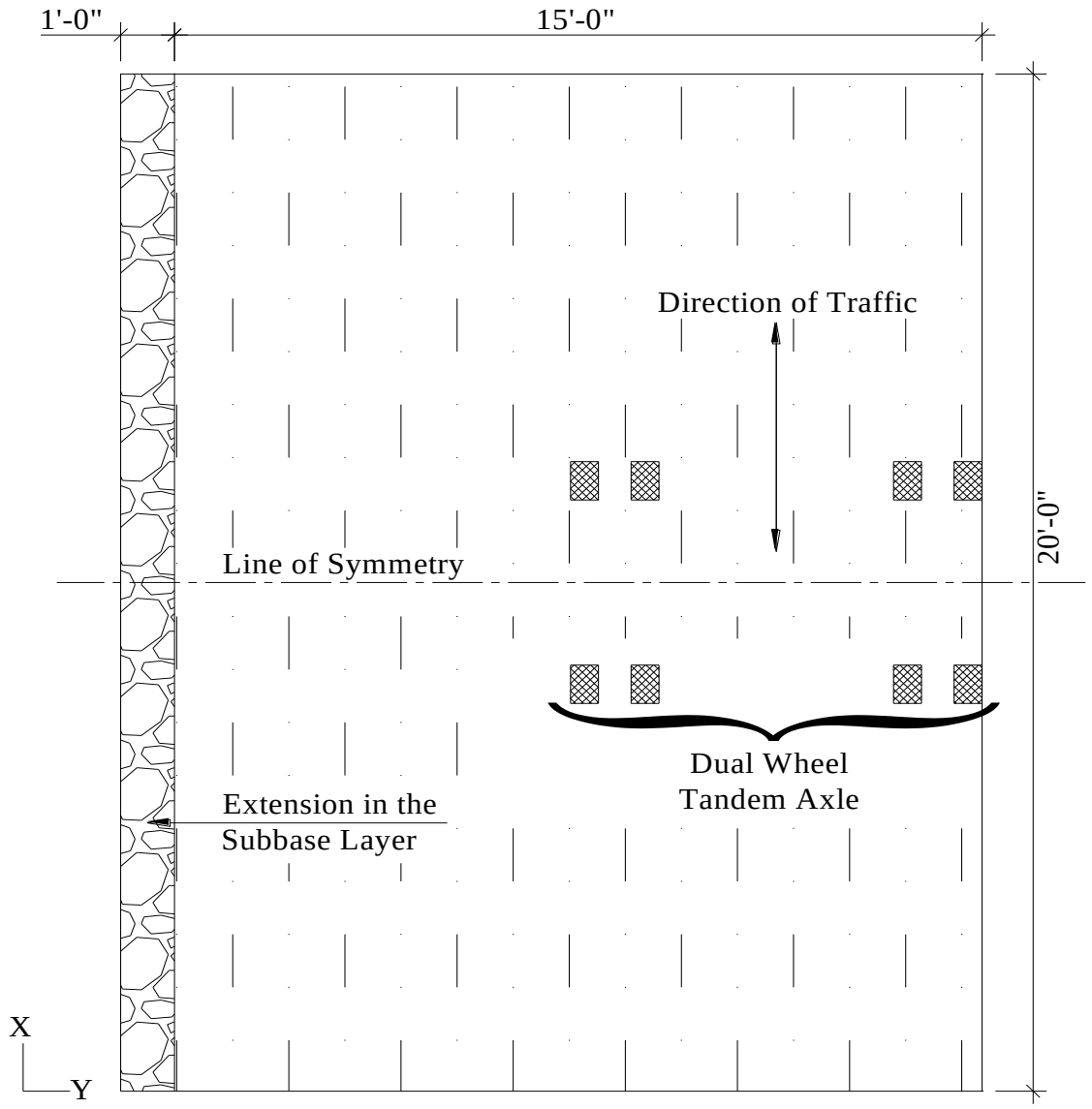

Figure 3.7: Wheel location at edge of the pervious pavement panel with line of symmetry in the y-direction

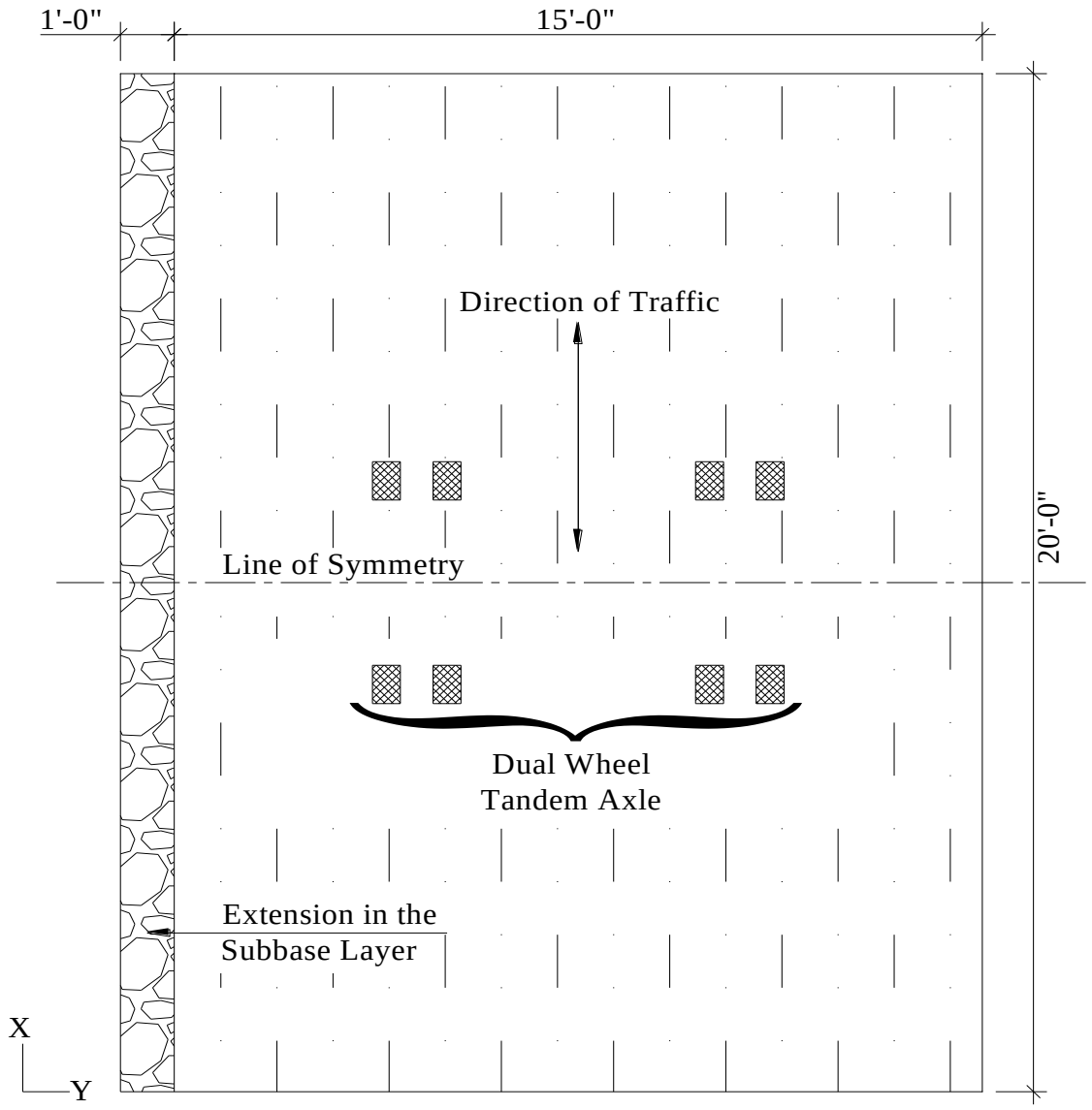

Figure 3.8: Wheel location at center of the pervious pavement panel with line of symmetry in the y-direction

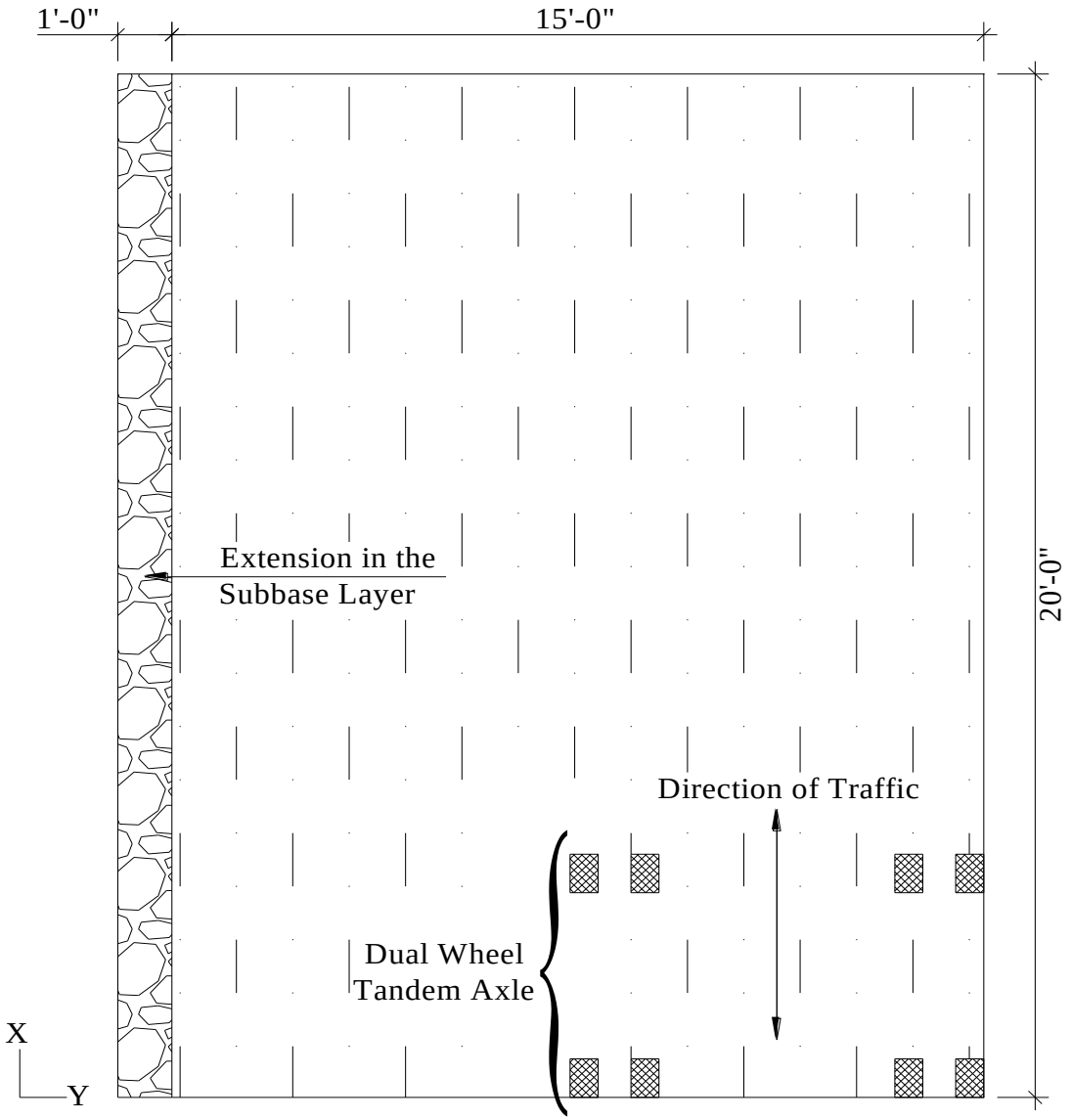

Figure 3.9: Wheel location at corner of the pervious pavement panel with no line of symmetry

In the FE method, the structure should be discretized into many elements, i.e. the mesh dimensions should be small enough to capture the necessary detail for more accurate analysis results for pavement panels. However, finer meshes increase the number of elements, which increases the computational time and memory usage of the computer hardware. A common practice is to use a convergence analysis, starting from a coarse mesh analysis through a finer mesh analysis to determine the maximum number of elements required for adequate analysis results using the least computational time and memory usage. In addition, the meshing pattern should be finer at the point of interest or at the critical locations where detailed analysis is required and coarser meshes may be used where detailed analysis in not necessary. Usually, in FEA, for structures subjected to different patterns of loading, a finer mesh is required around the loading zone, at the interface/joints of the material for better understanding of the load transfer mechanism. The meshing patterns of the pavement for corner, edge and center loading are given

in Appendix A (Figures A.1, A.2 and A.3, respectively). The finest mesh was in and around the tire contact areas while the mesh became coarser with increased distance from the tire contact area. The element type chosen was an 8-node hexahedron, as depicted in Figure 3.10.

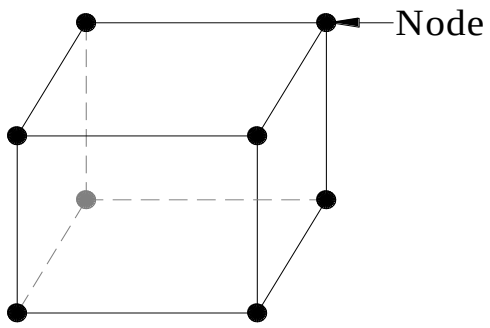

Figure 3.10: 8-node solid element from ADINA

3.4 FE Analysis Results

First, the analyses were performed for all three loading conditions in order to compare the results with the classical analytical theory for traditional concrete pavement (Alam et al., 2011a). In addition, these analyses were used to evaluate the critical loading conditions for deflection and for tensile and compressive stresses in pervious concrete pavement system panels. Typical deflected shape and deflection and tensile, and compressive stress contours obtained from ADINA for the corner, edge, and center loadings are given in Appendix A (Figure A.4-A.15). All of these depicted contours were for 8-inch (203 mm) pervious concrete layers with 10-inch (254 mm) thickness in the subbase layer.

The maximum deflections, tensile stresses, and compressive stresses obtained from these analyses for the three loading conditions are compared in Figures 3.11a, b, and c respectively. The maximum flexural stress was observed for the edge loading condition, and the maximum deflection was observed for corner loading. This validates the assumption that the pervious concrete pavement system follows the same flexural stress and deflection trends as typically observed for traditional concrete pavement systems. In addition, it was found that, in the pervious concrete pavement system, the compressive stress is comparatively higher, reflecting its porous matrix. The critical loading condition for compressive stress was found to be corner loading. From the three loading conditions it can be surmised that the wheel location at the center of the pavement is neither critical for deflection nor for stress (tensile and compressive) measures. Thus, the center loading condition was not considered in any additional analyses. In the additional analyses, deflection and compressive stress were further considered for corner loading, and tensile stress was further considered for edge loading.

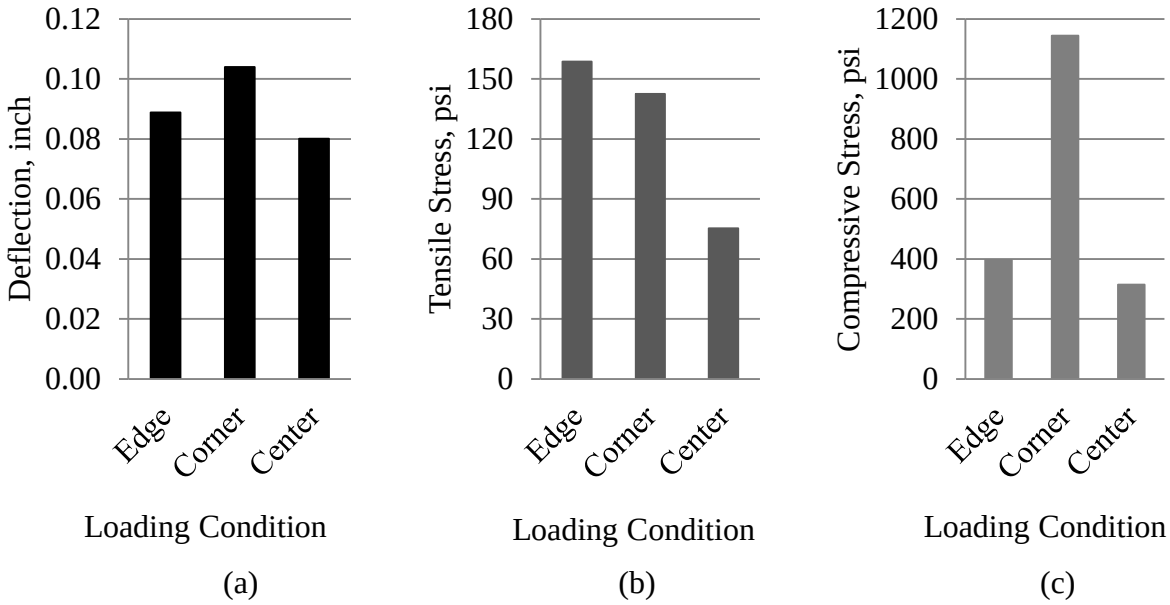

Figure 3.11: Maximum (a) Deflection, (b) Critical Tensile Stress, and (c) Critical Compressive Stress for the three different loading types based on FE Analyses (Alam et al., 2011a and 2011b)

3.4.1 *Comparison with Tensile and Compressive Strength*

The thickness of the pervious concrete layers from the field application varied from 5 inches (127 mm) to 8 inches (203 mm). Thus, FE analyses were performed for every inch interval in the pervious concrete layer within this range (i.e. 5-inch (127 mm), 6-inch (152mm), 7-inch (178 mm), and 8-inch (203 mm)) for both the corner loading and the edge loading conditions. The subbase depths modeled were 4 inches (102 mm) and 10 inches (254 mm) for each thickness modeled in the pervious concrete layer. The critical tensile stress for edge loading and critical deflection and compressive stress for corner loading are listed in Appendix B (Table B.1). Although deflection was not measured for the pervious pavement placement in the field, this parameter is listed for future reference.

The predicted tensile stress from the FE analyses is compared against the measured tensile strength in Figures 3.12a and b for the two subbase depths. Only those stresses which represent loaded trucks on the pavement were plotted. The points below the equity line indicate the likelihood of failure while the points above the equity lines represent satisfactory performance of the pavement. It can be concluded from Figure 3.12 that for both the 4-inch (102 mm) and the 10-inch (254 mm) subbase thickness, the 5-inch (127 mm) depth in the pervious concrete layer falls below the equity line and thus is prone to failure for these static loading conditions.

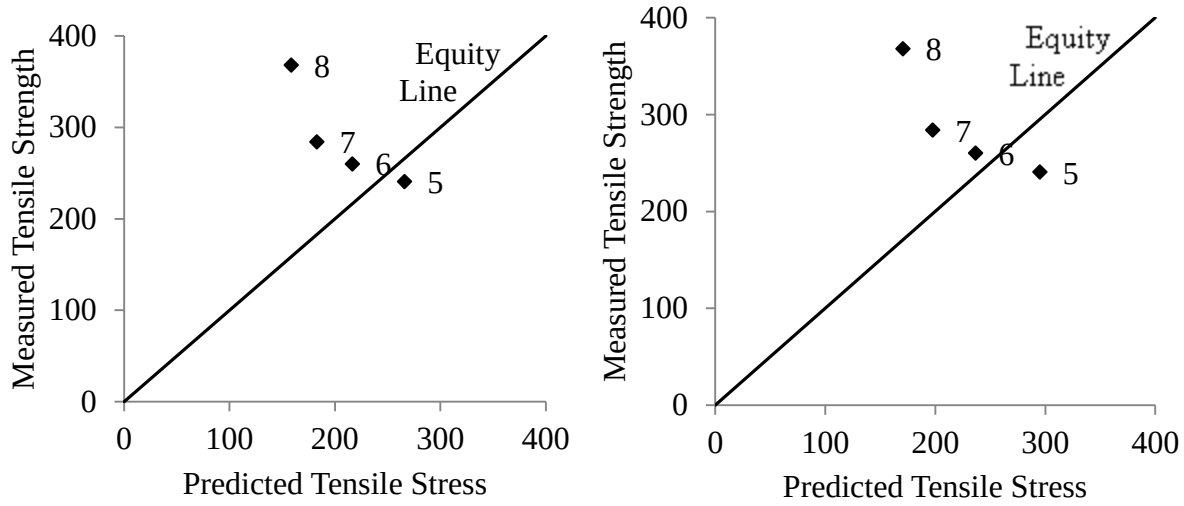

Figure 3.12: Tensile strength and stress comparison for (a) 10 inch (254 mm) subbase depth; (b) 4 inch (102 mm) subbase depth for 8 inch (203 mm), 7 inch (178 mm), 6 inch (152 mm), and 5 inch (127 mm) pavement thicknesses

Predicted flexural stresses from the FE analysis for different subbase thicknesses were compared with the material strength data (Alam et al., 2011b). The pervious pavement thickness was correlated with the intersecting point between the strength curve and the stress curve as can be seen where the thickness curves would cross the equity lines in Figure 3.12. Those points may be designated as the minimum depths required for static loading conditions. As expected, for the 4-inch (102 mm) depth subbase, the required thickness is higher as compared to the thickness required for the 10 inch (254 mm) depth subbase.The minimum depth required for static load is given in Table 3.5. The equivalent static load was for 45-kip (200-kN) tandem axle dual wheel load.

Table 3.5: Minimum required thickness of pervious concrete for static load (Alam et al., 2011b)

Subbase Thickness	Pervious Concrete layer Thickness
inch (mm)	inch (mm)
4 (102)	5.7 (137)
10 (254)	5.4 (145)

Comparisons between the measured compressive strength for the field samples and the predicted compressive stresses from the FE analyses are shown in Figure 3.13. In this case, all the points fall above the equity line which implies no compression failure in the pervious concrete pavement for these static loading conditions. It should be noted that various admixtures were used in the mix designs for these particular pervious concrete panels and the compressive strength of pervious concrete could vary from 500 psi (3.45 MPa) to 4000 psi (27.58MPa) (Onstenk et al., 1993; Tennis et al., 2004; Vassilikou et al., 2011). The predicted compressive stresses found from these analyses ranged between 1145 psi and 1403 psi for a 10-inch (254 mm) depth subbase, and between 1245 psi and 1619 psi for a 4-inch (102 mm) depth subbase, which indicates there is some possibility of failure due to compression in a pervious concrete pavement

if mix designs with the lower strengths are used. Although using highly porous pervious concrete with low compressive strength is not likely, if it is, compressive strength will need to be considered as an additional design parameter in the structural design of pervious concrete pavement. Note that, compressive strength is not a design parameter for the design of traditional concrete pavement.

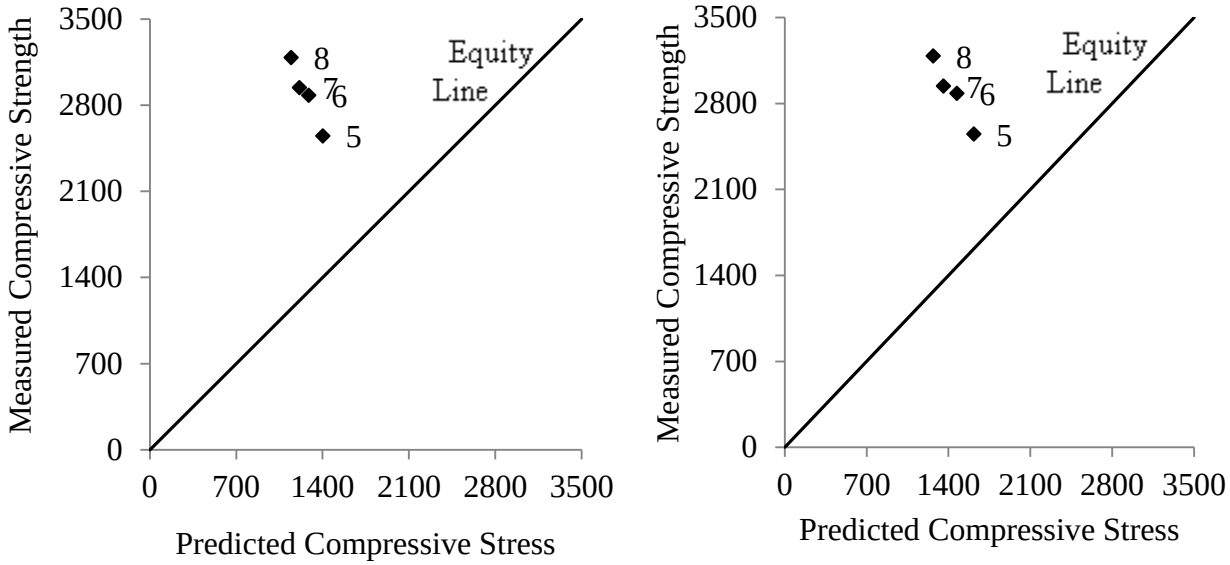

Figure 3.13: Compressive strength and stress comparison for (a) 10 inch (254 mm) subbase depth; (b) 4 inch (102 mm) subbase depth for 8 inch (203 mm), 7 inch (178 mm), 6 inch (152 mm), and 5 inch (127 mm) pavement thicknesses

3.4.2 Comparison with PCI Rating

The design of concrete pavement depends on long term performance of the pavement, which is determined from the allowable number of load repetitions. The allowable number of load repititions is then compared with the annual average daily truck traffic (AADT) to calculate the predicted years of service for the particular pavement sytem. For traditional concrete pavements, there are emipirical methods to calculate the allowable number of load repetitions over the pavement. The method usually involves determing the stress ratio factor, which is a function of the modulus of rupture and the predicted tensile stress for the pavement material. This factor is later used to determine the allowable number of load repetitions for a particular load application (i.e. single axle, tandem axle) on the pavement using standard empirical charts (Huang, 2004).

These empirical equations to determine the number of load repetitions, and eventually to determine the years of service for the pavement system, have not yet been developed for pervious concrete. However, a PCI rating may reflect the pavement performance for the number of years of use at the evaluation time. Thus, the PCI rating could be regarded as a preliminary long term performance rating tool. PCI ratings determined for the field application (Table 3.3) considered in this study were after six years of service under frequent loading by trucks, which was related by Goede (2009) to the service life of a collector street. During this time span, the pervious pavement had seen 40 fully loaded concrete trucks running over it each day, which is equivalent to 62,640 cycles of a fully loaded truck loading considering 261 service days in each year. The concrete truck traversing the pavement had a 45 kip wheel load, which makes the loading equivalent to 2.1 equivalent single axle loads (ESAL) (Goede and Haselbach, 2011). The

ESAL is the standard axle load and represents an 18-kip (80-kN) single axle load. Thus the pervious pavement at the Oregon site had 132,000 cycles of 18-kip (80-kN) ESAL repetitions.

The PCI ratings reported in Goede (2009) were further correlated with the pavement thicknesses (Alam et al. 2011b). The pervious concrete pavement thickness corresponding to the lowest PCI rating value on Table 3.3 may reflect the mimimum thickness required to resist cyclic or repetitive load applications. Only the lowest observed rating point was considered so that the design thickness becomes more conservative. As shown in Figure 3.4, according to the ASTM standard (2009), any PCI rating below 55 is described as a poor pavement performance. For a pavement performance to be defined as fair, satisfactory, and good, the required PCI rating is 55-70, 70-85 and 85-100, respectively. The lowest PCI rating experienced for each thickness is given in Table 3.6 and compared to acceptable ranges of PCI ratings for pavements. Associated thicknesses for these PCI ranges were then linearly interpolated from the actual values and are also listed in Table 3.6. These interpolated values may represent the minimum required depths in the pervious concrete layers for fair, satisfactory, and good performance pavements.

Table 3.6: Lowest PCI values for various loaded panel thicknesses from the field application and comparisons to interpolated design values for cyclic loading (Goede, 2009; Alam et al., 2011b)

Actual Depth of Pervious Concrete Layer	Interpolated Thickness for Desired PCI Rating	Lowest PCI Values in Field	Ranges of Acceptable PCI Ratings
in (mm)	in (mm)		
4 (102)		8	
5 (127)		8	
6 (152)		8	
8 (203)		50	
	8.3 (211)		55 (fair)
	9.1 (231)		70 (satisfactory)
	9.9 (251)		85 (good)
10 (254)		87	

The percentage increase in the thickness for cyclic loading compared to the thickness required for static loading is 46%, 60%, and 74% for fair, satisfactory, and good performance pavement, respectively for the 4-inch (102 mm) depth subbase. Therefore, also considering the complexity and variability of pervious concrete, it is concluded that a factor of safety equivalent of two (2) be recommended when calculating the design thickness of the pervious concrete layer based on static stress analyses, as a conservative approach for design.

Chapter 4

Generalized Finite Element Model for Pervious Pavement

4.1 Introduction

The pervious concrete pavement analysis in Chapter 3 was to evaluate the field application in Oregon. The pavement dimensions and material properties considered were representative of this field site. In this chapter, the FE model has been extended for generalized cases with a variety of thicknesses in both the pervious concrete and the subbase layer. Typical loads, i.e. 18-kip (80-kN) and 36-kip (180-kN) forces, from single axle dual wheel and tandem axle dual wheel load, respectively, were used.

4.2 Pavement Configuration

The panel dimensions in the longitudinal and transverse direction of the pavement remain the same as in the previous field analysis (15 ft (4.5 m) and 20 ft (6.0 m)), but along the vertical direction, the depth of the pervious layer and the subbase layer have been modified to represent a range of typical designs. It was found in the previous field analysis that, for cyclic loading, the minimum required depth for fair, satisfactory, and good performance pavement was 8.3 inch (211 mm), 9.1 inch (231 mm), and 9.9 inch (251 mm), respectively (Alam et al. 2011b). In the generalized model, the thickness values of the pervious concrete layer that were considered were 8 inches (203 mm), 10 inches (254 mm), and 12 inches (305 mm), which are typical roadway pavement thicknesses. Since the intended use of the subbase layer in the pervious concrete pavement is to serve as a detention pond, comparatively higher thicknesses were considered in the subbase layer and these were 12 inches (305 inch) and 24 inches (610 mm).

4.3 Material Properties, Loading, and Meshing

The mechanical properties of pervious concrete largely depend on the porosity of the mixture. Usually, the average porosity of pervious concrete varies from 15%-25% (ACI). The porosity considered earlier was 21% for the field sample. To represent the worst possible material property with respect to strength, the porosity considered for the generalized model was 25%. For this 25% average porosity, the modulus of elasticity of pervious concrete in the top quarter, middle half, and bottom quarter are listed in Table 4.1 (based on Equations 2.1, 2.2, 2.11, 2.12, 2.13, and 2.14). The unit weight considered was 118 pcf (1890 kg/m^3). The modulus of elasticity for the subgrade and the subbase were the same as considered for the field application modeling.

Table 4.1: Material properties for generalized FE analysis

Material		Porosity	Modulus of Elasticity	Poisson's Ratio
		%	ksi (GPa)	
Pervious Concrete	Top quarter	19.75	2667.0 (18.4)	0.22
	Middle half	25.00	1638.0 (11.3)	0.22
	Bottom quarter	30.25	939.4 (6.5)	0.22
Subbase		--	20.0 (0.14)	0.40
Subgrade		--	5.0 (0.034)	0.40

The loading considered was an 18-kip (80-kN) single axle dual wheel load and a 36-kip (160-kN) tandem axle dual wheel load. The single axle load and tire contact area configuration are shown in Figure 4.1. Both of the loading types have the same tire contact pressure that is equivalent to 80 psi (MPa).

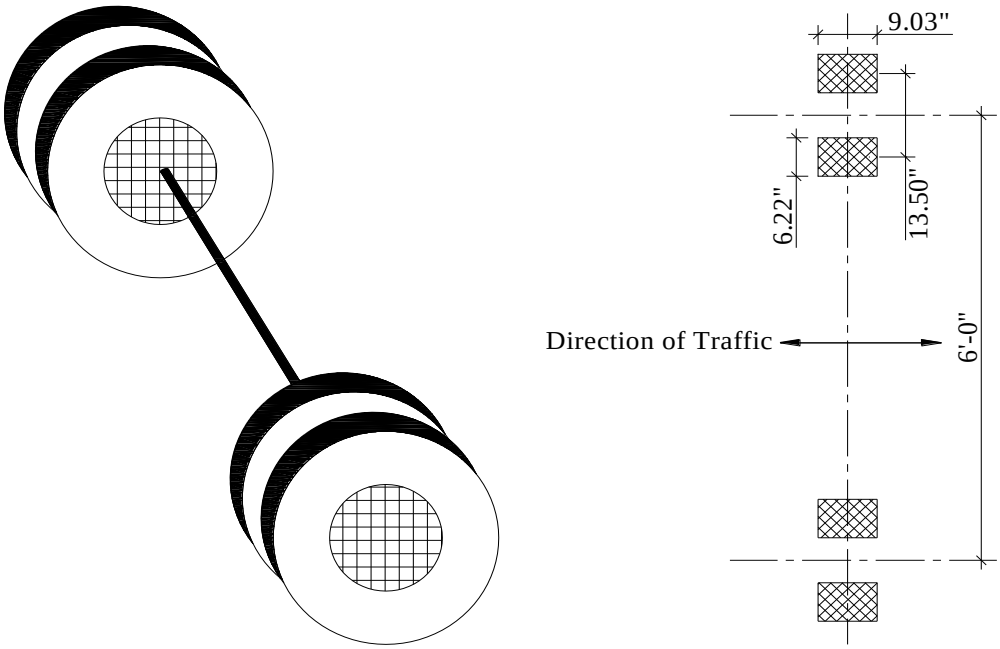

(a) (b)

Figure 4.1: Single axle load (a) Dual wheel tire; (b) Tire contact area (Alam et al., 2011a)

The modeling of the pervious concete pavement was accomplished by applying the vertical porosity distribution in pervious concrete technique developed by Alam et al. (2011a). Element type and meshing pattern were similar to those of the previous analysis, with finer meshes around the tire contact area and coarser meshes away from the truck. The meshing pattern for the tandem axle dual wheel load is shown in Appendix A. The meshing pattern for the single axle dual wheel load is given in Appendix C (Figure C.1 to C.2) for the corner loading and edge loading. Wheel locations at the center of the pavement were not considered as it was determined that center loading is not critical for any of the stress and deflection measures in the field validation of pervious pavement.

4.4 FE Analysis Results and Comparison

FE analysis was performed for three different thicknesses in the pervious concrete layer, for the two different load conditions, and for each of the critical wheel positions for deflection and compressive stress (corner loading) and for tensile stress (edge loading). Representative plots of the deflected shape, displacement (z-direction), and tensile and compressive stress contours for the 18-kip (80-kN) single axle dual wheel load are given in Appendix C (Figure C.3 to C.10). Figures C.3 to C.10 represent pavement configurations of 8 inches (203 mm) in the pervious concrete layer and 12 inches (307 mm) in the subbase layer. The critical deflection and compressive stresses for corner loading and critical tensile stresses for edge loading are listed in Appendix D (Table D.1 and D.2). It should be mentioned that the selfweight of the pavement system was considered in all these analyses.

The overall comparative summary results from the 24 sets of analyses are presented in the following sections. A summary of the conditions evaluated are tabulated in Table 4.2.

Table 4.2: Summary of the pavement configurations used for the generalized model

Model No	Pervious Concrete Thickness	Subbase Thickness	Loading	Wheel Position
	inch (mm)	inch (mm)	kip (kN)	
1	8 (203)	12 (305)	18 (80)	Corner
2				Edge
3			36 (160)	Corner
4				Edge
5		24 (610)	18 (80)	Corner
6				Edge
7			36 (160)	Corner
8				Edge
9	10 (254)	12 (305)	18 (80)	Corner
10				Edge
11			36 (160)	Corner
12				Edge
13		24 (610)	18 (80)	Corner
14				Edge
15			36 (160)	Corner
16				Edge
17	12 (305)	12 (305)	18 (80)	Corner
18				Edge
19			36 (160)	Corner
20				Edge
21		24 (610)	18 (80)	Corner
22				Edge
23			36 (160)	Corner
24				Edge

4.4.1 Critical Displacment Analysis (Corner Loading)

Figures 4.2 and 4.3 present the total pavement system displacement for the three pervious concrete layer thicknesses and two subbase layer thicknesses for the 36-kip (160-kN) and 18-kip (80-kN) loading scenarios, respectively. These displacements include the self weight of the system. The higher loading scenario of 36-kip (160-kN) has a high overall displacement for the same system configuration. In general, increasing the subbase thickness will increase the stiffness of the system and thus will reduce the dispacement in the system. (This fact was previously established for the FE modeling based on the field application.) In contrast, from Figures 4.2 and 4.3, it can be seen that, with the increase of subbase thickness, the pavement displacement increases. This is a result of the inclusion of self weight of the pavement system in the FE analysis (Alam et al., 2011a). The higher subbase thicknesses produce additional loads in the pavement system and have varying impacts on the overall displacement of the pavement system. While analyzing for 36-kip (160-kN) tandem axle load, increasing the pervious concrete layer thickness from 8 inches (203 mm) to 10 inches (254 mm) seems to improve the displacement due to the additional material stiffness impacts, but as this thickness increases to 12 inches (305 mm), the additional selfweight apparently has the opposite effect.

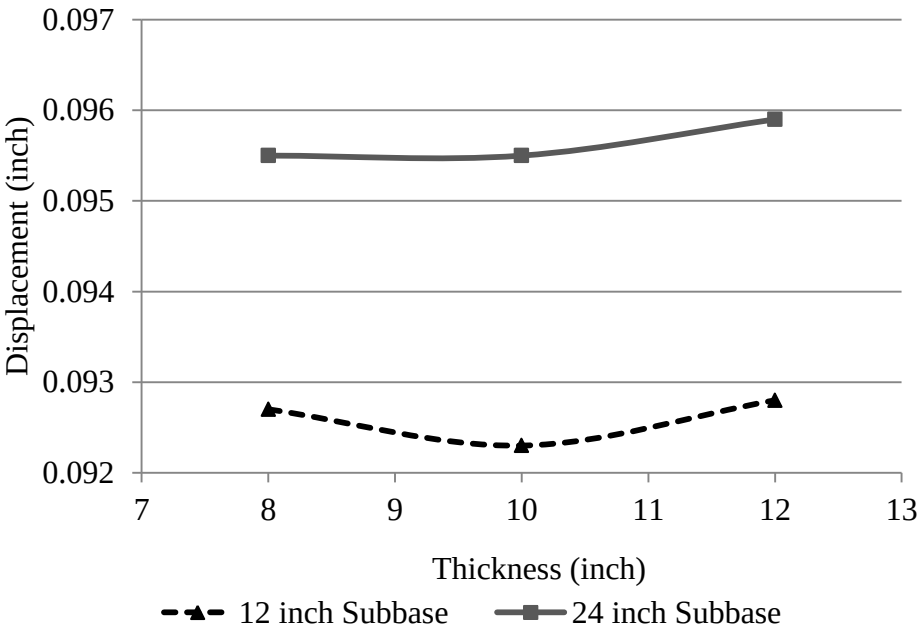

Figure 4.2: Displacement in the pavement sytem for 36-kip (160-kN) tandem axle dual wheel load for different pervious concrete and subbase thicknesses

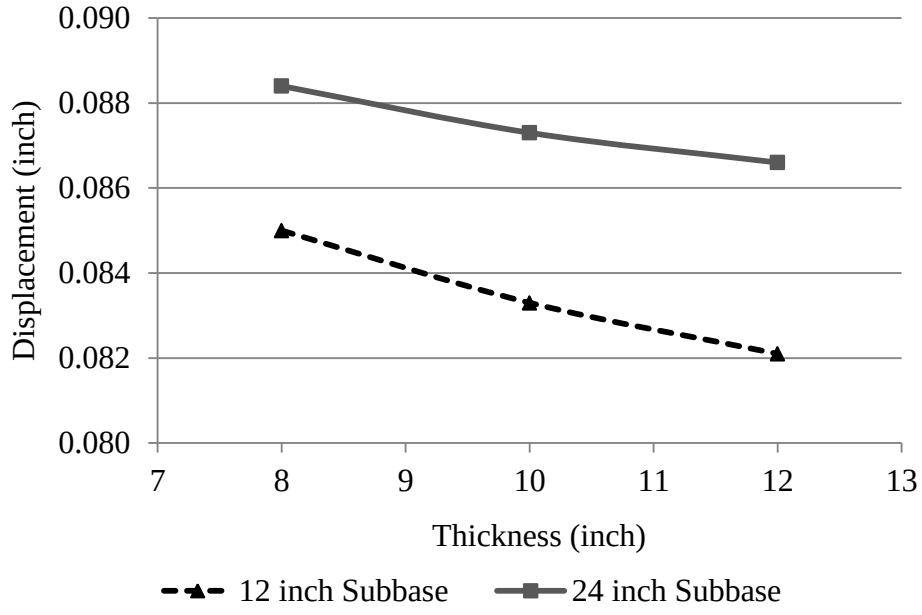

Figure 4.3: Displacement in the pavement sytem for 18-kip (80-kN) single axle dual wheel load for different pervious concrete and subbase thicknesses

4.4.2 Comparison of Flexural Strength to Static Loading Stress and Estimated Cyclic Loading Stress

The tensile stresses a for 36-kip (160-kN) dual wheel tandem axle and a 18-kip (80-kN) single axle dual wheel tire are shown in Figures 4.4 and 4.5. The critical wheel location was at the edge

of the pavement. The tensile stress decreases with the increase in the thickness of the pervious concrete layer and also with the increase in the subbase thickness due to increased stiffeness of the pavement system. The tensile stress for the 18-kip (80-kN) single axle load is higher compared to the tensile stress for the 36-kip (160-kN) tandem axle load. While, for the 18-kip (80-kN) single axle load, the maximum stress occurs right below the wheel location, the maximum tensile stress for the 36-kip (160-kN) tandem axle load occurs away from the wheel location (Figure 4.6). Thus, the intensity of the tire pressure is lower for the 36-kip (160-kN) tandem axle load, resulting in lower tensile stresses. The contour plots in Figure 4.6 are for the 12-inch (305 mm) pervious concrete and 24-inch (610 mm) subbase thickness combination in the pavement system. To compare with the modulus of rupture of pervious concrete, the limiting line was plotted in the tensile stress plot. The tensile stresses were also plotted with a factor of safety (FOS) of 2 to represent the stress requirements for cyclic loading. It shows that even with a FOS of 2, the tensile stresses in the previous concrete are much lower than the average modulus of rupture of the pervious concrete.

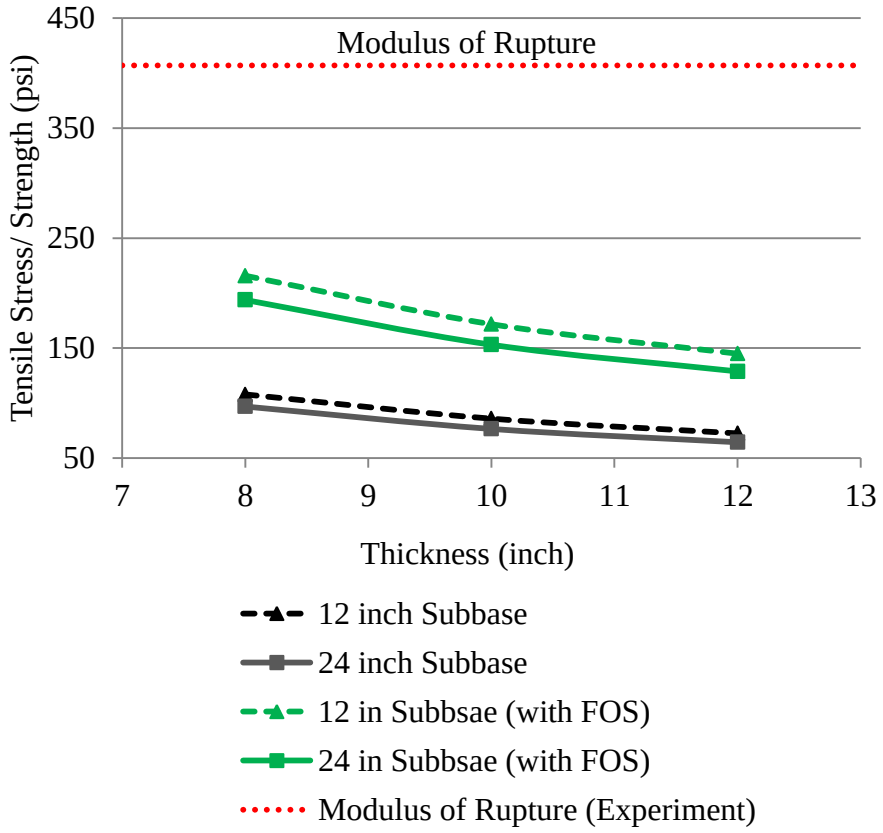

Figure 4.4: Flexural stress/strength comparision 36-kip (160-kN) tandem axle dual wheel load

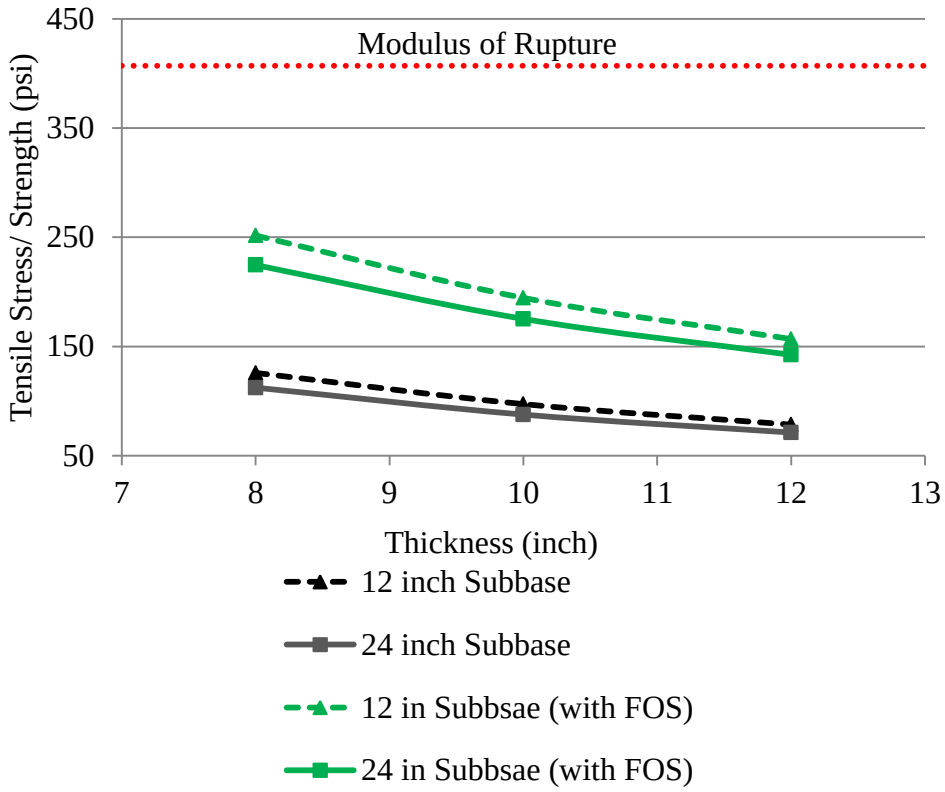

Figure 4.5: Flexural stress/strength comparision 18-kip (80-kN) single axle dual wheel load

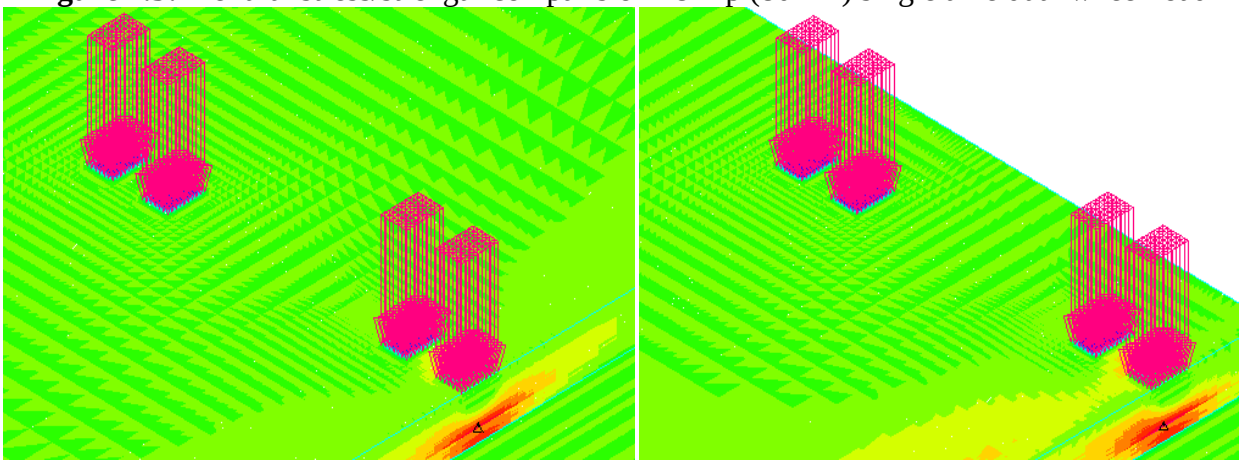

(a) (b)

Figure 4.6: Snapshots of tensile stress contours for a) 18-kip (80-kN) single axle dual wheel load; b) 36-kip (160-kN) tandem axle dual wheel load

4.4.3 Comparison of Compressive Stress

The compressive stresses in the pavement system for the wheel position at the corner of the pavement for different thickness values were plotted (Figures 4.7 and 4.8) for the 36-kip (160-kN) dual wheel tandem axle and 16-kip (80-kN) single axle dual wheel loads. The compressive stress decreases with the increase in thickness of the pervious concrete layer as well as with the

increase in the subbase thickness. In contrast to the tensile strees, the compressive stress is higher for the 36-kip (160-kN) tandem axle load as compared to the compressive stress for the 18-kip (80-kN) single axle load. The higher compressive stress for 36-kip (160-kN) tandem axle load is attributed to the confinement of four wheels at the corner of the pavement compared to two wheels in the pavement system for the 18-kip (80-kN) tandem axle load. The comparison with the compressive strength of pervious concrete from the previous material characterization experiments shows that the stress in the pavement system for both of the loading conditions is not very significant fot this particular field application. (Note that the field application has undisclosed aggregate additives. Most applications do have admixtures included, however.)

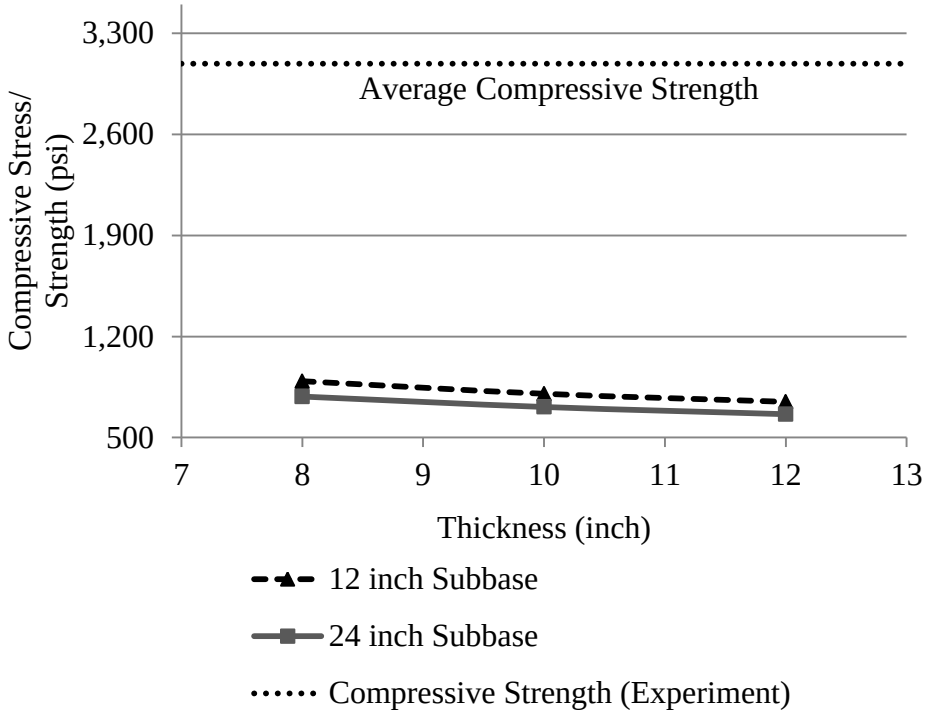

Figure 4.7: Compressive stress/strength comparison for 36-kip (160-kN) tandem axle dual wheel load

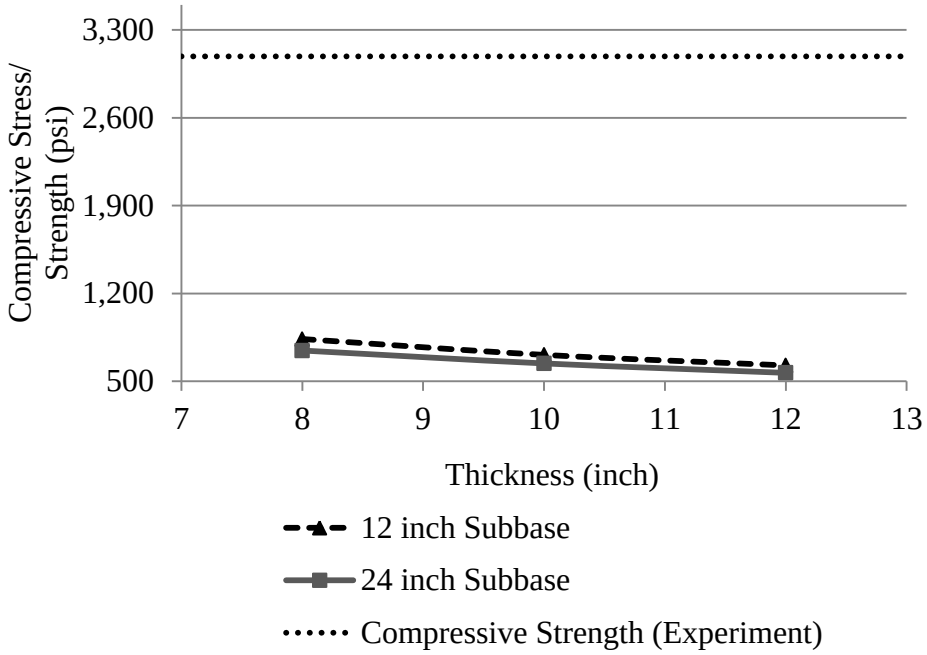

Figure 4.8: Compressive stress/strength comparison for 18-kip (80-kN) single axle dual wheel load

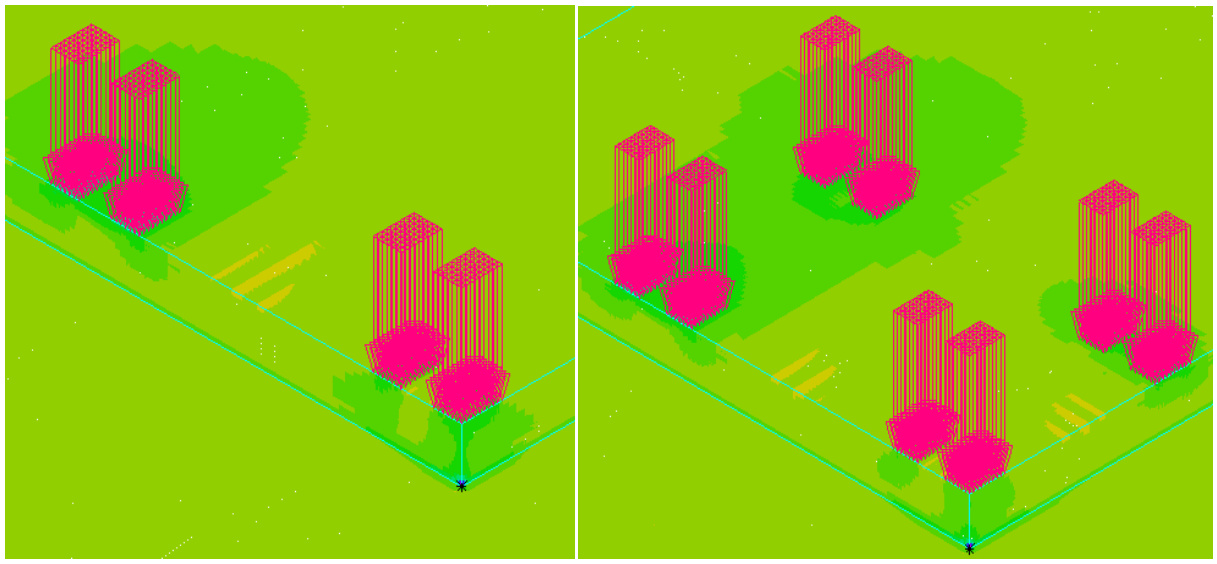

(a) (b)

Figure 4.9: Snapshots of compressive stress contours for a) 18-kip (80-kN) single axle dual wheel load and b) 36-kip (160-kN) tandem axle dual wheel load

4.5 Summary

Based on the analyses for these 24 pavement combinations and also based on the comparison with experimental strength results, it can be concluded that pervious concrete is a viable pavement for roadway shoulders. The performance of pervious concrete was also previously shown to be promising under cyclic loading.

Chapter 5

Dowel Bar and Shoulder Usage in Pervious Pavement

5.1 Introduction

In the previous chapters, pervious concrete pavement systems were analyzed for different load combinations and pavement configurations. Since only one panel in the pavement was modeled, with no transverse joints, it was not required to model the cases with the inclusion of dowel bars between a shoulder and a mainline section, although an extension of 12 inch (300 mm) in the subbase layer at the outward edge of the pavement was considered. In this chapter, considerations for the possible inclusion of dowel bars between pavement slabs are discussed.

5.2 Dowel Bars

Dowel bars are used in the transverse joints of many pavements to transfer load to the adjacent slab (Huang, 2004). The other purpose of using dowels is to minimize faulting and pumping in the pavement (PCA, 1984). However, there have been no reported applications of dowel bars in pervious concrete pavement. (ACPA, 2011). In order to further confirm that the use of dowel bars in pervious concrete might not be applicable, and therefore not worthy of detailed finite element analyses, a pervious concrete sidewalk was also investigated to determine the relative vertical movement and grade change with respect to a traditional concrete pavement.

5.2.1 Pervious Concrete Sidewalk

A pervious concrete sidewalk installed in October of 2010 on the east side of the Valley Playfields at Washington State University was investigated to evaluate its performance at subfreezing temperatures and also its structural performance. This was done in comparison with a neighboring traditional portland cement concrete sidewalk. The test site is shown in Figure 5.1(a). On one side of this sidewalk there is a playfield with artificial turf and on the other side there is soil and then a pond at least 50 ft (15.24 m) away from the sidewalk. The width of the sidewalk is 14 ft (4.27 m) for most of the length (See Figure 5.1(b)) and the approximate length of the pervious concrete portion of the sidewalk is 308 ft (93.88 m). In the longitudinal direction the pervious concrete sidewalk is divided along the middle with a sawcut and in the transverse direction the pervious concrete sidewalk is divided into forty sections. While the width of each panel is 7 ft (2.13 m), the lengths of the pervious concrete sections along the longitudinal direction vary from 2 ft (0.61 m) to a maximum of 8 ft (2.44 m). Figure 5.1(b) shows the panel numbering in the pervious concrete sidewalk for observation references.

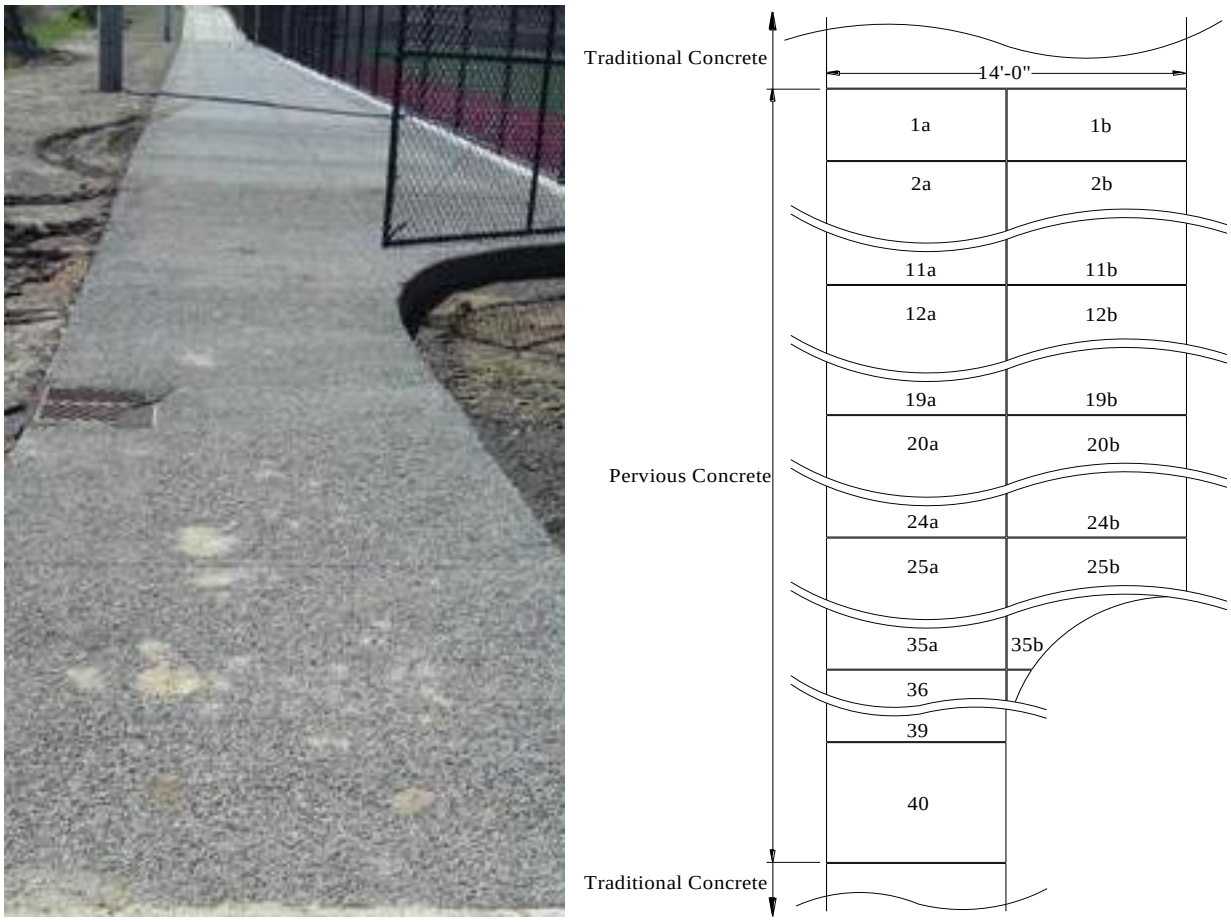

(a) (b)

Figure 5.1: (a) Sidewalk installed at WSU Valley Playfields (eastside); (b) Panel numbering for this pervious concrete sidewalk

The forty sections in the longitudinal direction of the pervious concrete sidewalk portion were designated as forty panels. Each one had a Part a (west part) and some had a Part b (east part) in the transverse direction. The numbering of these panels is shown in Figure 5.1a.

5.2.2 Relative Grade Change in Pervious and Traditional Concrete

Measurements were taken almost every week during this research period to determine the vertical movement of the pervious concrete and traditional concrete at their interface. The objective of this study is to compare the grade change in pervious concrete with that of traditional concrete and to correlate it to temperature. Measurements were taken using a SmartLevel at the interface of these two materials for seven observation points, each 2 ft (0.61 m) apart along the transverse direction of the sidewalk as shown in Figure 5.2.

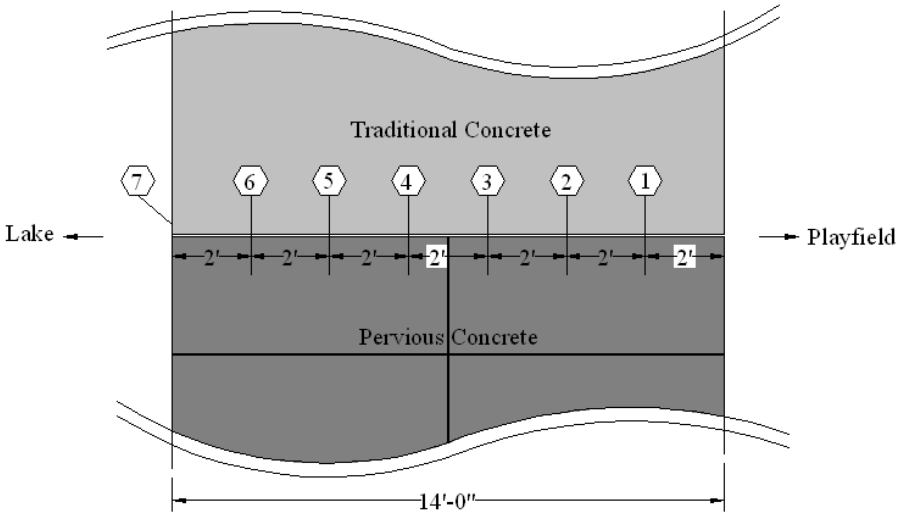

Figure 5.2: Observation point location for measuring the grade change in pervious concrete and traditional concrete

The summary of these data obtained is given in Table 5.1. Because of the presence of snow on the sidewalk on several days, no measurements were taken at several observation points. The weather condition given in Table 5.1 is to provide information on how the temperature in the pavement might vary with the air temperature depending on weather conditions of that particular day. When the air temperature is lower, the pavement temperature does not vary appreciably, but when the air temperature is higher, the pavement temperature increases more rapidly.

Table 5.1: Average grade change in traditional and pervious concrete

Date	Pavement Temperature	Air Temperature	Weather Condition	Average Grade Change	
				Traditional Concrete	Pervious Concrete
	° F	° F		Deg	Deg
2/15/2011	39.4	35.1	Light Rain	0.76	1.23
2/25/2011	8.6	8.6	Mostly Cloudy	0.43	1.43
3/3/2011	39.6	39.0	Partly Cloudy	0.54	1.18
3/11/2011	49.9	37.9	Sunny	0.87	1.08
3/23/2011	59.0	51.1	Sunny/ Partly Cloudy	0.88	0.95
3/31/2011	63.1	55.0	Cloudy	0.88	1.37
4/8/2011	70.3	50.0	Sunny	0.82	1.45
4/21/2011	62.4	46.0	Cloudy/ Light Rain	0.70	1.32

The average grade change in the traditional concrete and pervious concrete for the corresponding pavement temperature is plotted in Figure 5.3. While it is very difficult to comment on the relationship of the grade change of both the traditional concrete and the pervious concrete sidewalk with respect to temperature, it can be surmised that the total variations are similar with temperature in both systems and the effect is negligible.

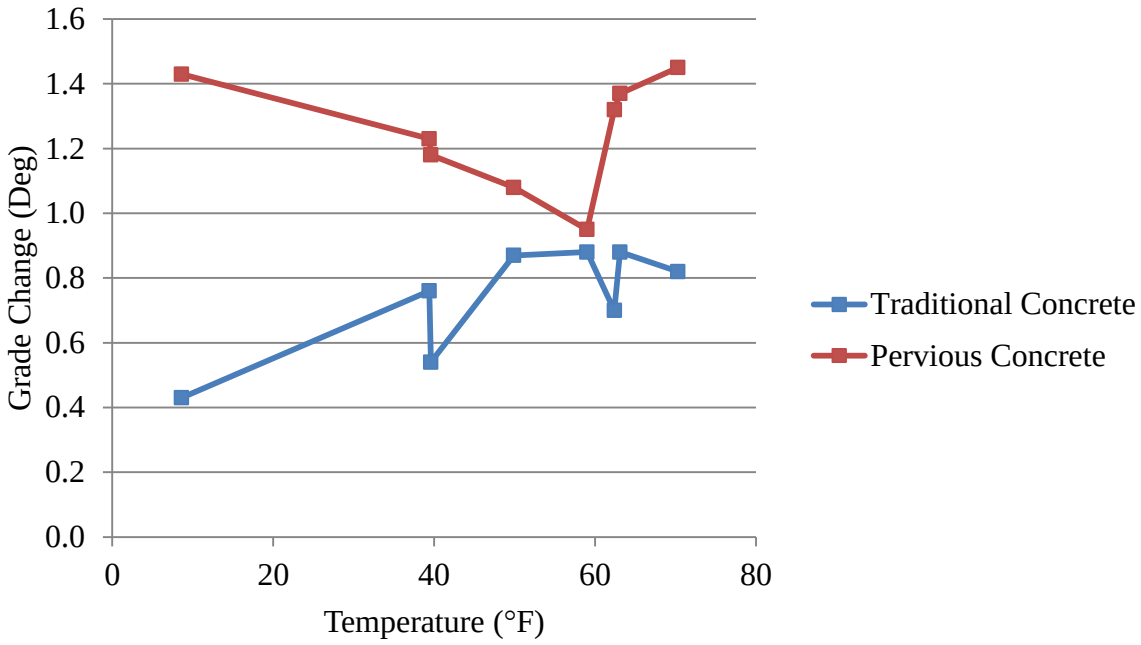

Figure 5.3: Vertical movement of traditional and pervious concrete for corresponding temperature

5.2.3 Vertical Height Difference

Abutting the pervious concrete, a curb runs the entire length along the field side of the sidewalk, as shown in Figure 5.4(a) where vertical deflection has been measured between the two. Weekly measurements were taken at both the end and the middle of the panel, as shown in Figure 5.4(b). Out of seventy panels (counting each one on each side of the longitudinal cut), four panels were selected to investigate the vertical movement. Two of them were selected randomly i.e. Panel 2b and Panel 25b. The selection of Panel 12b and Panel 20b was due to the fact that both of these panels had transverse cracks running across the width of the sidewalk.

(a)

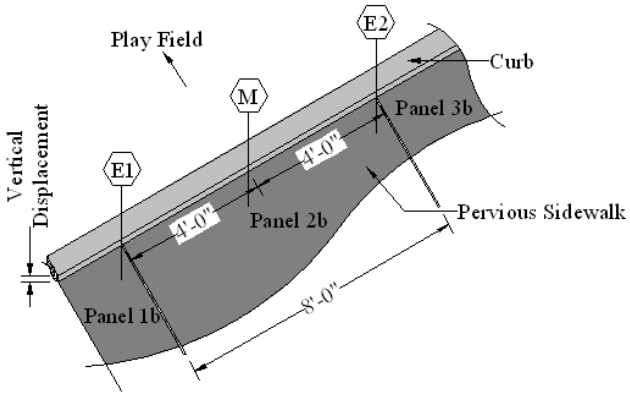

(b)

Figure 5.4: (a) Curb running between the sidewalk and playfield; (b) Location of observation points for vertical deflection measurements

The average vertical height difference calculated for each observation point is listed in Table 5.2. (Note from Tables 5.1 and 5.2 that on several days there could be variations in pavement temperature since data for grade change and vertical displacement were recorded within a time interval of 15 minutes to 25 minutes.)

Table 5.2: Vertical height difference between the pervious concrete sidewalk and curb

Date	Pavement Temperature	Air Temperature	Average Vertical Height Difference			
			Panel 2b	Panel 12b	Panel 20b	Panel 25b
	° F	° F	inch	inch	inch	inch
2/15/2011	39.4	35.1	1.563	1.458	1.438	1.188
2/25/2011	8.6	8.6	1.563	1.396	1.333	1.146
3/3/2011	39.6	39.0	1.625	1.563	1.458	1.375
3/11/2011	49.8	37.9	1.542	1.479	1.313	1.208
3/23/2011	59.0	51.1	1.542	1.479	1.458	1.208
3/31/2011	59.0	55.0	1.521	1.542	1.458	1.229
4/8/2011	71.0	50.0	1.604	1.500	1.396	1.229
4/21/2011	62.4	46.0	1.563	1.604	1.479	1.292

The average vertical height difference between the pervious concrete sidewalk and the curb for each panel that was under investigation was plotted against the pavement temperature and the plot is shown in Figure 5.5. All of these panels have varying vertical displacements for the range of temperatures observed on the corresponding days. There is a cyclic relationship between the vertical movement of the sidewalk and the associated pavement temperature.

Even though there were some minor vertical displacement trends seen due to temperature variations between the pervious concrete slabs and the curb, they were relatively insignificant between the two different pavement types with only minor grade changes noted. Measurable displacements between the two different pavement types were never noted.

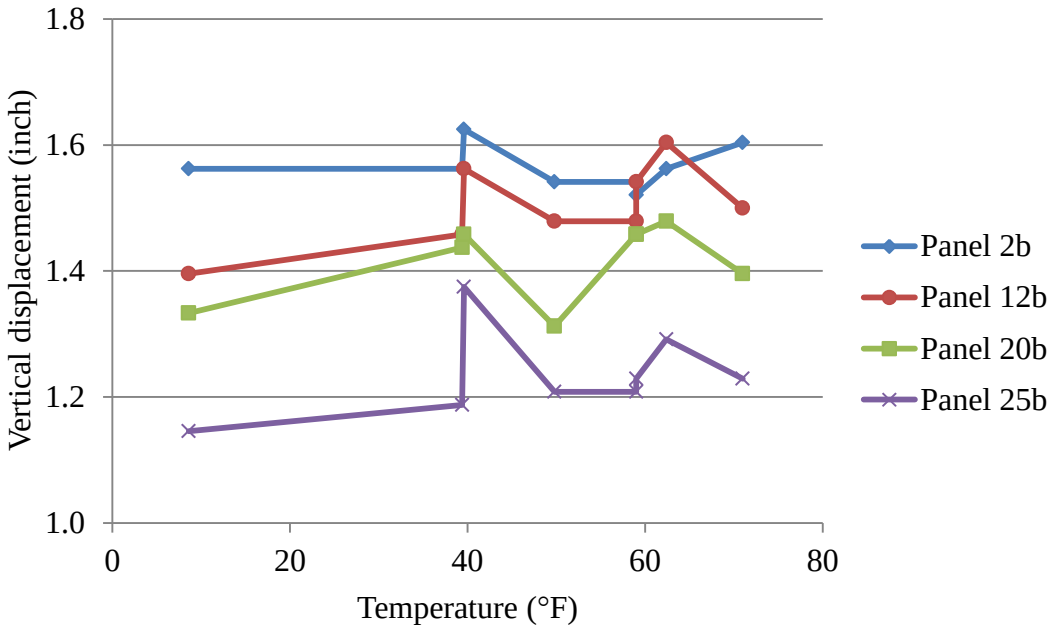

Figure 5.5: Vertical movement of the panels against pavement temperature

5.3 Shoulders

Highway shoulders are defined as the adjacent portion of a highway used for emergency purposes, for stopped vehicles, and for lateral support of the surface and subbase courses (AASHTO, 1968; Huang et. al 2004). From these definitions, it must be assumed that the shoulders adjacent to the pavement will have the same tire loading as considered for the mainline slab. Thus, the same analysis performed in Chapter 4 can be considered to be valid for shoulders. The analysis of the mainline slab in Chapter 4 reveals that a pervious concrete layer thickness equivalent to 8 inches (200 mm) appears to be adequate to support an 18-kip (80-kN) single axle load and a 36-kip (160-kN) tandem axle load. Further analyses under actual loading conditions are still warranted to more accurately provide for a design methodology. These analyses indicate that typical depths of pervious concrete from 8 to 12 inches might be effective for highway shoulders depending on the application and intensity of use.

Chapter 6

Conclusion

6.1 Research Summary

An FE modeling procedure for pervious concrete pavement systems was developed in this research. The model was then used to analyze a field placement in Oregon. In the next step, the FE model was used to analyze pavement for typical load applications. Finally, the presence of dowel bars and relationships for shoulder applications in the pavement were discussed. A summary of the FE analyses are as follows.

6.1.1 The Basic FE Modeling Procedure

- ADINA finite element software was used to model the pervious concrete pavement system.
- The modeling procedure developed in this study included consideration of the vertical porosity distribution in the pervious concrete layer, and the pervious concrete layer was divided into three vertical sections i.e. top quarter, middle half, and bottom quarter.
- Vertical porosity distribution equations (Haselbach and Freeman, 2006) were used to calculate the porosity of the corresponding layer.
- The related mechanical properties of pervious concrete for different porosities were obtained from the experimental study of the field placement in Oregon (Goede, 2009).
- The mechanical properties of the subbase and the subgrade were obtained from previous pavement related research.
- The pervious concrete, subbase, and subgrade were assumed to be elastic materials and perfectly bonded at the interface of the corresponding layer.
- The subgrade layer was extended to 108 inches (2100 mm) in depth to simulate the infiniteness of this layer.

6.1.2 The Field Placement Simulations

- In the first phase analysis for the field placement, the tire pressure considered represented the concrete trucks that were used to traverse the field site and a tandem axle dual wheel tire was modeled.
- For uniform distribution of tire pressure around and below the tire, mapped meshing was considered in both the planar and the vertical directions.
- Three different loading condition based on the wheel position were considered and these are edge, corner, and center loading conditions.
- Linear static analyses of the pavement system were performed throughout the study.
- The tensile stress and deflection in the pervious pavement system responded similarly, for the same loading condition, when compared with analytical and FE analysis of traditional concrete pavement.
- The wheel position at the center of the pavement is not critical, either for stresses or deflection.
- The compressive stress response in the pervious concrete pavement system is comparatively higher than that of traditional concrete pavement systems.
- The stresses and deflections decrease with increases in the thickness of either the pervious concrete layer or the subbase layer.

- When comparing with the material strength data for the field site against static analyses, the pavement system requires a thickness of more than 5 inches (125 mm) in the pervious concrete layer.
- To compare with cyclic or repetitive loading, the stresses obtained from the FE analyses were evaluated by relating them to the PCI condition index of the field site.
- The cyclic loading calculation indicated that a factor of safety equivalent to almost 2 resulted for minimum depth in the pervious concrete layer equivalent to 8.3 inches (211 mm), 9.1 inches (231 mm), and 9.9 inches (251 mm) for fair, satisfactory, and good performance pavement, respectively.

6.1.3 The Analyses for Roadway Applications

- In the second phase analysis for application to typical roadways, both 18-kip (80-kN) single axle dual wheel loading and 36-kip (160-kN) tandem axle loading were considered, and edge and corner loading were considered in the modeling.
- The material properties of pervious concrete were obtained for a 25% mean porosity.
- The subbase depth considered was 12 inches (300 mm) and 24 inches (600 mm) to mimic the intended use of pervious concrete for stormwater usage.
- There were some different responses in the pavement system for deflection when the subbase depth is very high. It was found that for a 24-inch (600 mm) depth in the subbase layer, the deflection is higher than the deflection for 12-inch (300 mm) depth in the subbase for the same pavement thickness. Also, a higher thickness in the concrete layer increases the deflection in the pavement system. This could be credited to the consideration of the self-weight of the pavement system in the analysis.
- The stress response was as expected, with a decrease in stress with an increase in the pervious concrete and subbase layer thicknesses.
- For the critical loading conditions, the tensile and flexural stresses are well below the material strength, even with a consideration of a factor of safety of 2 for tensile stresses.
- Shoulders in the pavement system usually have the same loading type as in the roadway and therefore these recommendations are appropriate since the static stresses will be the same for both, but conservative with respect to cyclic loading as the stresses will be lower for fewer load repetitions in the shoulder.
- Modeling and analysis of dowel bars was not considered as it was found that dowel bars are not used in pervious concrete pavement.
- A pervious pavement sidewalk at Washington State University was observed in order to assess the frost heave action and measurements were also taken to determine the vertical height difference in the sidewalk compared to panels of traditional concrete. The frost heave effect was minimal and the measured height differences in the sidewalk were not significant.

6.2 Recommendations

The following recommendations are made based on the FE analyses of the pervious pavement systems:

- From the validation against the classical analytical theory and a field placement of pervious concrete pavement, the FE method was shown to be an appropriate modeling procedure for pervious concrete pavement system to investigate other properties.

- Tensile stress and deflection are primary design parameters for pervious concrete in these FE analyses, although the compressive stress in the pervious pavement should be considered as a design parameter for very low strength (highly porous) applications.
- When increasing the thicknesses of the pervious concrete and/or subbase layer, the deflections need to be analyzed for all possible variations.
- Based on the static analyses, pervious concrete can be used as an alternate paving material in the shoulder of pavement systems.
- For the particular material properties used in this research, pervious concrete may be appropriate for use in high volume traffic applications for highways with additional factors of safety. However, more research is required to quantify its fatigue properties.

6.3 Future Research

The complex characteristics of pervious concrete were modeled through FE methods using a vertical porosity distribution approach. One limitation of this model is the assumption of the perfect bond between the interfaces of the different layers. Another limitation is that only one pervious panel was modeled.

Future modeling should include multiple slabs in the pavement system as well as inclusion of a coefficient of friction between the different layer interfaces. As a porous material, and depending on the hydrologic design of the pervious pavement system, water might exist in the pervious concrete or subbase layer after a storm event. Thus, the water inside the pores might create some additional stresses in the pavement system and should be investigated.

In this study, only linear static analyses were performed and further analyses should be performed considering both material and load nonlinearity. The stresses were compared against limited material strength data and require validation against stress measures in the pavement system for various traffic loading conditions.

Finally, failure modes in pervious concrete systems might also include durability issues such as raveling. Thus, a combination empirical/theoretical model approach including both strength/stress related impacts and surface durability considerations might need to be developed to more comprehensively provide designers with tools for expanded applications.

References

AASHTO (1968). AASHO highway definitions. Special Committee on Nomenclature, *American Association of State Highway officials*.

Abaqus (2010). *The Abaqus software*. Version ABAQUS/CAE 6.10-1

ACI Committee 325 (2002). ACI 325.12R-02: Guide for design of jointed concrete pavements for streets and local roads. *American Concrete Institute*.

ACI Committee 522 (2006). ACI 522R-06: Pervious concrete. *American Concrete Institute*.

American Concrete Pavement Association (ACPA) (2011). *PerviousPave background, purpose, assumptions and equations*. Rosemont, Illinois.

ADINA (2010). *ADINA - Finite Element Analysis Software.* Version 8.7.2.

Alam, A., Haselbach, L. and Cofer, W. (2011a). Three-dimensional finite element modeling and analysis of pervious concrete pavement: simplified vertical porosity distribution approach. In preparation.

Alam, A., Haselbach, L. and Cofer, W. (2011b). Validation of the Performance of Pervious Concrete in a Field Application with Finite Element Analysis (FEA). *For Presentation ASTM Pervious Concrete Symposium Dec 4*.

ASTM Standard C39 (2005). Standard test method for compressive strength of cylindrical concrete specimens. *ASTM International*, West Conshohocken, PA, 2005, DOI: 10.1520/C0039-05, www.astm.org.

ASTM Standard C78 (2002). Standard test method for flexural strength of concrete (Using simple beam with third-point loading). *ASTM International*, West Conshohocken, PA, 2002, DOI: 10.1520/C0078-02, www.astm.org.

ASTM Standard C469 (2002). Standard test method for static modulus of elasticity and Poisson's ratio of concrete in compression. *ASTM International*, West Conshohocken, PA, 2002, DOI: 10.1520/C0469-02, www.astm.org.

ASTM Standard D6433 (2007), Standard practice for roads and parking lots pavement condition index surveys. *ASTM International*, West Conshohocken, PA, 2003, DOI: 10.1520/D6433-07, www.astm.org.

ASTM D 6433-09 (2009). *Standard Practice for Roads and Parking Lots Pavement Condition Index Surveys*. *ASTM International*, West Conshohocken, Pennsylvania, DOI: 10.1520/D6433-09.

Adu-Osei, A., Little, D. N., and Lytton, R. L. (2001). Structural characteristics of unbound aggregate bases to meet AASHTO 2002 design requirements: interim report. Report No. ICAR/502-1, *Aggregates Foundation for Technology, Research, and Education*, Arlington, VA 22201-3062, USA.

Bentz, D. P. (2008). Virtual Pervious Concrete: Microstructure, Percolation, and Permeability. *ACI Materials Journal*, V. 105, No. 3, pp. 297-301.

Bowles, J. E. (1996). *Foundation Analysis and Design*. 5th Ed, The McGraw-Hill Companies.

Boyer, M., Haselbach, L. and Cofer, W. (2012). Heat transfer finite element modeling in pervious concrete: impacts of vertical porosity distributions. *Accepted for Presentation in TRB Annual Meeting.*

Cho, Y., B. F. McCullough and J. Weissmann (1996). Considerations on Finite-Element Method Application in Pavement Structural Analysis. In *Transportation Research Record: Journal of the Transportation Research Board*, No. 1539, Transportation Research Board of the National Academies, Washington, D.C., pp. 96–101.

Crouch, L. K., Pitt, J., & Hewitt, R. (2007). Aggregate effects on pervious portland cement concrete static modulus of elasticity. *Journal of Materials in Civil Engineering*, *19:7*, 561-567.

Coduto, D. P. (1994). *Foundation Design Principles and Practices*. Prentice-Hall, Inc., Englewood Cliffs, NJ 07632, USA.

Davids, W. (2010). EverFE: Software for the 3D Finite Element Analysis of Jointed Plain *Concrete Pavements*. http://www.civil.umaine.edu/EverFE/

Delatte, N.J., Miller, D., & Mrkajic, A. (2007). Portland cement pervious concrete pavement: Field performance investigation on parking lot and roadway pavements. *RMC Research & Education Foundation*.

Delatte, N., (2008). *Concrete Pavement Design, Construction, and Performance*. Taylor & Francis, New York, NY, USA.

Ferguson, B. K. (2005). *Porous pavement*. Taylor & Francis, Boca Raton, Florida, USA.

Garber, N. J. and Hoel, L. A., (2002). *Traffic & Highway Engineering*. 3rd ed., Brooks/Cole, Pacific Grove, CA.

Ghafoori, N., & Dutta, S. (1995). Pavement thickness design for no-fines concrete parking lots. *Journal of Transportation Engineering*, Vol. 121, No. 6, pp. 476-484.

Goede, W. (2009). Pervious concrete: Investigation into structural performance and evaluation of the applicability of existing thickness design methods. *MS Thesis*, Washington State University, Pullman, WA.

Goede, W. and L. Haselbach (2011). Investigation into the Structural Performance of Pervious Concrete. *J. of Transportation Engineering*, doi:10.1061/(ASCE)TE.1943-5436.0000305.

Haselbach, L. M. and Freeman, R. M. (2006). Vertical porosity distributions in pervious concrete pavement. *ACI Materials Journal*, Vol. 103, No. 6, pp. 452-458.

Huang, Y. H., (2004). *Pavement Analysis and Design*. 2nd ed., Pearson Prentice Hall, Upper Saddle River, NJ, USA.

McCormac, J. C. and Nelson, J. K., (2005). *Design of Reinforced Concrete*. 7th Ed. John Wiley & Sons, Inc. Hoboken, NJ, USA.

Mackerle, J. (1998). Finite element and boundary element analysis of bridges, roads and pavements- A bibliography (1994--1997). *Finite Elements in Analysis and Design*, Vol. 29, pp. 65-73.

Miller, J. S. and Bellinger, W. Y. (2003). Distress identification manual for long-term pavement performance program (fourth revised edition). *Publication No. FHWA-RD-03-031*.

Montes, F., Valavala, S., & Haselbach, L. M. (2005). A new test method for porosity measurements of Portland cement pervious concrete. *Journal of ASTM International*, 2:1, 1-13.

Onstenk, E., A. Aguado, E. Eickschen and A. Josa (1993). Laboratory study of porous concrete for its use as top-layer of concrete pavements. *Fifth International Conference on Concrete Pavement Design and Rehabilitation*, West Lafayette, IN, Vol. 2, pp. 125-139.

Portland Cement Association (PCA), (1984). *Thickness design for concrete highway and stress pavements*. EB109.01P, Shokie, Ill.

Rohne, R. J. and Izevbekhai, B., I. (2009). Early performance of pervious concrete pavement. *TRB 2009 Annual Meeting*.

Somayaji, S. (2001). *Civil Engineering Materials*. Prentice-Hall, Inc., Upper Saddle River, NJ 07458, USA

Tennis, P., Leming, M., & Akers, D. (2004). *Pervious Concrete Pavements*. Skokie, IL: Portland Cement Association.

Vassilikou, F., N. Kringos, M. Kotsovos, and A. Scarpas, (2011). Application of Pervious Concrete for Sustainable Pavements: A Micro-Mechanical Investigation. In *Highways; Pavements; Materials.* CD-Rom. Transportation Research Board of the National Academies, Washington, D.C.

Wang, C., Salmon, C., & Pincheira, J. (2007). *Reinforced Concrete Design*. 7th Ed., Hoboken, NJ: John Wiley & Sons, Inc., page 13.

Wanielista, M., & Chopra, M. (2007). Performance assessment of Portland Cement pervious pavements:Report 2 of 4: Construction and maintenance assessment of pervious concrete pavements. Retrieved from http://www.stormwater.ucf.edu/research/Final%20Report%202%20of%204%20Construction%20and%20Maintenance%20Jan.pdf.

Yang, J., & Jiang, G. (2003). Experimental study on properties of pervious concrete pavement materials. *Cement and Concrete Research*, *33*, 381-386.

Yang, Z., Ma, W., Shen, W., & Zhou, M. (2008). The Aggregate Gradation for the Porous Concrete Pervious Road Base Material. *Journal of Wuhan University of Technology-Materials Science Edition*, *23:3*, 391-394.

Appendix A

PAVEMENT MODEL AND ANALYSIS RESULTS FOR FIELD APPLICATION

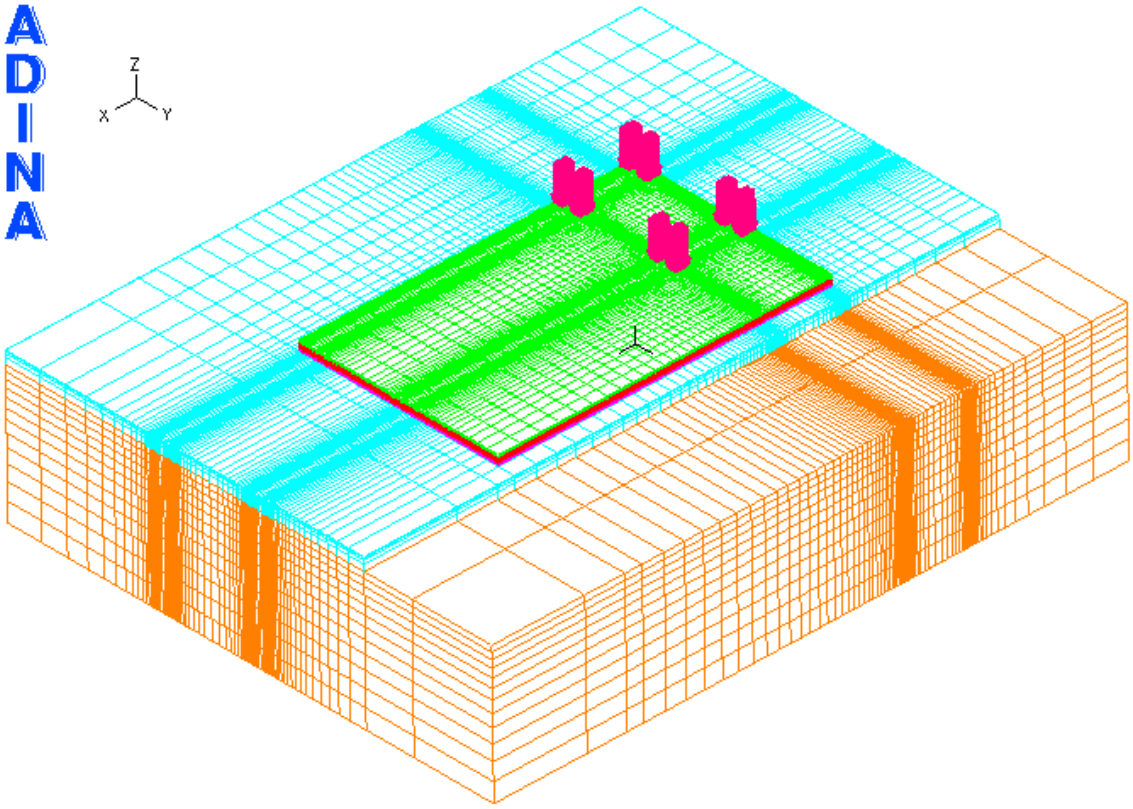

Figure A.1: Meshing pattern for wheel location at the corner of the pavement

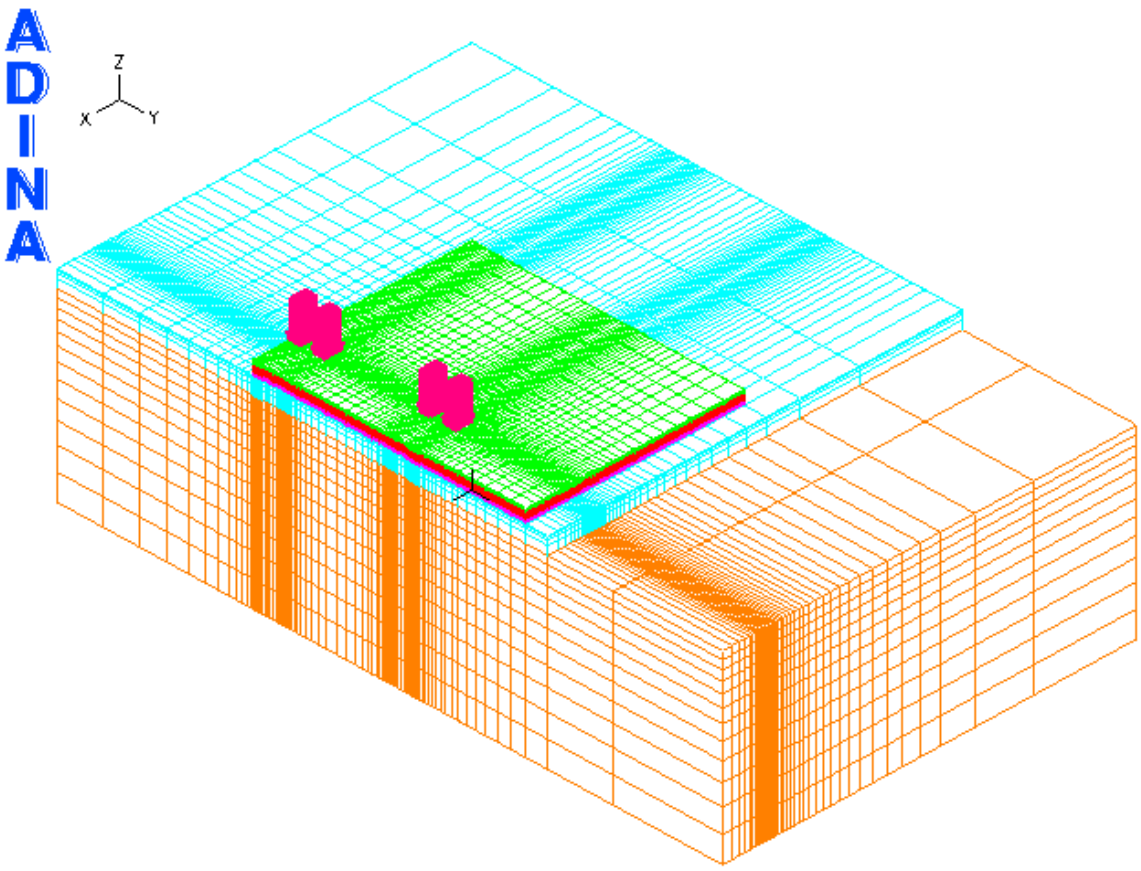

Figure A.2: Meshing pattern for wheel location at the center of the pavement

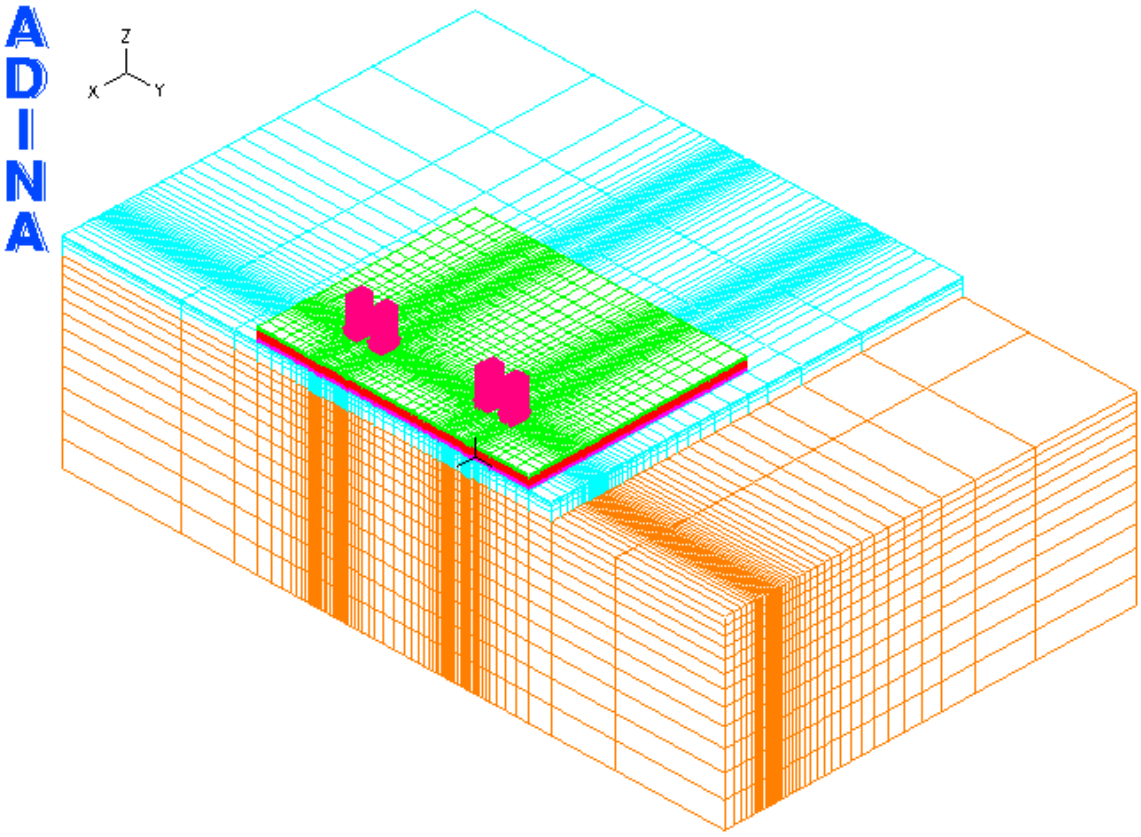

Figure A.3: Meshing pattern for wheel location at the center of the pavement

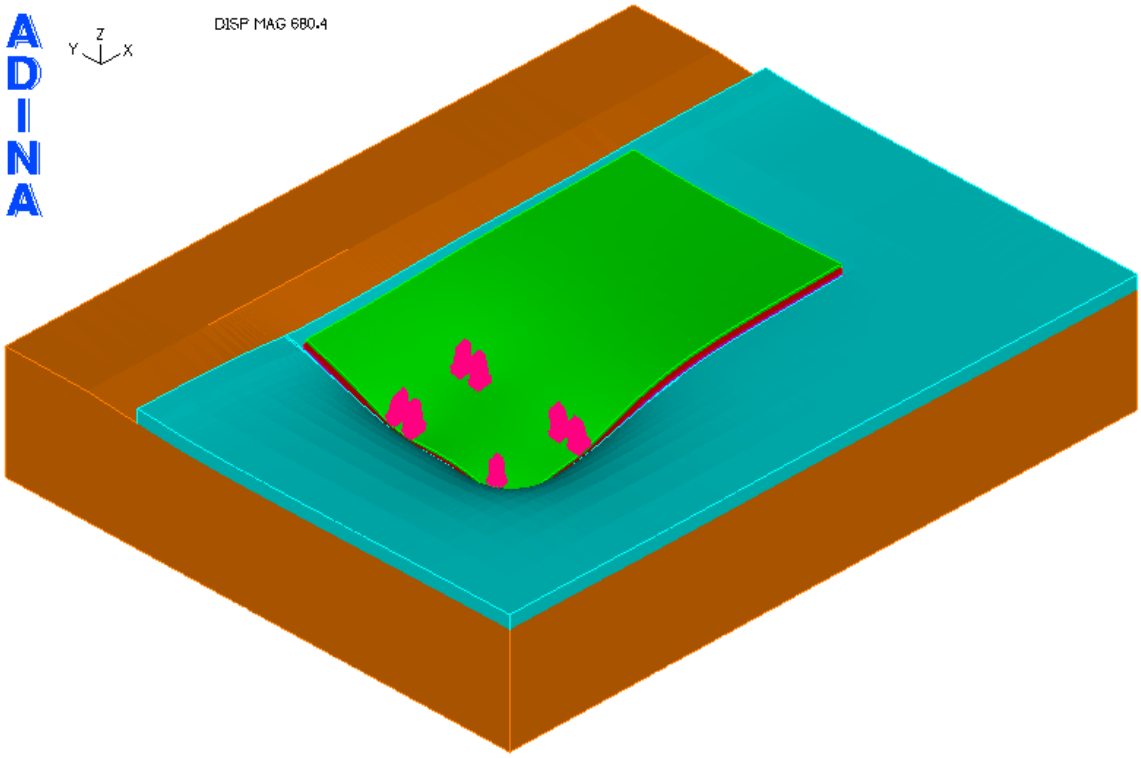

Figure A.4: Deflected shape for corner loading

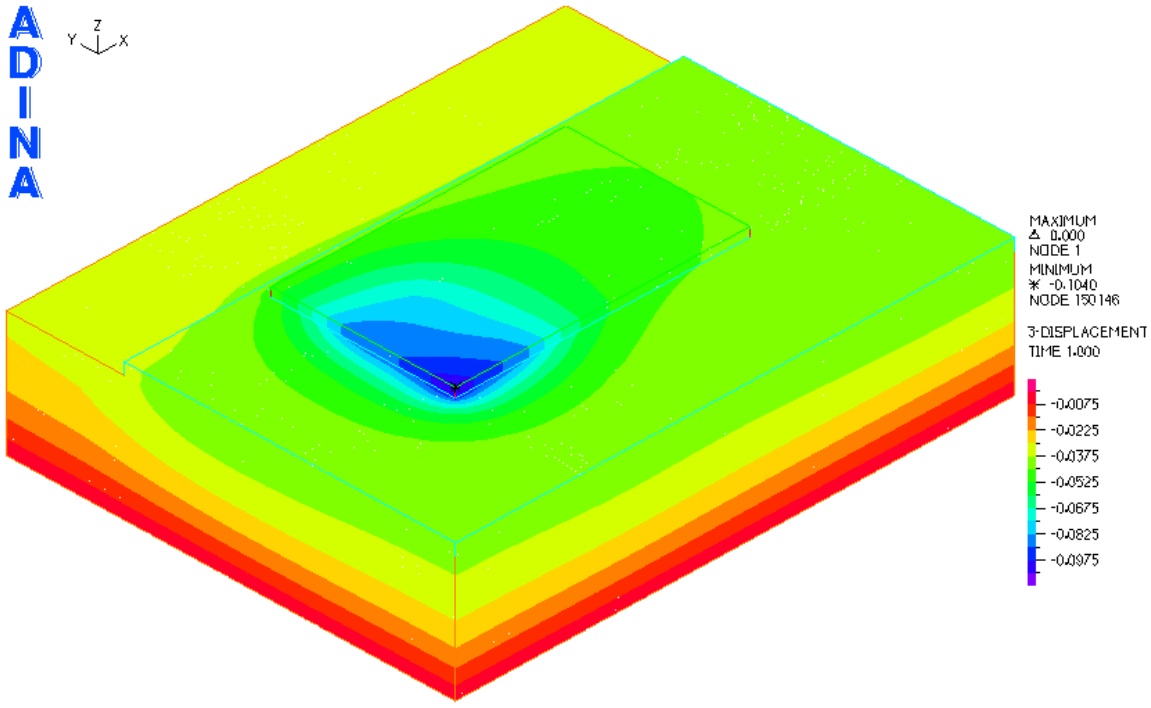

Figure A.5: Deflection contour in the vertical z-direction for corner loading

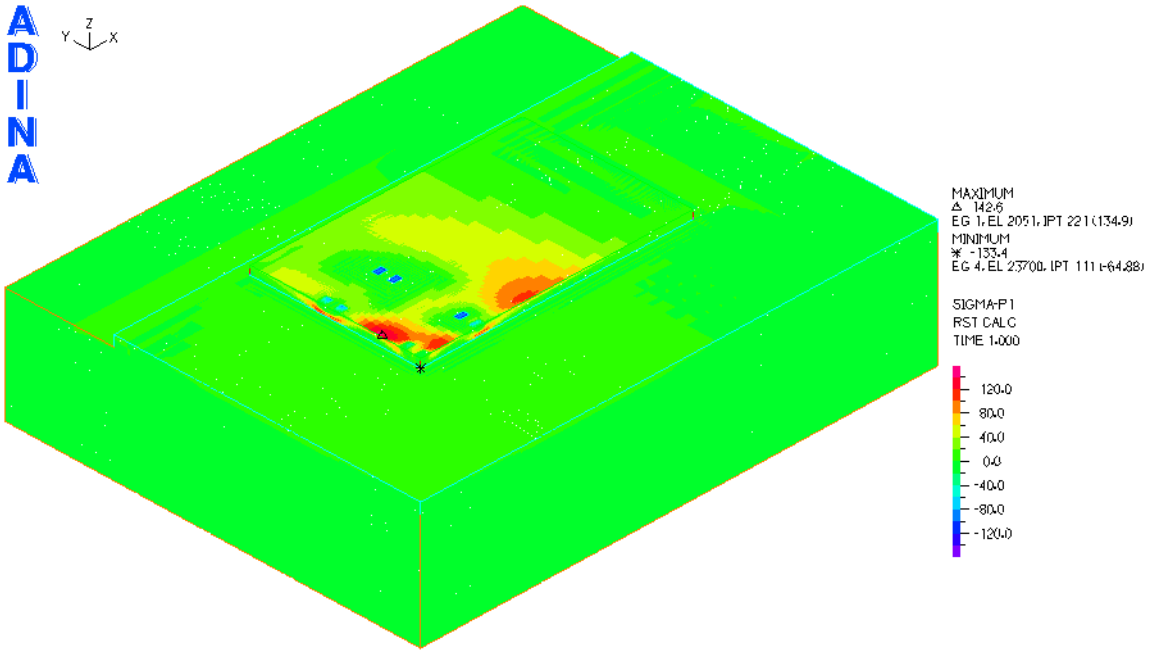

Figure A.6: Tensile stress contour for corner loading

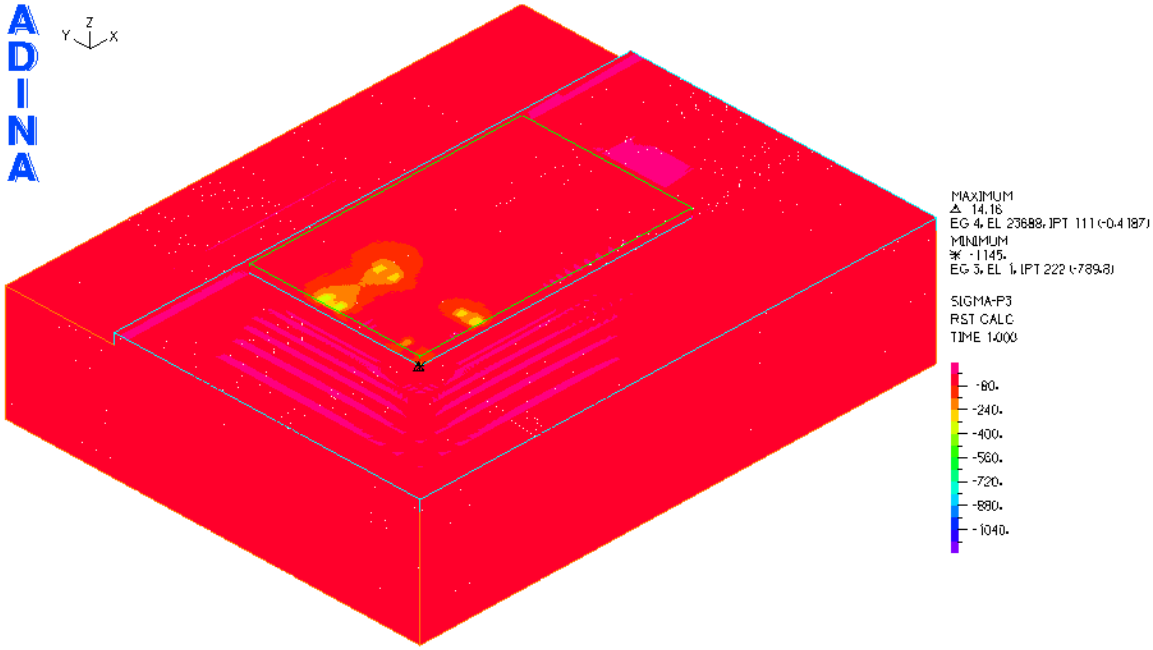

Figure A.7: Compressive stress contour for corner loading

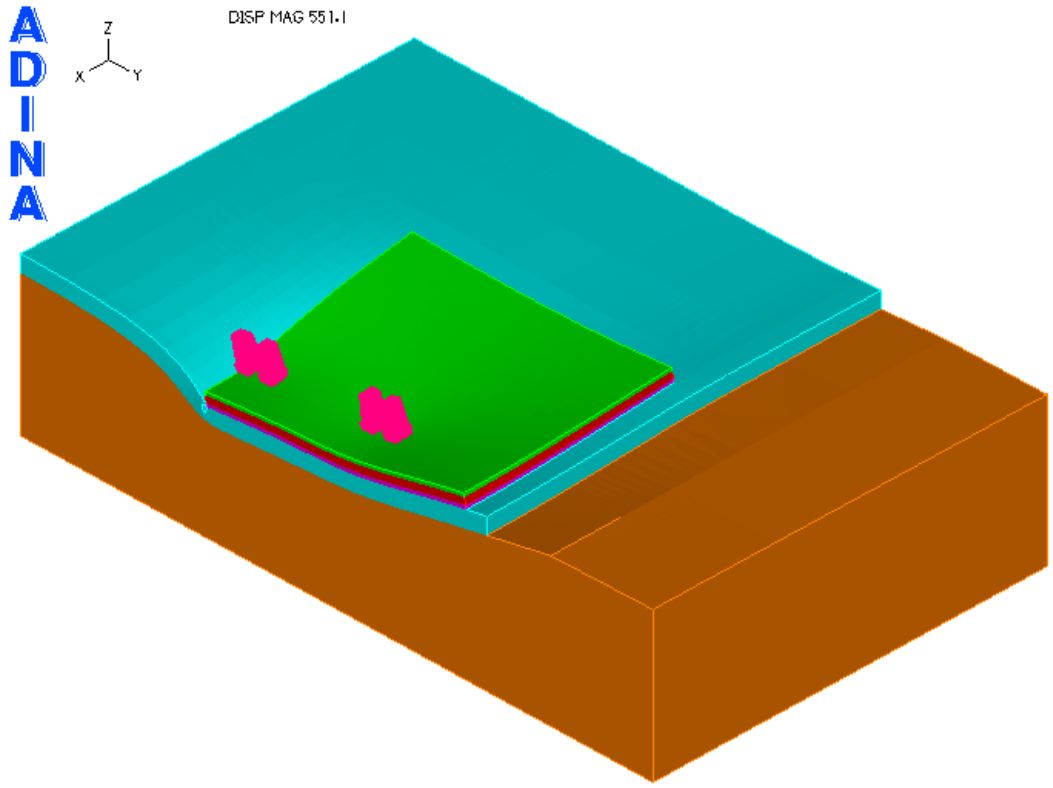

Figure A.8: Deflected shape for edge loading

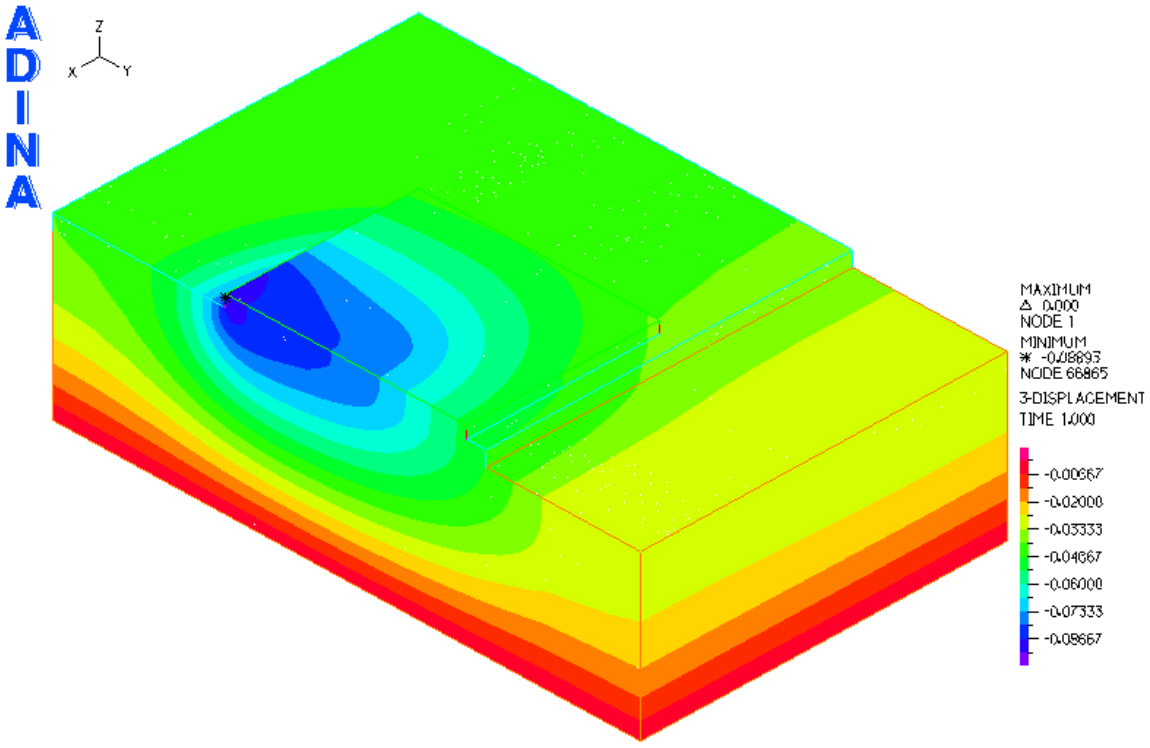

Figure A.9: Deflection contour in the vertical z-direction for edge loading

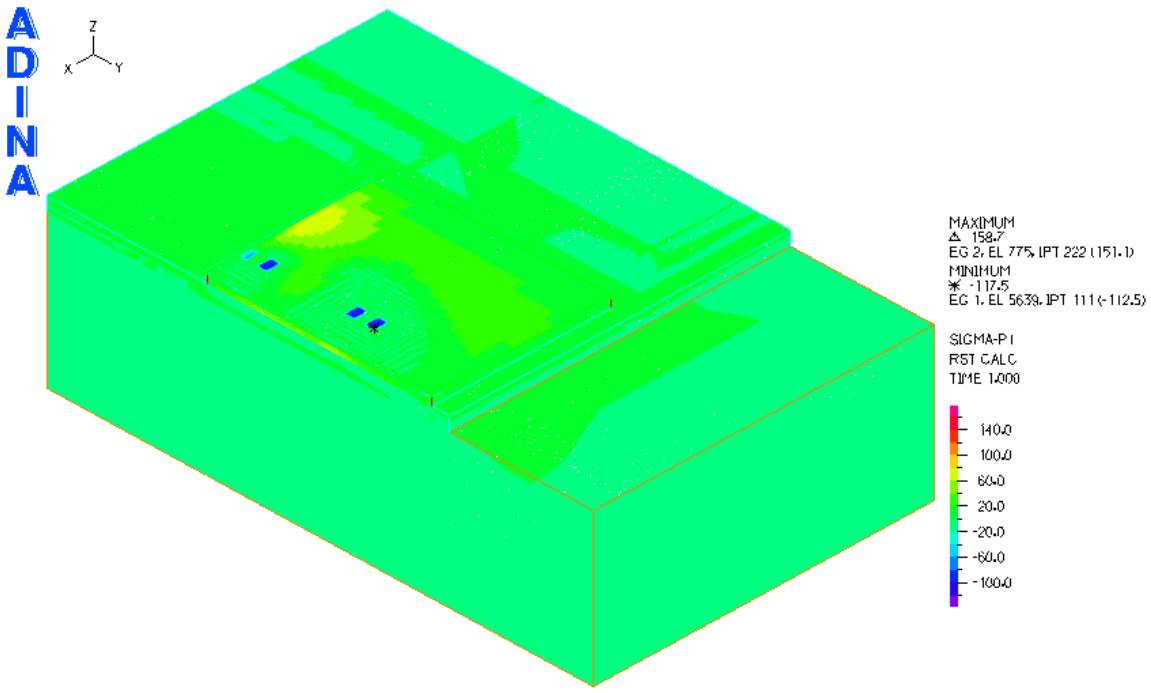

Figure A.10: Tensile stress contour for edge loading

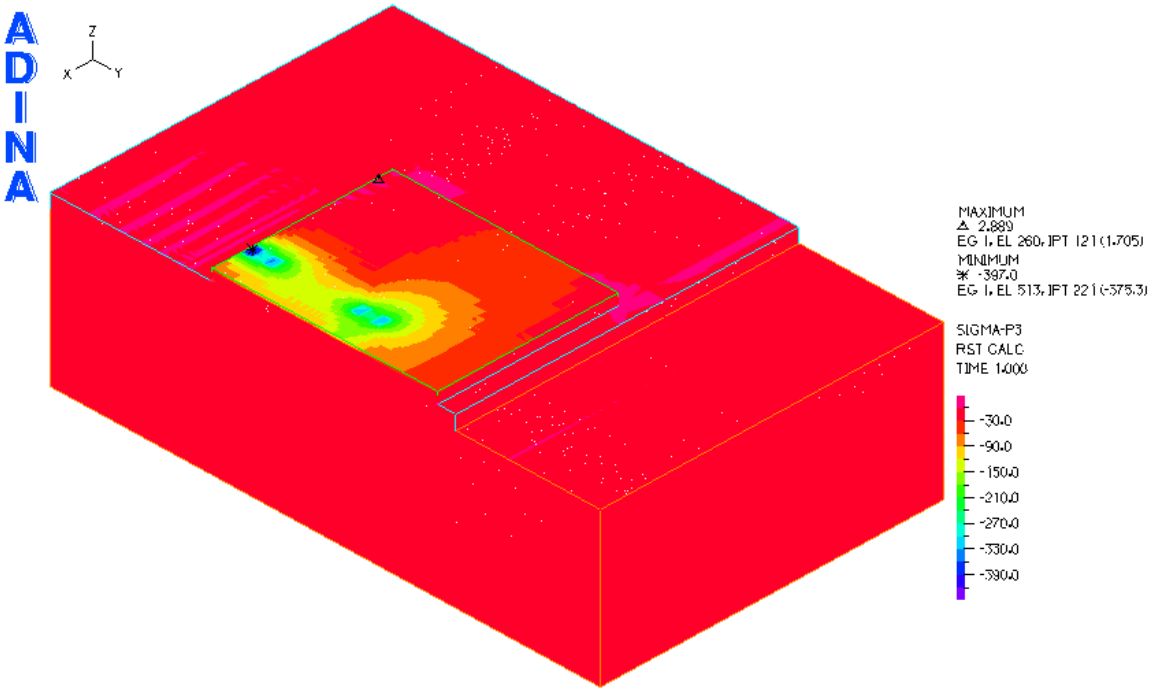

Figure A.11: Compressive stress contour for edge loading

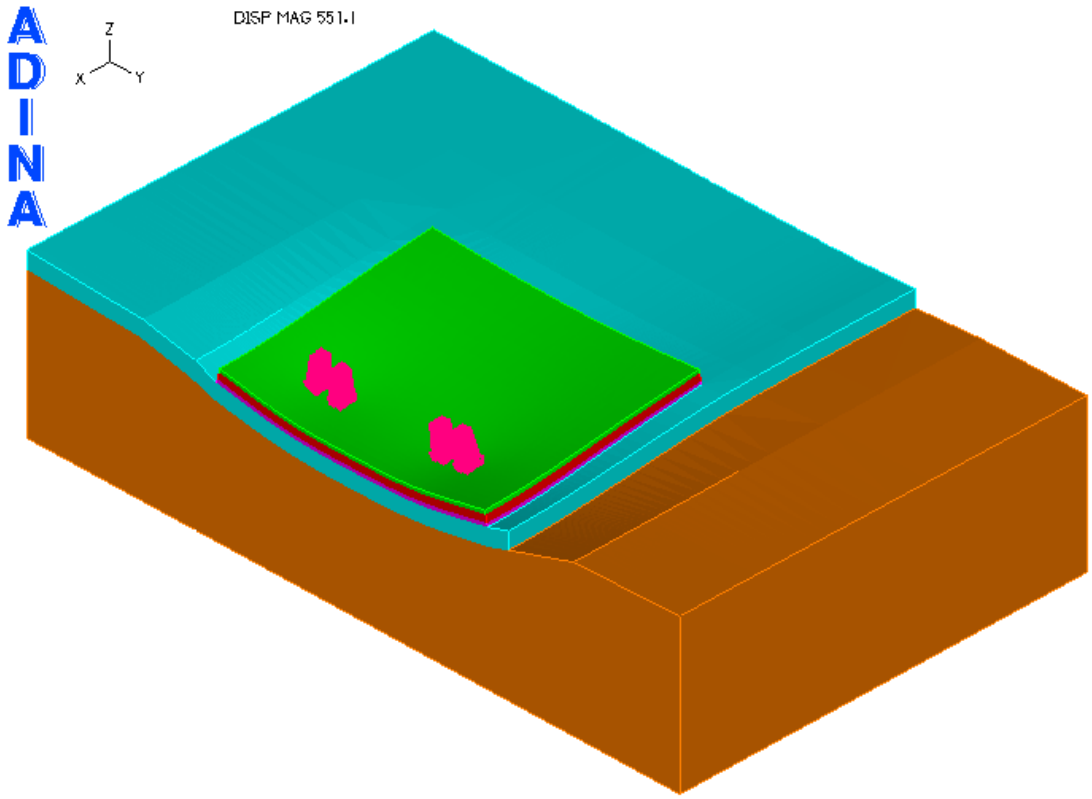

Figure A.12: Deflected shape for center loading

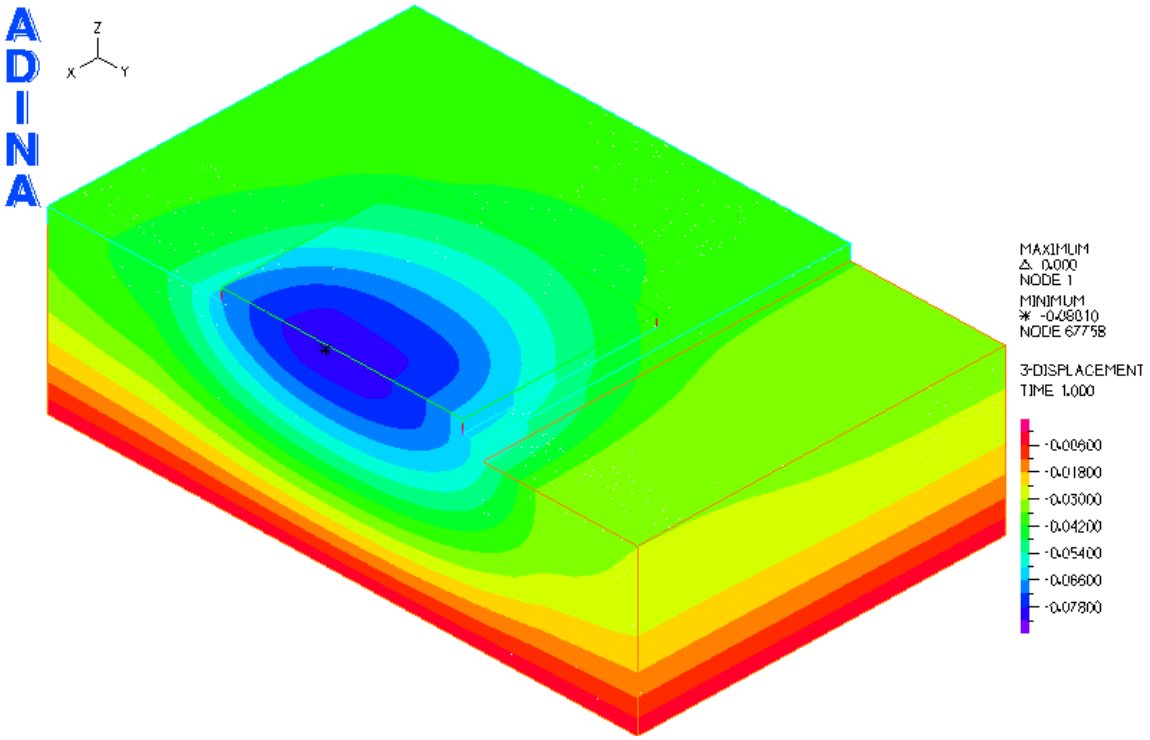

Figure A.13: Deflection contour in the vertical z-direction for center loading

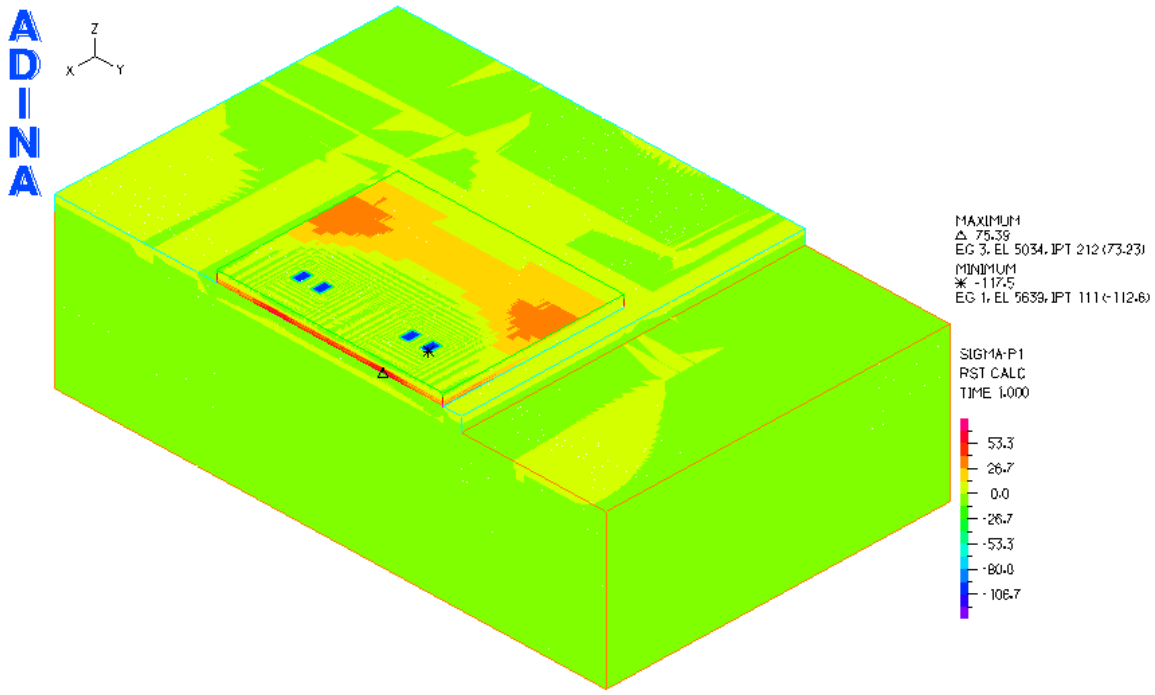

Figure A.14: Tensile stress contour for center loading

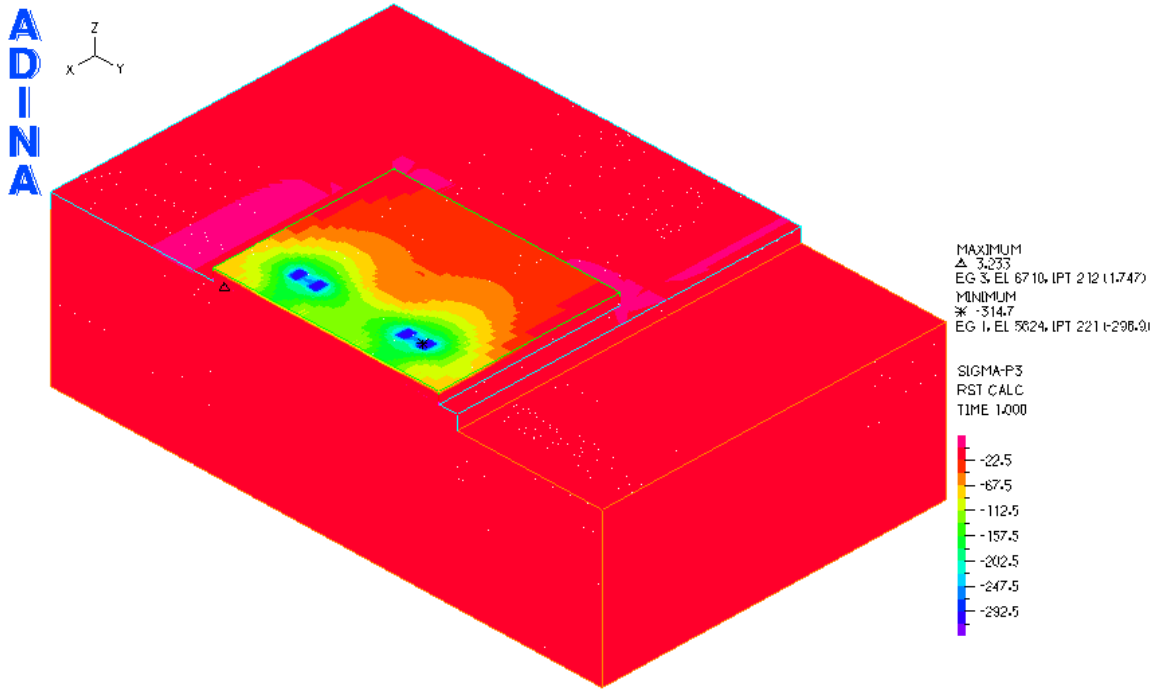

Figure A.15: Compressive stress contour for center loading

Appendix B

Analysis Results for Field Application

Table B.1: Deflection, tensile, and compressive stress for field condition truck loading

Subbase Thickness	Thickness of Pervious Concrete	Deflection	Tensile Stress	Compressive Stress
inch (mm)	inch (mm)	inch (mm)	psi (MPa)	psi (MPa)
4 (102)	5 (127)	0.1134	295.2	1619
	6 (152)	0.1111	236.7	1473
	7 (178)	0.1095	197.8	1360
	8 (203)	0.1084	170.7	1272
8 (203)	5 (127)	0.1060	266.2	1403
	6 (152)	0.1050	216.8	1288
	7 (178)	0.1044	182.9	1214
	8 (203)	0.1040	158.7	1145

Appendix C

Meshing and Analysis Results for Generalized Pavement Model

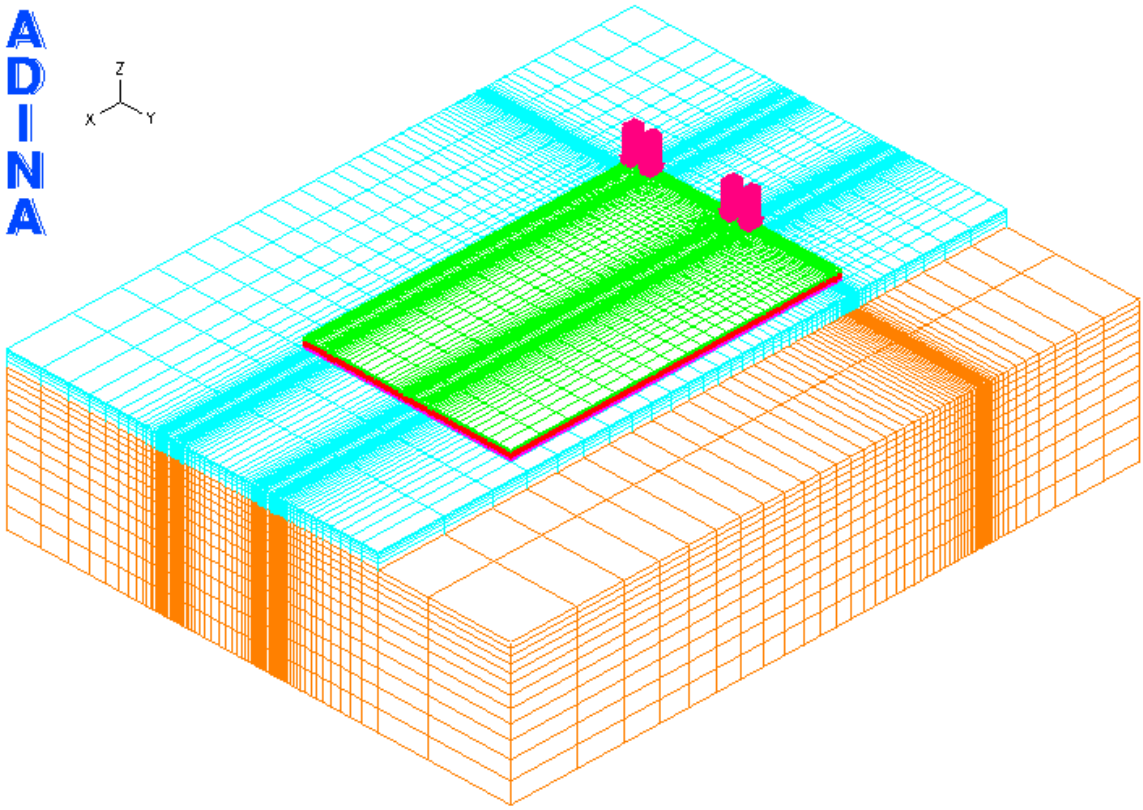

Figure C.1: Meshing pattern for single axle dual wheel location at the corner of the pavement

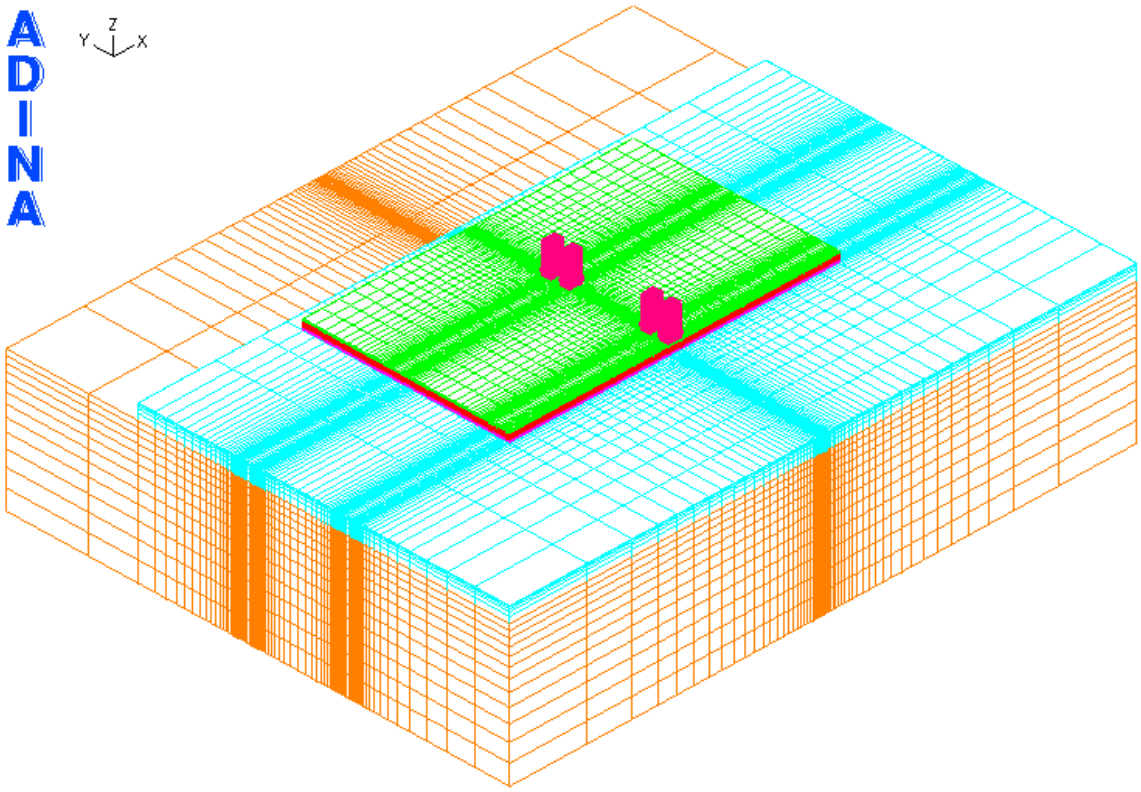

Figure C.2: Meshing pattern for single axle dual wheel location at edge of the pavement

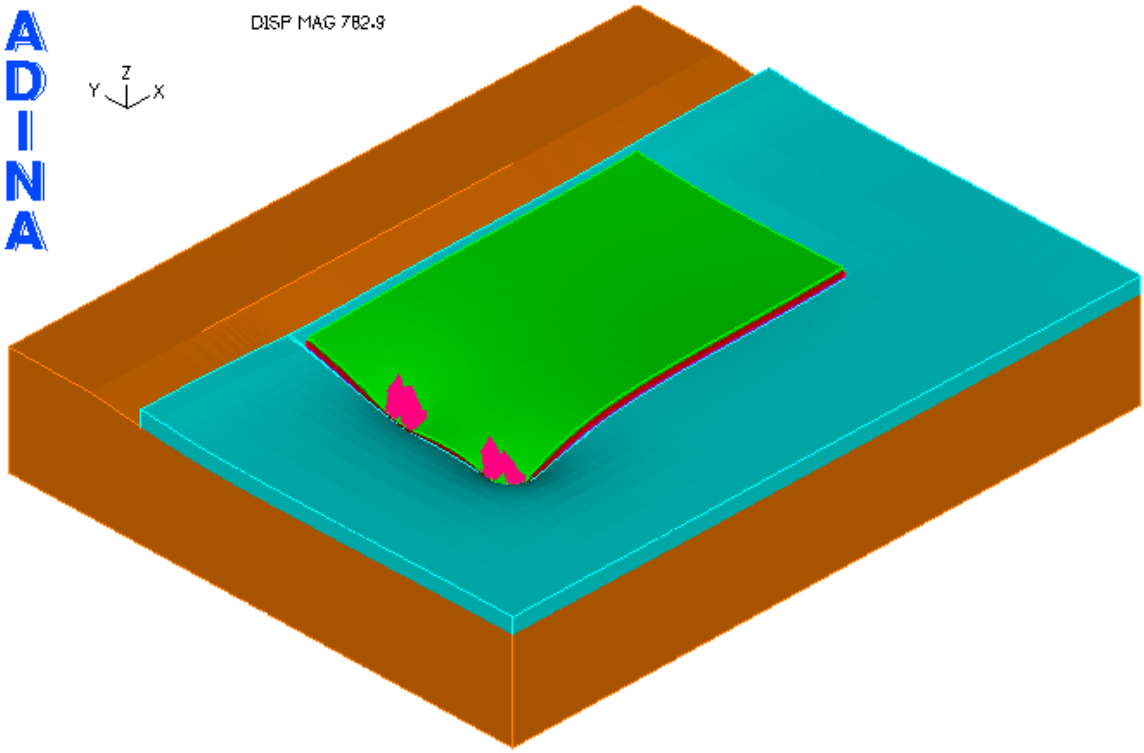

Figure C.3: Deflected shape for single axle dual wheel at corner of the pavement

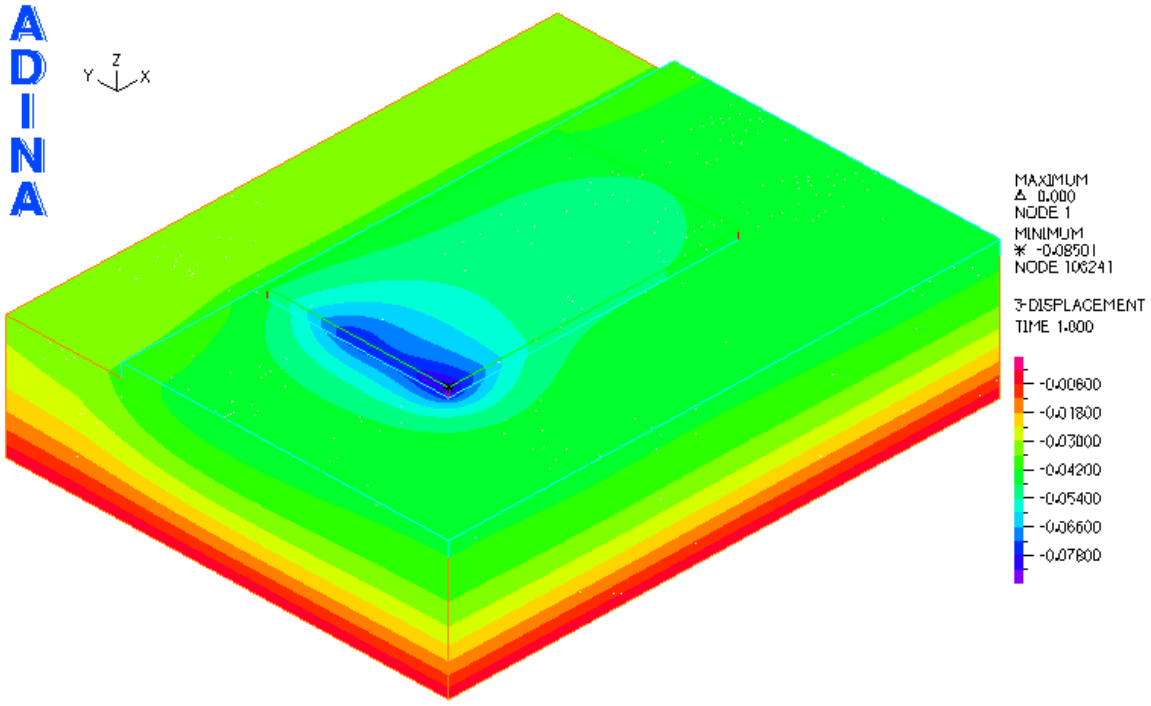

Figure C.4: Displacement contour in the vertical x-direction for single axle dual wheel at corner of the pavement

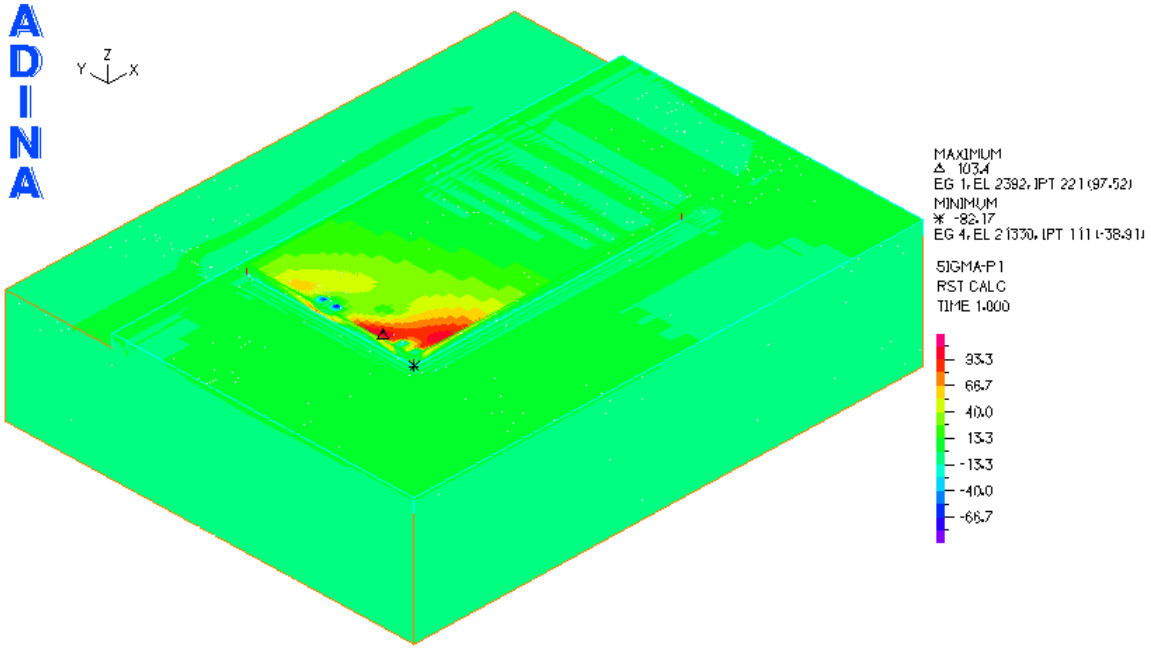

Figure C.5: Tensile stress contour for single axle dual wheel at corner of the pavement

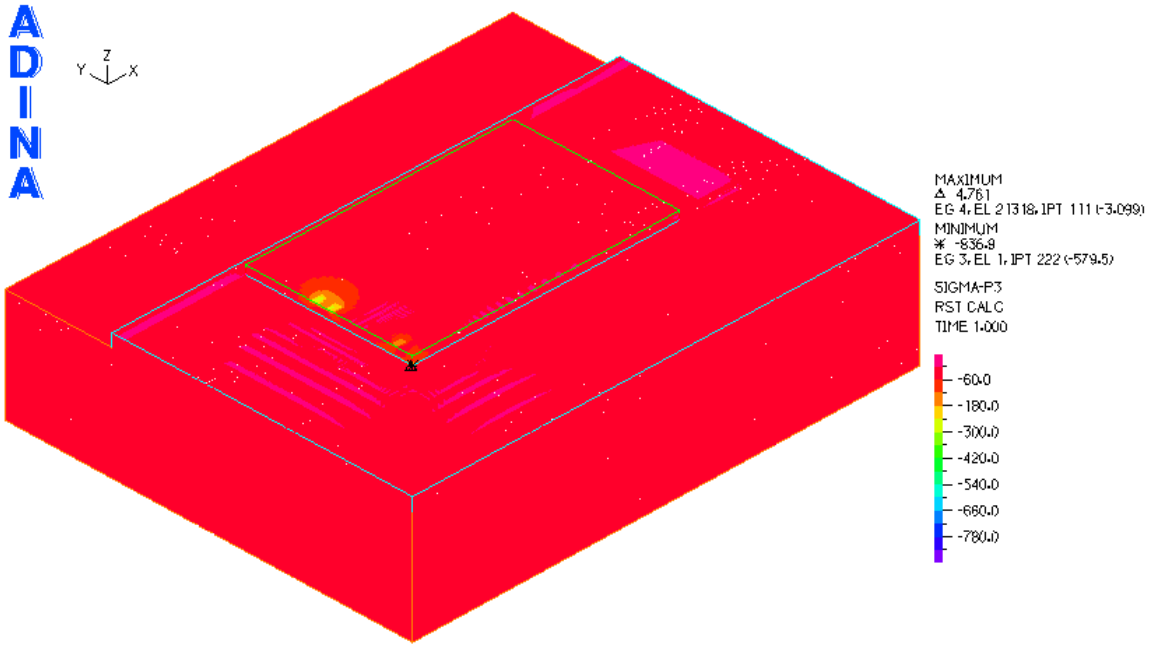

Figure C.6: Compressive stress contour for single axle dual wheel at corner of the pavement

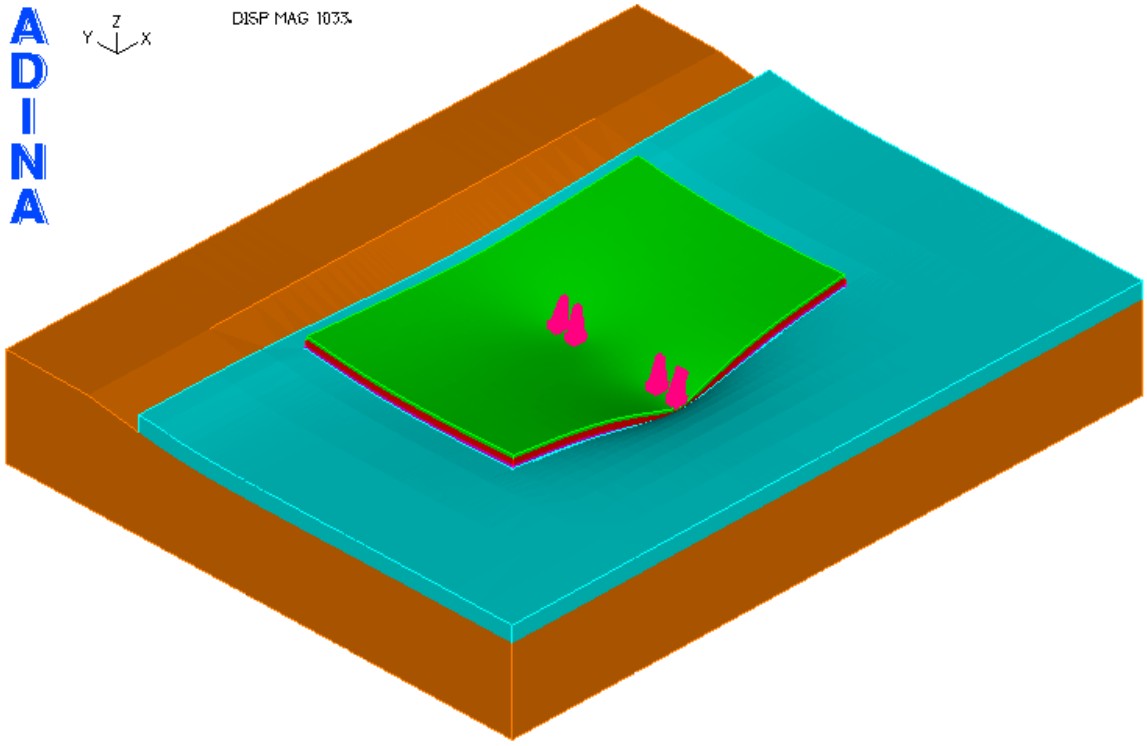

Figure C.7: Deflected shape for single axle dual wheel at edge of the pavement

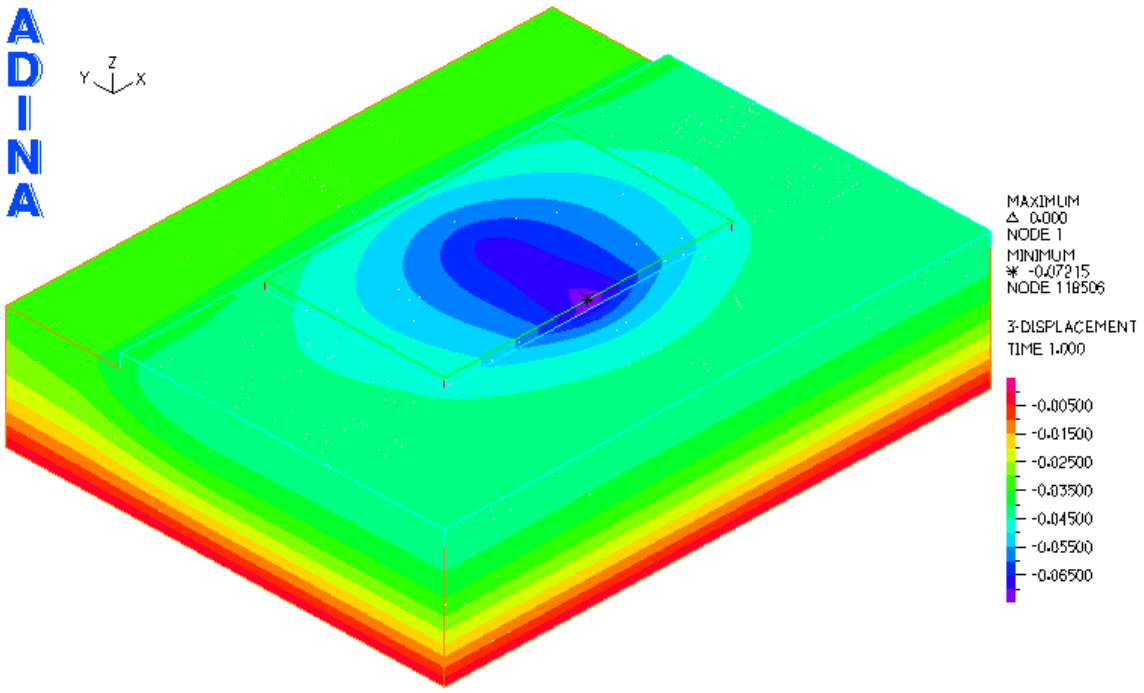

Figure C.8: Displacement contour in the vertical x-direction for single axle dual wheel at edge of the pavement

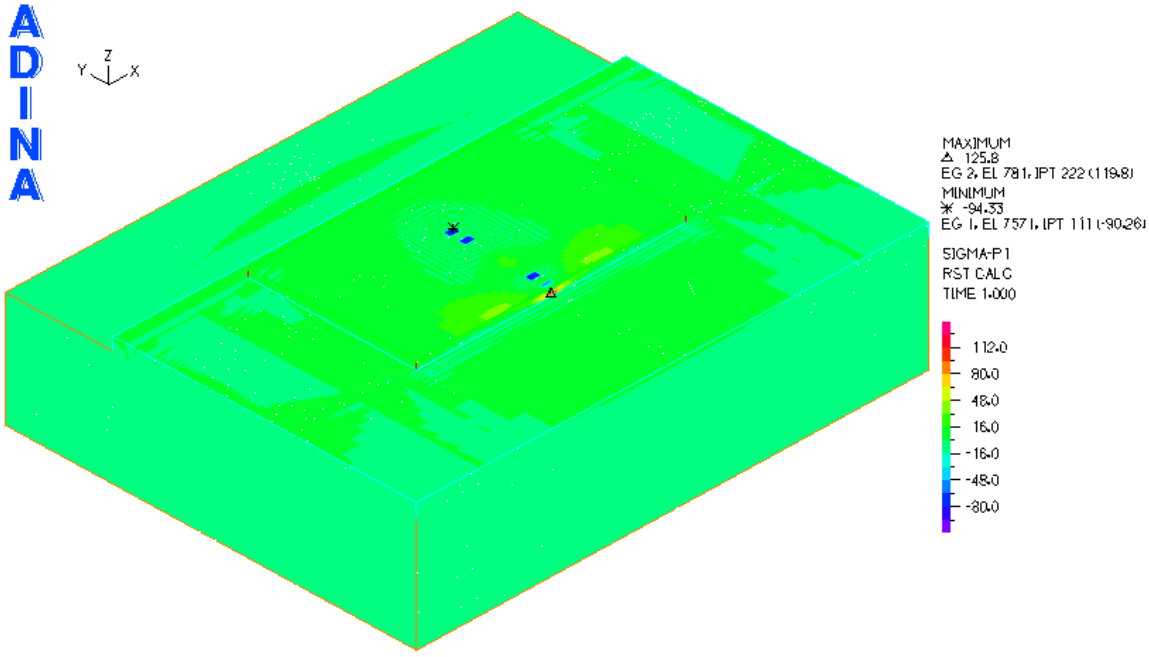

Figure C.9: Tensile stress contour for single axle dual wheel at edge of the pavement

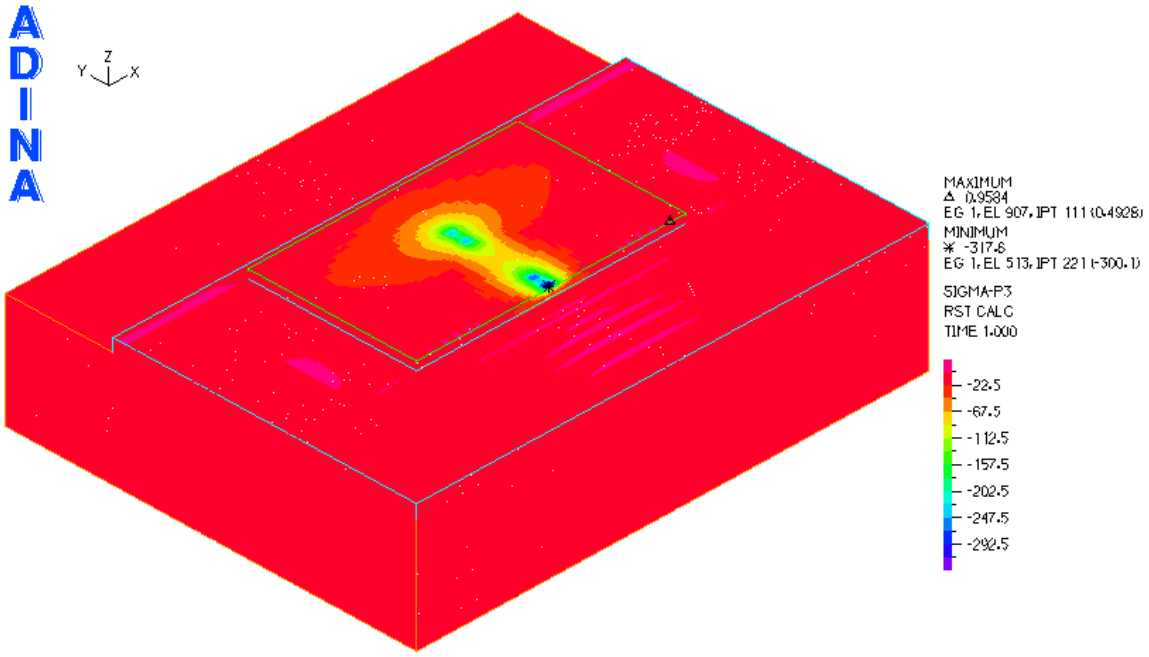

Figure C.10: Compressive stress contour for single axle dual wheel at edge of the pavement

Appendix D

FE Analysis Results for Generalized Model

Table D.1: Deflection, tensile, and compressive stress for 36-kip (160-kN) tandem axle dual wheel load

Subbase Thickness	Thickness of Pervious Concrete	Deflection	Tensile Stress	Compressive Stress
inch (mm)	inch (mm)	inch (mm)	psi (MPa)	psi (MPa)
12 (305)	8 (203)	0.0927	107.9	890.6
	10 (254)	0.0923	85.87	803.6
	12 (305)	0.0928	72.47	747.6
24 (610)	8 (203)	0.0955	96.89	784.2
	10 (254)	0.0955	76.53	712.0
	12 (305)	0.0959	64.41	662.0

Table D.2: Deflection, tensile, and compressive stress for 18-kip (80-kN) single axle dual wheel load

Subbase Thickness	Thickness of Pervious Concrete	Deflection	Tensile Stress	Compressive Stress
inch (mm)	inch (mm)	inch (mm)	psi (MPa)	psi (MPa)
12 (305)	8 (203)	0.0850	125.8	836.9
	10 (254)	0.0833	97.24	710.7
	12 (305)	0.0821	78.42	626.4
24 (610)	8 (203)	0.0884	112.3	745.2
	10 (254)	0.0873	87.62	642.5
	12 (305)	0.0866	71.18	567.2